

Multicomponent Description of Dust Forming Stellar Shells

vorgelegt von
Dipl.- Phys. Karen Lingnau
aus Berlin

Der Fakultät II - Mathematik und Naturwissenschaften
der Technischen Universität Berlin
zur Erlangung des akademischen Grades
Doktor der Naturwissenschaften
- Dr. rer. nat. -

genehmigte Dissertation

Promotionsausschuss:

Vorsitzender: Prof. Dr. Mario Dähne

Berichter: Prof. Dr. Erwin Sedlmayr

Berichter: Prof. Dr. Heike Rauer

Tag der wissenschaftlichen Aussprache: 10.7.2012

Berlin 2012

D 83

Contents

1	Introduction	11
2	Theoretical Background	15
2.1	Hydrodynamics	15
2.1.1	Equation of Continuity	17
2.1.2	Conservation of Momentum	19
2.1.3	Conservation of Energy	24
2.2	Dust Complex	31
2.2.1	Thermodynamics	31
2.2.2	Dust Equations	37
2.3	Radiative Transfer	40
2.4	The Numerical Problem	43
2.4.1	Differential-algebraic Equations	43
2.4.2	Shooting Method	44
3	Models Including Interactions between Gas and Dust	47
3.1	Stationary Wind Model in Spherical Symmetry	47
3.2	Time-Dependent Model	49
4	Multi-Component Description of a Stellar Wind	53
4.1	Aim	53
4.2	The Restriction To C-Rich Cases	54
4.3	Single Fluid Model	56
4.4	Two-Fluid-Model	62
4.4.1	Applied Equations	63
4.4.2	Results of the Two-Component Description	64
4.5	Decoupled Description of the Dust Component	65
4.5.1	Results of the Decoupled Description and Consequences for the Two Fluid Description	68
4.6	Closer Inspection of the Equations of the Model	72
4.7	Results of the Studies	76

4

CONTENTS

5 Conclusions and Outlook

79

A

83

List of Tables

4.1	The implemented models	57
4.2	Comparison of the implemented models	61
4.3	Table demonstrating differences of dust density based on moment equations and mass flux	75

List of Figures

2.1	The coupled problem of a dust-driven wind (adopted from Winters et al. [109])	16
2.2	Model for the radiation field (adopted from the work of L.B. Lucy [84])	41
2.3	Shooting method (schematic). Trial integrations satisfying the boundary condition at one endpoint lead to discrepancies from the designated boundary condition at the other endpoint. These are used to adjust the starting conditions, until boundary conditions at both endpoints are satisfied.	46
4.1	Velocity structure of a stellar wind with a luminosity of $4.35 \cdot 10^3 \cdot L_{\odot}$ (Euler-method)	58
4.2	Velocity structure of a stellar wind with a luminosity of $7.64 \cdot 10^3 \cdot L_{\odot}$ (Euler-method)	58
4.3	Velocity structure of a stellar wind with a luminosity of $1.28 \cdot 10^4 \cdot L_{\odot}$ (Euler-method)	59
4.4	Velocity structure of a stellar wind with a luminosity of $4.35 \cdot 10^3 \cdot L_{\odot}$ (Limex)	59
4.5	Velocity structure of a stellar wind with a luminosity of $7.64 \cdot 10^3 \cdot L_{\odot}$ (Limex)	60
4.6	Velocity structure of a stellar wind with a luminosity of $1.28 \cdot 10^4 \cdot L_{\odot}$ (Limex)	60
4.7	Comparison of the implemented numerical models: E.g. velocity structure of a stellar wind with a luminosity of $1.28 \cdot 10^4 \cdot L_{\odot}$	62
4.8	Velocity structure: Comparison of the single fluid description and the two fluid description of a stellar wind with a luminosity of $1 \cdot 10^4 \cdot L_{\odot}$.	64
4.9	The decoupled model with derived drift velocity with a stellar luminosity of $1 \cdot 10^4 \cdot L_{\odot}$	66
4.10	Velocity structure of a stellar wind with a luminosity of $1 \cdot 10^4 \cdot L_{\odot}$ (Euler-method)	67
4.11	Gas and drift velocity structure	68

4.12	Dust and gas densities, calculated as coupled single fluid around the onset of dust formationl	69
4.13	Acceleration terms, calculated as coupled single fluid around the onset of dust formation	70
4.14	Velocity structure, calculated as coupled single fluid around the onset of dust formation	70
4.15	Density structure of the model without a differential equation for the gas component calculated as coupled single fluid around the onset of dust formation	71
4.16	Comparison of the acceleration terms	73
4.17	Comparison of the dust densities	74
4.18	Comparison of the drift velocities	74

Zusammenfassung

In den kühlen, ausgedehnten Hüllen weitentwickelter Sterne auf dem asymptotischen Riesenast (AGB) bilden sich kleine Festkörper. Dieser Staub führt durch den auf ihn wirkenden Strahlungsdruck zu einem massiven Materiestrom bzw. Wind. Eine realistische Beschreibung dieses aus vielen chemischen Komponenten bestehenden Materiestroms erfordert die konsistente Behandlung der Hydrodynamik, der Staubbildung, des Strahlungstransports und der Chemie der Gasphase aller am Wind beteiligten Komponenten. Das langfristige Ziel, das dieser Arbeit zu Grunde liegt, ist ein Mehrkomponenten-Hydrodynamik-Modell, das den Materiestrom sowohl der einzelnen unterschiedlichen Staub bildenden Moleküle, als auch das der daraus gebildeten Staubteilchen mit den unterschiedlichen Größen adäquat beschreibt. In dieser Arbeit wird ein Teilaspekt behandelt, der die Wechselwirkung zwischen der Gasphase und dem Staubanteil im betrachteten Materiestrom untersucht. An Hand eines stationären, sphärisch symmetrischen Modells wird in einem ersten Schritt das Verhalten des Gleichungssystems betrachtet. Die Wechselwirkungen der Staub- mit der Gasphase werden durch Austauschterme dargestellt, die sich aus der detaillierten Darstellung der hydrodynamischen Gleichungen ergeben. Es werden die speziellen Anforderungen und die daraus resultierenden Schwierigkeiten für die numerische Behandlung des erweiterten Gleichungssystems aufgezeigt.

Abstract

The outer regions of the cool, extended shells of evolved stars on the asymptotic giant branch (AGB) are the source of small grains. Driven by radiation, the newly formed dust leads to a massive outflow, respectively wind from the star. In order to model this outflow in a realistic way, a consistent description of hydrodynamics, dust formation, radiative transfer, and chemistry of the gas phase with all involved components is needed. In the long term, the basic goal consists in a multicomponent model of hydrodynamics including all dust-forming molecules as well as their successor dust particles with individual size and composition. The part of the project exploring the interactions between gas and dust in the outflow is subject matter of this work. Based on a stationary model in spherical symmetry, the behaviour of the underlying system of equations is studied. Interactions between the gas and the dust phase are introduced by coupling terms derived from the detailed elaboration of the hydrodynamic equations. The specific conditions and the resulting difficulties for the numerical treatment of the extended system of equations are discussed.

Chapter 1

Introduction

At the end of their lives, all stars lose material in form of excessive temporally non-regular eruptions, explosive like novae or supernovae or in the form of massive winds. These materials form new stars and planets or other interplanetary bodies. Stars of spectral type K, M, S, or C, with a surface temperature lower than that of the Sun, so called Late Type Stars, are the most important source of interstellar material in the universe. The gas effusing from these stars is cold and neutral and mainly manifests as molecules. The outflow cools down by expansion and forms condensates of heavy elements at temperatures lower than 1000 K. At the moment where the temperature in the outflow is sufficiently low and the density of condensible material is high enough, its dynamics will be dominated by radiation pressure. According to the dust-composition the grains react to the stellar radiation and therefore may exhibit a large radiation pressure. The gain of momentum due to the dust driven wind is partially transferred to the surrounding gas via collisions. Observed shells around Late Type Stars are composed of condensate originating from stellar outflows in form of a dense, slow wind with potential high mass loss rates.

In general, models of physics of circumstellar envelopes treat the gas-dust complex as an entity assuming gas and dust are completely coupled by friction. Indeed, considering this coupling as not preassumed, this leads to another description of the problem. Different species and sizes of dust grains implicate different force terms due to interactions between different species and the gas as well as the radiation field due to the diverse nature of the considered material. In consequence, any model of physics of circumstellar envelopes should include the behaviour of every constituent concerning gas and dust species as well as the size of the considered dust particle. However, these effects are commonly neglected. This work deals with the feasibility of a multicomponent description, and attempts to extend the knowledge of the possibilities of modelling the outflow of AGB-stars. The purpose consists in analysing both the mathematical and technical difficulties accompanying the computation of a system of highly non-linear differential algebraic equations (DAE) in an overdetermined system. To begin with,

the applied equations are considered in the case of a stationary, spherically symmetric outflow.

In order to obtain an extensive treatise of the effects due to a multicomponent medium, the coupled system of conservation equations has to be extended by particular equations for each involved species and the subsequent resulting coupling terms. Whether the implementation of a multicomponent description is successful or the method fails, the potential of an enhancement applying the multicomponent description compared to the previous applied models must be questioned and discussed.

Dust formation in circumstellar shells of C-stars is studied by e.g. H.-P. Gail, E. Sedlmayr. They investigated the dust formation by a spherically expanding stationary flow using a wind equation which passes dust driven through the sonic point. Dust formation is devised in a modified form by using the moments of the local size distribution of the dust particles. The flow consists of one component, where dust and gas are completely coupled by friction, see e.g. [46], [48], [52], [51] [35], [100], [50], [49], [54], [98], [47], and [99]. I. Cherchneff et al. focused on the chemistry of dust condensation simulating the temperature, density, and velocity profiles of evolved stellar envelopes. They used a theoretical formalism capable of describing the average steady gas density and flow velocity, cf. [16], [17], [19], and [18].

The first investigation into the outflow in winds of evolved stars on the asymptotic giant branch (AGB) with respect to the two-fluid nature was done by D. Krüger [77]. His studies comprise the influences of interactions between gas and dust in a C-rich environment.

Several subsequent investigations deepened this subject, given that radiative acceleration of newly-formed dust grains and transfer of momentum from the dust to the gas plays an important role for driving winds of AGB-stars.

The role and effects of the gas-dust interaction on the mass loss and wind formation are studied in detail the effects of the grain drift in time dependent models by e.g. Sandin, [94], [95], [96].

Y. Simis et al. presented two-fluid time-dependent hydrodynamics in spherical symmetry with included equilibrium gas chemistry as well as grain nucleation and growth, [102].

In Chapter 2, an overview of the theoretical part is given. It comprises the hydrodynamics, the dust formation, and a short survey of radiation transfer. The treatment of hydrodynamics includes the special approach with regard to the topics of the work, i.e. the coupling between the gas and the dust phase determined by derived coupling terms. These coupling terms are deduced from the completely elaborated conservation equations of mass, motion, and energy. The section describing dust formation involves the thermodynamics, as well as the classical nucleation theory completed by the mo-

ment equations representing the local size distribution of the dust particles. The numerical treatment of the equations imports characteristics beyond the common treatment of a system of ordinary differential equations. These will be introduced in Section 2.4.

The Chapter 3 concentrates on the works with comparable aim, where coupling terms are introduced, describing interactions between gas and dust. Several examples are presented.

The purpose of this work is subject of Section 4.1. The applied equations with the fully derived terms are introduced as well as the differences from previous works. A program code for the single fluid model was developed which utilises the explicit Euler method. Subsequent, the model was extended by the multicomponent equations. Finally, the results comprise the difficulties resulting from the considered complexity of the system and the conclusion for the treatment of multicomponent fluids.

Chapter 2

Theoretical Background

An investigation of dynamical behaviour of circumstellar dust shells starts by appointing the equations to model the complex of hydrodynamics, dust formation, radiative transfer, and chemistry of the gas phase. The modeling results in a simultaneous solution of a coupled system of partial differential equations in conjunction with the equations of the dust-complex with chemistry. These equations are completed by algebraic state equations like pressure or describing material properties like opacity. Furthermore these equations depend on the temperature structure which is specified by solving the radiative transfer. The influence of multicomponent gas and dust composite on the coupled system of equations i.e. the interaction between gas and dust is expressed by coupling terms. Figure 2.1 shows the correlation diagram of the coupled problem of a dust-driven wind.

2.1 Hydrodynamics

In general, conservation of any physical quantity u may be described in the following way [1] according to the Reynolds transport theorem

$$\frac{d}{dt} \int_V u dV = - \int_{\partial V} \mathbf{f}(u) \cdot \mathbf{n} dA + \int_V g dV, \quad (2.1)$$

wherein $\mathbf{f}(u)$ denominates the flow, g the source term, V the considered volume and \mathbf{n} the normal vector of the surface A . With the *Gauss theorem*

$$\int_{\partial V} \mathbf{f}(u) \cdot \mathbf{n} dA = \int_V \nabla \cdot \mathbf{f}(u) dV, \quad (2.2)$$

equation (2.1) leads to

$$\int_V \left(\frac{\partial}{\partial t} u + \nabla \cdot \mathbf{f}(u) - g \right) dV = 0. \quad (2.3)$$

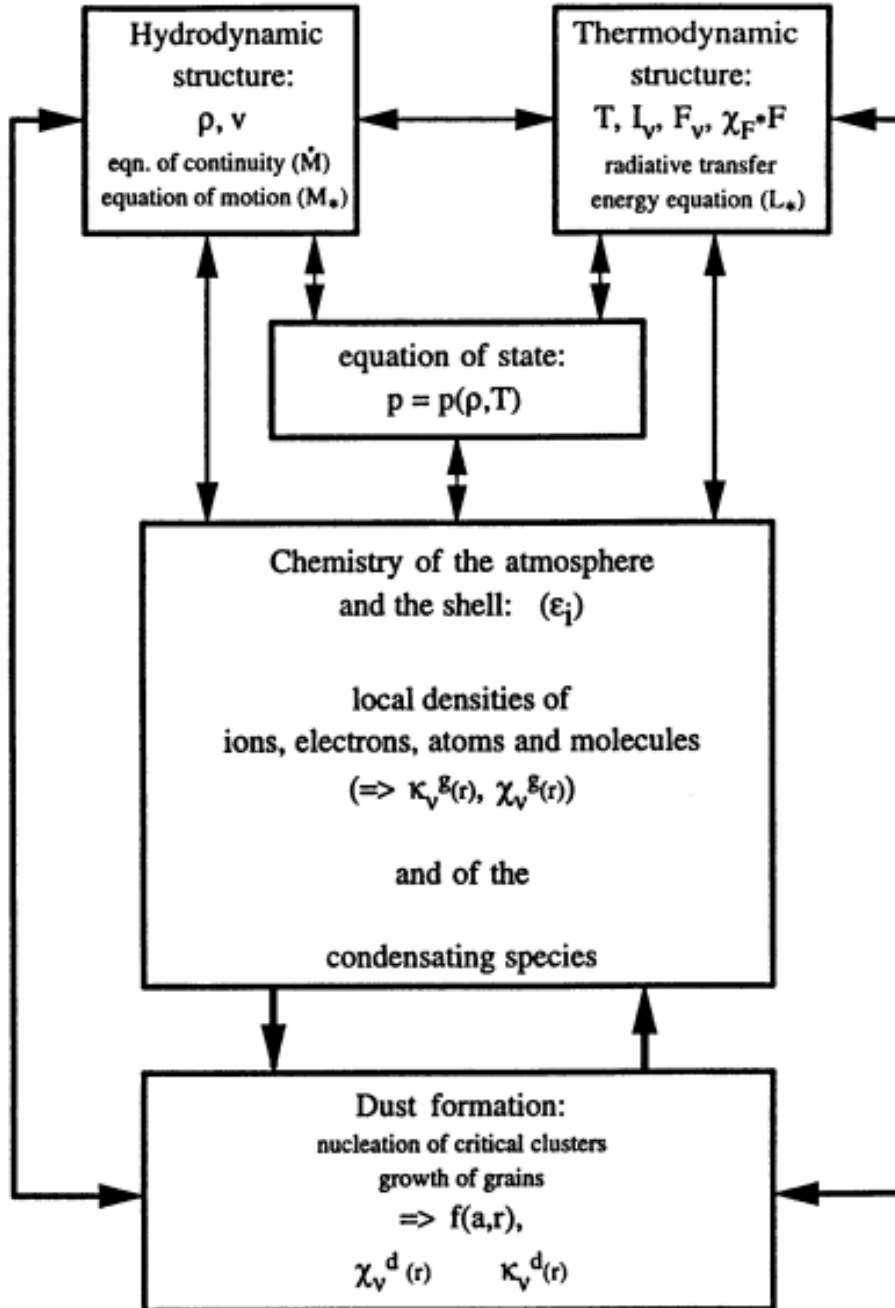


Figure 2.1: The coupled problem of a dust-driven wind (adopted from Winters et al. [109])

As this relation is valid for any arbitrary volume, the equation may be written in differential mode

$$\frac{\partial}{\partial t}u + \nabla \cdot \mathbf{f}(u) = g. \quad (2.4)$$

By neglecting viscosity, vorticity, and heat conduction, the Euler equations of gas dynamics can be applied to describe stellar outflows. The following equations describe the nonlinear conservation laws of gas dynamics in their common use. In addition of the usually applied equations, new terms are inserted, describing the interactions between the several components of the gas and the dust phase. The complete elaboration, leading to the newly derived terms is exemplarily given for the gas component in the Appendix A.

2.1.1 Equation of Continuity

The equation of continuity emanates from mass conservation after the Reynolds transport theorem. If V is a volume element of a fluid with density $\rho(t)$ the mass $m(t)$ can be obtained by integration

$$m(t) = \int_V \rho(t) dV. \quad (2.5)$$

The mass flow per unit time through an infinitesimal surface element is the mass flux density $\rho(t) \mathbf{v} d\mathbf{A}$. With $d\mathbf{A} = \mathbf{n} dA$, wherein \mathbf{n} is the normal of the surface, the equation turns into

$$\rho(t) \mathbf{v}(t) \cdot d\mathbf{A} = \rho(t) \mathbf{v}(t) \cdot \mathbf{n} dA. \quad (2.6)$$

For mass conservation it is essential that the amount of mass leaving the surface of V in direction of $\mathbf{n} dA$ is equal to the entire change of mass in the considered volume, i.e.

$$\frac{d}{dt}m(t) = \frac{d}{dt} \int_V \rho(t) dV = - \int_{\partial V} \rho(t) \mathbf{v} \cdot \mathbf{n} dA. \quad (2.7)$$

Under the condition that ρ is sufficiently smooth (e.g. derivation in terms of t being limited), the source term g equals zero and applying the differential conservation equation (2.4), mass conservation can be written as

$$\frac{\partial}{\partial t}\rho(t) + \nabla \cdot (\mathbf{v}(t)\rho(t)) = 0. \quad (2.8)$$

Taking into account time and local dependence, mass conservation takes the following form

$$\frac{\partial}{\partial t}\rho(\mathbf{r}, t) + \nabla \cdot (\mathbf{v}(\mathbf{r}, t) \rho(\mathbf{r}, t)) = 0. \quad (2.9)$$

In case of an extensive chemical mixture, following [58], the equation can be split into the main constituents namely gas and dust

$$\frac{\partial}{\partial t}\rho_g(\mathbf{r}, t) + \nabla \cdot (\mathbf{v}_g(\mathbf{r}, t) \rho_g(\mathbf{r}, t)) = q_g(\mathbf{r}, t), \quad (2.10)$$

$$\frac{\partial}{\partial t} \rho_d(\mathbf{r}, t) + \nabla \cdot (\mathbf{v}_d(\mathbf{r}, t) \rho_d(\mathbf{r}, t)) = q_d(\mathbf{r}, t). \quad (2.11)$$

The exchange terms q mean that condensation leads to a depletion of condensible material in the gas component and to an increase of condensed material of the dust component. This has to be taken into consideration by solving the mass conservation equations. With the homogeneous nucleation rate J_* (2.120), (2.126) the exchange term describing the depletion of condensible material in the gas component is the following mass flux density

$$q_g(\mathbf{r}, t) = -J_*(\mathbf{r}, t)m_d, \quad (2.12)$$

where m_d is the mass of the cluster of the condensed material, expressed by the volume density of the considered dust species multiplied by the average particle volume of the cluster as given in equation (2.128)). On the other hand, condensed material equals to a depletion of condensible material. This leads to

$$q_d(\mathbf{r}, t) = -q_g(\mathbf{r}, t) = J_*(\mathbf{r}, t)m_d. \quad (2.13)$$

At last, the equations may be written as a sum over all their components, with m , the mass of the considered species and n , its number density in the flow. Each gas species is labeled by i , between 1 and I , each dust species by β and each species β , between 1 and B , is also subdivided by its size α between 1 and A^β , the biggest size bin of the species β . Thus,

$$\sum_{i=1}^I m_g^i n_g^i(\mathbf{r}, t) = \rho_g(\mathbf{r}, t) \quad (2.14)$$

and

$$\sum_{\beta=1}^B \sum_{\alpha=1}^{A^\beta} m_d^\beta(a^\alpha) n_d^{\beta,\alpha}(\mathbf{r}, t) = \rho_d(\mathbf{r}, t), \quad (2.15)$$

where a^α is the radius of the grain of size α , assumed to be of spherical shape.

Every component can be considered individually with respect to the dependency of time t and location r . So, for each gas component i the mass conservation equation gives

$$\frac{\partial}{\partial t} m_g^i n_g^i(\mathbf{r}, t) + \nabla \cdot (m_g^i n_g^i(\mathbf{r}, t) \mathbf{v}^i(\mathbf{r}, t)) = q_g^i(\mathbf{r}, t). \quad (2.16)$$

And for the dust components β with respect to the size α one obtains:

$$\begin{aligned} & \frac{\partial}{\partial t} m_d^\beta(a^\alpha) n_d^{\beta,\alpha}(\mathbf{r}, t) + \\ & \nabla \cdot (m_d^\beta(a^\alpha) n_d^{\beta,\alpha}(\mathbf{r}, t) \mathbf{v}^{\beta,\alpha}(\mathbf{r}, t)) = q_d^{\beta,\alpha}(\mathbf{r}, t), \end{aligned} \quad (2.17)$$

with

$$\sum_{i=1}^I q_g^i + \sum_{\beta=1}^B \sum_{\alpha=1}^{A^\beta} q_d^{\beta,\alpha} = 0. \quad (2.18)$$

The exchange terms q_g^i , and $q_d^{\beta,\alpha}$ represent not only the exchange between gas and dust, but also the exchange among several gas species and/or several dust species and/or dust grain sizes.

2.1.2 Conservation of Momentum

The source terms of the equation of motion are in general the radiative and gravitational acceleration. In order to set up an equation of motion for both gas and dust, interactions between the two components of the fluid as well as the source terms have to be described.

2.1.2.1 The Drag Force

Gas and dust particles exchange momentum as a result of collisions between the several components. The momentum gain of the gas particles after a collision with a grain spreads to other gas particles by subsequent random thermal collisions with other gas particles. So, the momentum gain of the gas phase acts on the entire gas. The momentum loss of the dust grains acts as a frictional force on individual dust grains. This causes a deceleration of their relative motion with respect to the gas phase.

The discrete nature of the momentum exchange process induces tiny random velocity changes of the grains due to the Brownian motion. In a circumstellar environment, the density of dust particles is not large enough to lead to a significant number of dust-dust collisions due to Brownian motion. So, irregular motions superposed on the average motion of the dust grains are negligible in most cases. Further, non-central collisions between gas particles and a dust particle may provide a torque on the grain in addition to momentum change. The description of the drag forces bases on [58]. The drag force is a volume force as a consequence of frictional coupling between dust and gas components with significant relative motions between the radiation pressure driven grains and the gas particles. The drag force measures the momentum transfer from the dust components to the gas. Therefore, it has to be added in the equation of motion for the gas and subtracted in the equations of motion for the dust components. The drag force is related to the different frictional situations of surface interaction of gas and dust particles. The following specifications describe the transfer of momentum by sticking, thermal accommodation, and specular or diffuse reflection. Considering collisions, the description depends on a couple of factors as it involves the masses of the colliding particles, the collision frequency, and the velocities of each considered component as well as the ratio between the drift velocity and the thermal velocity. In the following, the drag force will be introduced under the assumption that only one kind of gas phase species is present. If the gas phase is a mixture of different species, the entire drag force has to be determined by summing up the several drag forces for all the involved species. The applied terms to determine the drag forces are:

- πa^2 : the cross section area of the involved dust species with the corresponding radius a ,
- n_g and n_d : the number densities of the considered gas and dust species,
- k_B : the Boltzmann constant,
- T_g and T_d : the gas and dust temperatures,
- m_d : the mass of a grain of the considered dust species,
- m_g : the mean mass of a gas particle, expressed by the individual particle masses of the different gas species i and their respective mass fractions γ_g^i

$$m_g = \left(\sum_{i=1}^I \frac{\gamma_g^i}{m_g^i} \right)^{-1}, \quad (2.19)$$

- $\mathbf{v}_{\text{drift}}$, the drift velocity of the dust with respect to the gas phase

$$\mathbf{v}_{\text{drift}}(\mathbf{r}, t) = \mathbf{v}_d(\mathbf{r}, t) - \mathbf{v}_g(\mathbf{r}, t), \quad (2.20)$$

- and \mathbf{S} : the ratio between the drift velocity and the thermal velocity

$$\mathbf{S} = v_{\text{drift}}/v_{\text{th}}, \quad (2.21)$$

with the thermal velocity

$$v_{\text{th}} = \sqrt{\frac{2k_B T_g}{m_g}} \quad (2.22)$$

Specular Reflection

If the interaction time between the gas particle and the surface atoms of the dust particles is short, a collision results only in elastic scattering. The drag force caused by specular reflection is represented by the following equation

$$\mathbf{f}_{\text{drag,specular}} = \left(\frac{64}{9\pi} + \mathbf{S}^2 \right)^{1/2} \pi a^2 n_d(a) \frac{m_g m_d}{m_g + m_d} n_g v_{\text{th}} \mathbf{v}_{\text{drift}}. \quad (2.23)$$

Diffuse Reflection

If impinging gas particles are reflected from a dust grain surface with a microscopic roughness, they return from the grain's surface with a velocity obeying a comoving Maxwellian distribution function. So the drag force due to diffuse reflection can be written as

$$\mathbf{f}_{\text{drag,diffuse}} = \left(\frac{16}{3\pi} + \mathbf{S}^2 \right)^{1/2} \pi a^2 n_d(a) m_g n_g v_{\text{th}} \mathbf{v}_{\text{drift}}. \quad (2.24)$$

Sticking

The growth of particles bases on impinging gas particles which are not reflected. The particle sticking would be important for momentum exchange (expressed by the correspondent drag force) between the gas and dust component

$$\mathbf{f}_{\text{drag,sticking}} = \left(\frac{4}{\pi} + \mathbf{S}^2 \right)^{1/2} \pi a^2 n_d(a) \frac{m_g m_d}{m_g + m_d} n_g \mathbf{v}_{\text{drift}} \quad (2.25)$$

Thermal Accomodation

Impinging gas particles do not permanently stick on the surface of the grain. Just like for the diffuse reflection, they return to the gas phase after a period of adsorption to the surface with a velocity obeying a comoving Maxwellian distribution function. The temperature of the grains T_d may be different from the gas kinetic temperature T_g of the gas particles. Therefore the drag force by thermal accomodation follows as

$$\mathbf{f}_{\text{drag,acc}} = \left(\frac{4}{\pi} \left(1 + \frac{1}{3} \sqrt{\frac{T_d}{T_g}} \right)^2 + \mathbf{S}^2 \right)^{1/2} \pi a^2 n_d(a) m_g n_g v_{\text{th}} \mathbf{v}_{\text{drift}}. \quad (2.26)$$

More details can be found in *Physics and Chemistry of Circumstellar Dust Shells* by H.P. Gail and E. Sedlmayr [58].

The drag force applied in this work follows Draine [31] and will be discussed in Section 3.1.

2.1.2.2 Equation of Motion

Following the Reynolds transport theorem, the equation of conservation of momentum is based on the equation (2.4):

$$\frac{\partial}{\partial t} (\rho(\mathbf{r}, t) \mathbf{v}(\mathbf{r}, t)) + \nabla \cdot ((\rho(\mathbf{r}, t) \mathbf{v}(\mathbf{r}, t)) \otimes \mathbf{v}(\mathbf{r}, t)) = -\nabla \cdot p_g(\mathbf{r}, t) + \mathbf{f}_{\text{rad}}(\mathbf{r}, t) - \mathbf{f}_{\text{grav}}(\mathbf{r}, t). \quad (2.27)$$

Therein p_g represents the scalar part of the symmetric pressure tensor (the considered densities are small) and $\mathbf{v}(\mathbf{r}, t) \otimes \mathbf{v}(\mathbf{r}, t)$ denominates the dyadic product of the velocities.

$$\mathbf{f}_{\text{grav}}(\mathbf{r}, t) = \rho(\mathbf{r}, t) \mathbf{g}(\mathbf{r}, t) \quad (2.28)$$

represents the external force per volume influencing the exposed material due to a gravitational acceleration \mathbf{g} directed inwards.

$$\mathbf{f}_{\text{rad}}(\mathbf{r}, t) = \frac{1}{c} \int_0^\infty \xi_\nu(\mathbf{r}, t) \mathbf{F}_\nu(\mathbf{r}, t) d\nu \quad (2.29)$$

represents the external force per volume as a radiative acceleration directed outwards due to the influence of the local spectral radiative momentum flux $(1/c)\mathbf{F}_\nu$. The extinction of radiation is expressed by the momentum transfer coefficient ξ_ν . In general, all external forces per volume are vectored.

Considering complete coupling between the gas and dust component (one-fluid approach), conservation of momentum changes after subtraction of the equation for conservation of mass to

$$\rho(\mathbf{r}, t) \left(\frac{\partial}{\partial t} \mathbf{v}(\mathbf{r}, t) + (\mathbf{v}(\mathbf{r}, t) \cdot \nabla) \mathbf{v}(\mathbf{r}, t) \right) = -\nabla \cdot p_g(\mathbf{r}, t) + \mathbf{f}_{\text{rad}}(\mathbf{r}, t) - \mathbf{f}_{\text{grav}}(\mathbf{r}, t). \quad (2.30)$$

Just as with mass conservation, in case of an extensive chemical mixture, the equation can be split into their constituents gas and dust, with m , the mass of the considered species, n , its number density in the flow. Taking into account the interactions between the two phases of the fluid, a new source term has to be added, namely the drag force. The drag force \mathbf{f}_{drag} has to be considered here as the sum of the different frictional situations of possible processes of surface interaction of gas and dust particles.

With these requirements the equation of motion for the gas turns into

$$\begin{aligned} \frac{\partial}{\partial t} (\rho_g(\mathbf{r}, t) \mathbf{v}_g(\mathbf{r}, t)) + \nabla \cdot (\rho_g(\mathbf{r}, t) \mathbf{v}_g(\mathbf{r}, t) \otimes \mathbf{v}_g(\mathbf{r}, t)) = \\ -\nabla \cdot p_g(\mathbf{r}, t) + \mathbf{f}_{g,\text{rad}}(\mathbf{r}, t) - \mathbf{f}_{g,\text{grav}}(\mathbf{r}, t) + \mathbf{f}_{\text{drag}}(\mathbf{r}, t) \end{aligned} \quad (2.31)$$

and for the dust follows

$$\begin{aligned} \frac{\partial}{\partial t} (\rho_d(\mathbf{r}, t) \mathbf{v}_d(\mathbf{r}, t)) + \nabla \cdot (\rho_d(\mathbf{r}, t) \mathbf{v}_d(\mathbf{r}, t) \otimes \mathbf{v}_d(\mathbf{r}, t)) = \\ \mathbf{f}_{d,\text{rad}}(\mathbf{r}, t) - \mathbf{f}_{d,\text{grav}}(\mathbf{r}, t) - \mathbf{f}_{\text{drag}}(\mathbf{r}, t). \end{aligned} \quad (2.32)$$

Then, using equation (2.10), the equation of motion for the gas component turns after subtraction of the corresponding equation of mass conservation into

$$\begin{aligned} \rho_g(\mathbf{r}, t) \left(\frac{\partial}{\partial t} \mathbf{v}_g(\mathbf{r}, t) + (\mathbf{v}_g(\mathbf{r}, t) \cdot \nabla) \mathbf{v}_g(\mathbf{r}, t) \right) = \\ -\nabla \cdot p_g(\mathbf{r}, t) + \mathbf{f}_{g,\text{rad}}(\mathbf{r}, t) - \mathbf{f}_{g,\text{grav}}(\mathbf{r}, t) + \mathbf{f}_{g,\text{drag}}(\mathbf{r}, t) - \mathbf{v}_g(\mathbf{r}, t) q_g(\mathbf{r}, t) \\ = -\nabla \cdot p_g(\mathbf{r}, t) + \mathbf{f}_{g,\text{rad}}(\mathbf{r}, t) - \mathbf{f}_{g,\text{grav}}(\mathbf{r}, t) + \mathbf{f}_{g,\text{drag}}(\mathbf{r}, t) - \mathbf{q}_{g,\text{acc}}(\mathbf{r}, t) \end{aligned} \quad (2.33)$$

with

$$\mathbf{q}_{g,\text{acc}} = \mathbf{v}_g(\mathbf{r}, t) q_g(\mathbf{r}, t) = -J_*(\mathbf{r}, t) m_d \mathbf{v}_g(\mathbf{r}, t) \quad (2.34)$$

(see equation (2.12)). Therefore, $-q_g(\mathbf{r}, t) = J_*(\mathbf{r}, t) m_d$ leads to a gain of momentum for the gas phase.

Using (2.11), the equation of motion of the dust turns into

$$\rho_d(\mathbf{r}, t) \left(\frac{\partial}{\partial t} \mathbf{v}_d(\mathbf{r}, t) + (\mathbf{v}_d(\mathbf{r}, t) \cdot \nabla) \mathbf{v}_d(\mathbf{r}, t) \right) =$$

$$\begin{aligned}
& \mathbf{f}_{d,\text{rad}}(\mathbf{r}, t) - \mathbf{f}_{d,\text{grav}}(\mathbf{r}, t) - \mathbf{f}_{d,\text{drag}}(\mathbf{r}, t) - \mathbf{v}_d(\mathbf{r}, t)q_d(\mathbf{r}, t) \\
& = \mathbf{f}_{d,\text{rad}}(\mathbf{r}, t) - \mathbf{f}_{d,\text{grav}}(\mathbf{r}, t) - \mathbf{f}_{d,\text{drag}}(\mathbf{r}, t) - \mathbf{q}_{d,\text{acc}}(\mathbf{r}, t)
\end{aligned} \tag{2.35}$$

with

$$\mathbf{q}_{d,\text{acc}} = \mathbf{v}_d(\mathbf{r}, t)q_d(\mathbf{r}, t) = J_*(\mathbf{r}, t)m_d\mathbf{v}_d(\mathbf{r}, t) \tag{2.36}$$

(see equation (2.13)). For the dust, the expression $q_d(\mathbf{r}, t)$ leads to a loss of momentum towards the gas phase.

So, the newly derived remanents $\mathbf{q}_{\text{acc},g,d}$ are due to the added source term in the mass conservation equation, and represent the gain or loss of momentum from the one to the other phase as a consequence of particle growth by gas-dust collisions and take into account the velocity of impinging. Even though interactions between gas and dust by adsorption are included in the drag force term.

With respect to different species of gas and dust, each one with a specific size, the equations change into one equation for each species i, β , and size α , with $m_{g,d}$, the mass of the considered species, and $n_{g,d}$, its number density in the flow. Just as with the equations of mass conservation (equations (2.14), (2.15)), the equations (2.33), (2.35) turn into

$$\begin{aligned}
& m_g^i n_g^i(\mathbf{r}, t) \left(\frac{\partial}{\partial t} \mathbf{v}_g^i(\mathbf{r}, t) + (\mathbf{v}_g^i(\mathbf{r}, t) \cdot \nabla) \mathbf{v}_g^i(\mathbf{r}, t) \right) + \nabla \cdot p_g^i(\mathbf{r}, t) \\
& = \mathbf{f}_{g,\text{rad}}^i(\mathbf{r}, t) - \mathbf{f}_{g,\text{grav}}^i(\mathbf{r}, t) + \mathbf{f}_{g,\text{drag}}^i(\mathbf{r}, t) - \mathbf{q}_{g,\text{acc}}^i(\mathbf{r}, t)
\end{aligned} \tag{2.37}$$

and

$$\begin{aligned}
& m_d^{\beta,\alpha} n_d^{\beta,\alpha}(\mathbf{r}, t) \left(\frac{\partial}{\partial t} \mathbf{v}_d^{\beta,\alpha}(\mathbf{r}, t) + (\mathbf{v}_d^{\beta,\alpha}(\mathbf{r}, t) \cdot \nabla) \mathbf{v}_d^{\beta,\alpha}(\mathbf{r}, t) \right) \\
& = \mathbf{f}_{d,\text{rad}}^{\beta,\alpha}(\mathbf{r}, t) - \mathbf{f}_{d,\text{grav}}^{\beta,\alpha}(\mathbf{r}, t) - \mathbf{f}_{d,\text{drag}}^{\beta,\alpha}(\mathbf{r}, t) \\
& \quad - \mathbf{q}_{d,\text{acc}}^{\beta,\alpha}(\mathbf{r}, t).
\end{aligned} \tag{2.38}$$

As for the equations of mass conservation, the momentum exchange terms $\mathbf{q}_{\text{acc},g}^i$, respectively $\mathbf{q}_{\text{acc},d}^{\beta,\alpha}$ represent not only the exchange between gas and dust, but also the exchange among the several gas species and/or the several dust species and/or the dust grain sizes.

In case of assumed spherical symmetry, the system of coupled equations is reduced to a system of one spatial coordinate r . Therefore, the gravitational acceleration $M_r G/r^2$ affecting the gas or dust particles with G , the gravitational constant and M_r , the attracting mass at the radial position r , leads to

$$f_{\text{grav}}(r, t) = \frac{M_r G}{r^2} \rho(r, t) \tag{2.39}$$

and

$$f_{\text{rad}}(r, t) = \frac{4 \pi}{c} \int_0^{\infty} \chi_{\nu} H_{\nu} d\nu \quad (2.40)$$

with c , the speed of light, $H = \int_0^{\infty} \chi_{\nu} H_{\nu} d\nu$, the integrated Eddington flux over all frequencies ν , and χ_{ν} , the opacities of the gas or dust species. In the case of radiative equilibrium (RE), with $4 \pi H = L_{\star}/(4 \pi r^2)$, the external force due to the radiative acceleration turns to

$$f_{\text{rad}} = \frac{L_{\star}}{4 \pi c r^2} \chi_{\text{H}}, \quad (2.41)$$

with the flux weighted mean opacity χ_{H} .

2.1.3 Conservation of Energy

The equation of conservation of energy follows the Reynolds transport theorem, based on the equation (2.4). In this case, the parameter u is represented by the energy density of the matter per unit mass, consisting of the specific energy e and the specific local kinetic energy $e_{\text{kin}} = \frac{1}{2}v^2$ of the hydrodynamical fluid, multiplied by mass density ρ

$$\begin{aligned} & \frac{\partial}{\partial t} \left[\rho(\mathbf{r}, t) \left(e(\mathbf{r}, t) + \frac{1}{2}v^2(\mathbf{r}, t) \right) \right] + \\ & \nabla \cdot \left[\rho(\mathbf{r}, t) \left(e(\mathbf{r}, t) + \frac{1}{2}v^2(\mathbf{r}, t) \right) \mathbf{v}(\mathbf{r}, t) + p(\mathbf{r}, t)\mathbf{v}(\mathbf{r}, t) \right] = Q_{\text{rad}}(\mathbf{r}, t). \end{aligned} \quad (2.42)$$

The local energy input rate to the internal states of the matter due to absorption and inelastic scattering of photons, and for the energy loss due to emission of photons is expressed by the radiative net energy source term Q_{rad} . This term provides also an immediate energy transfer to the thermal pool of matter.

The specific energy e consists of the thermal energy from random particle motion, the internal energy expressed by the internal degrees of freedom, the latent chemical energy and the kinetic energy due to relative motions of the different components.

The behaviour of the inner energy e can be obtained by scalar multiplication of the equation of motion (2.30) with \mathbf{v} and subsequent subtraction of these equation and of the replaced mass conservation equation (2.9) from the equation (2.42). In the context of cool dust forming circumstellar shells $Q_{\text{rad}}(\mathbf{r}, t) = Q_{\text{rad, int}}(\mathbf{r}, t)$ does apply. Radiative cooling or heating concerns only the internal state of matter. $Q_{\text{rad, int}}(\mathbf{r}, t)$ describes the net loss rate of energy of the radiation field due to these processes

$$\begin{aligned} & \rho(\mathbf{r}, t) \left(\frac{\partial}{\partial t} e(\mathbf{r}, t) + \mathbf{v}(\mathbf{r}, t) \cdot \nabla e(\mathbf{r}, t) \right) + p(\mathbf{r}, t) \nabla \cdot \mathbf{v}(\mathbf{r}, t) = \\ & \mathbf{v}(\mathbf{r}, t) \cdot \mathbf{f}_{\text{grav}}(\mathbf{r}, t) - \mathbf{v}(\mathbf{r}, t) \cdot \mathbf{f}_{\text{rad}}(\mathbf{r}, t) + Q_{\text{rad, int}}(\mathbf{r}, t) = Q(\mathbf{r}, t) + Q_{\text{rad, int}}(\mathbf{r}, t). \end{aligned} \quad (2.43)$$

The notations (2.42), (2.43) describe the one-fluid conservation equation of energy. The rate $Q(\mathbf{r}, t)$ is derived on the basis of the remnants by scalar multiplication of the complete equation of motion. It represents the mechanical power density due to the work performed by the external forces such as gravity and the force due to radiative acceleration. Therein \mathbf{f}_{grav} and \mathbf{f}_{rad} are the vectored volume forces acting on a considered species and its corresponding hydrodynamic velocity, i.e.

$$Q(\mathbf{r}, t) = Q_{\text{grav}}(\mathbf{r}, t) - Q_{\text{kin,rad}}(\mathbf{r}, t) = \mathbf{v}(\mathbf{r}, t) \cdot \mathbf{f}_{\text{grav}} - \mathbf{v}(\mathbf{r}, t) \cdot \mathbf{f}_{\text{rad}}. \quad (2.44)$$

These terms are valid for both one-fluid descriptions and multicomponent fluid descriptions, each with a corresponding index for gas or dust.

In order to consider an extensive chemical mixture, the equation can be split in its constituents gas and dust, which reads

$$\begin{aligned} & \frac{\partial}{\partial t} \left[\rho_{\text{g}}(\mathbf{r}, t) \left(e_{\text{g}}(\mathbf{r}, t) + \frac{1}{2} v_{\text{g}}^2(\mathbf{r}, t) \right) \right] + \\ \nabla \cdot & \left[\rho_{\text{g}}(\mathbf{r}, t) \left((e_{\text{g}}(\mathbf{r}, t) + \frac{1}{2} v_{\text{g}}^2(\mathbf{r}, t)) \mathbf{v}_{\text{g}}(\mathbf{r}, t) + p_{\text{g}}(\mathbf{r}, t) \mathbf{v}_{\text{g}}(\mathbf{r}, t) \right) \right] = Q_{\text{rad,int,g}}(\mathbf{r}, t). \end{aligned} \quad (2.45)$$

and

$$\begin{aligned} & \frac{\partial}{\partial t} \left[\rho_{\text{d}}(\mathbf{r}, t) \left(e_{\text{d}}(\mathbf{r}, t) + \frac{1}{2} v_{\text{d}}^2(\mathbf{r}, t) \right) \right] + \\ \nabla \cdot & \left[\rho_{\text{d}}(\mathbf{r}, t) \left((e_{\text{d}}(\mathbf{r}, t) + \frac{1}{2} v_{\text{d}}^2(\mathbf{r}, t)) \mathbf{v}_{\text{d}}(\mathbf{r}, t) \right) \right] = Q_{\text{rad,int,d}}(\mathbf{r}, t). \end{aligned} \quad (2.46)$$

The equation of conservation of the inner energy $e_{\text{g,d}}$ results in

$$\begin{aligned} & \rho_{\text{g}}(\mathbf{r}, t) \left(\frac{\partial}{\partial t} e_{\text{g}}(\mathbf{r}, t) + \mathbf{v}_{\text{g}}(\mathbf{r}, t) \cdot \nabla e_{\text{g}}(\mathbf{r}, t) \right) \\ = & - p_{\text{g}}(\mathbf{r}, t) \nabla \cdot \mathbf{v}_{\text{g}}(\mathbf{r}, t) - \mathbf{v}(\mathbf{r}, t)_{\text{g}} \cdot \mathbf{f}_{\text{drag}}(\mathbf{r}, t) + \mathbf{v}(\mathbf{r}, t)_{\text{g}} \cdot \mathbf{f}_{\text{g,grav}}(\mathbf{r}, t) - \mathbf{v}(\mathbf{r}, t)_{\text{g}} \cdot \mathbf{f}_{\text{rad,g}}(\mathbf{r}, t) \\ & - q_{\text{g}}(\mathbf{r}, t) \frac{1}{2} v_{\text{g}}^2(\mathbf{r}, t) - q_{\text{g}}(\mathbf{r}, t) e_{\text{g}}(\mathbf{r}, t) + Q_{\text{rad,int,g}}(\mathbf{r}, t) \\ = & - p_{\text{g}}(\mathbf{r}, t) \nabla \cdot \mathbf{v}_{\text{g}}(\mathbf{r}, t) - Q_{\text{drag,g}}(\mathbf{r}, t) + Q_{\text{grav,g}}(\mathbf{r}, t) - Q_{\text{rad,g}}(\mathbf{r}, t) \\ & - Q_{\text{kin,g}}(\mathbf{r}, t) - Q_{\text{int,g}} + Q_{\text{rad,int,g}}(\mathbf{r}, t) \end{aligned} \quad (2.47)$$

and

$$\begin{aligned} & \rho_{\text{d}}(\mathbf{r}, t) \left(\frac{\partial}{\partial t} e_{\text{d}}(\mathbf{r}, t) + \mathbf{v}_{\text{d}}(\mathbf{r}, t) \cdot \nabla e_{\text{d}}(\mathbf{r}, t) \right) \\ = & - \mathbf{v}(\mathbf{r}, t)_{\text{d}} \cdot \mathbf{f}_{\text{drag}}(\mathbf{r}, t) + \mathbf{v}(\mathbf{r}, t)_{\text{d}} \cdot \mathbf{f}_{\text{d,grav}}(\mathbf{r}, t) - \mathbf{v}(\mathbf{r}, t)_{\text{d}} \cdot \mathbf{f}_{\text{rad,d}}(\mathbf{r}, t) \\ & - q_{\text{d}}(\mathbf{r}, t) \frac{1}{2} v_{\text{d}}^2(\mathbf{r}, t) - q_{\text{d}}(\mathbf{r}, t) e_{\text{d}}(\mathbf{r}, t) + Q_{\text{rad,int,d}}(\mathbf{r}, t) \\ = & - Q_{\text{drag,d}}(\mathbf{r}, t) + Q_{\text{grav,d}}(\mathbf{r}, t) \\ & - Q_{\text{rad,d}}(\mathbf{r}, t) - Q_{\text{kin,d}}(\mathbf{r}, t) - Q_{\text{int,d}}(\mathbf{r}, t) + Q_{\text{rad,int,d}}(\mathbf{r}, t). \end{aligned} \quad (2.48)$$

Therein, the part of the equation represented by the equations of motion for the gas component (2.31) and for the dust component (2.32), scalar multiplied with $\mathbf{v}_{\text{g,d}}$, are replaced by their results. And in the same manner, the part of the equation that is represented by the mass conservation equations of gas (2.10) and dust (2.11) is replaced by the corresponding source terms. The term $Q_{\text{rad,int}}(\mathbf{r}, t)$ describing the radiative energy transfer from the internal states of the matter to the radiation field is represented by

$$Q_{\text{rad,int}}(\mathbf{r}, t) = 4\pi \int_0^\infty [\hat{\kappa}_\nu J_\nu - \eta_\nu^{\text{SP}}] d\nu, \quad (2.49)$$

with the isotropic spontaneous emission coefficient η_ν^{SP} , the net absorption coefficient $\hat{\kappa}_\nu$, and the mean spectral intensity J_ν .

The newly derived remanents of the subtraction of the equations of mass and momentum conservation in the case of extensive mixture of components lead to a series of terms besides these of the one-fluid description (see (2.43)). They result from the added source terms in the mass conservation equation and therefore the added and derived source terms by treatment of the equation of motion. The remanents introduce external energy source terms represented by the rates Q .

The term $Q_{\text{drag}}(\mathbf{r}, t)$ originates from the remanents of the equation of motion. Therein,

$$Q_{\text{drag}}(\mathbf{r}, t) = \mathbf{v}(\mathbf{r}, t)_{\text{g,d}} \cdot \mathbf{f}_{\text{drag}}(\mathbf{r}, t) \quad (2.50)$$

stands for the volume drag force acting on its corresponding hydrodynamic velocity. This volume force involves the difference of the velocities of the gas and the dust component, multiplied by the velocity of the considered species.

The terms

$$Q_{\text{kin,g}}(\mathbf{r}, t) = q_{\text{g}}(\mathbf{r}, t) \frac{1}{2} v_{\text{g}}^2(\mathbf{r}, t) = -\frac{1}{2} v_{\text{g}}^2(\mathbf{r}, t) J_*(\mathbf{r}, t) m_{\text{d}}, \quad (2.51)$$

respectively

$$Q_{\text{kin,d}}(\mathbf{r}, t) = q_{\text{d}}(\mathbf{r}, t) \frac{1}{2} v_{\text{d}}^2(\mathbf{r}, t) = \frac{1}{2} v_{\text{d}}^2(\mathbf{r}, t) J_*(\mathbf{r}, t) m_{\text{d}} \quad (2.52)$$

with (2.12) and (2.13) are the collisional gain and loss of kinetic energy of the gas or the dust phase due to the mass flux density by newly formed grains, respectively. Also for the inner energy e the collisional gain or loss leads to the equations

$$Q_{\text{int,g}}(\mathbf{r}, t) = q_{\text{g}}(\mathbf{r}, t) e_{\text{g}}(\mathbf{r}, t) = -J_*(\mathbf{r}, t) m_{\text{d}} e_{\text{g}}(\mathbf{r}, t), \quad (2.53)$$

$$Q_{\text{int,d}}(\mathbf{r}, t) = q_{\text{d}}(\mathbf{r}, t) e_{\text{d}}(\mathbf{r}, t) = J_*(\mathbf{r}, t) m_{\text{d}} e_{\text{g}}(\mathbf{r}, t). \quad (2.54)$$

Due to the mass flux density of newly formed grains, this term may represent the exchange of inner energy by condensation or growth (e_{th}) and excitation or deexcitation of internal states (e_{int}). Approaches, whether several terms may be replaced by simplified assumptions, may be found in [58].

In addition, to specify the extensive mixture of components, the equations may be split

into their constituents where each one has its own specific size. The equations change into equations for each species i, β , and size α as well as for momentum conservation. Therein $m_{\mathbf{g},\mathbf{d}}$ represents the mass of the considered species, whereas $n_{\mathbf{g},\mathbf{d}}$ represents its number density in the flow. Thus, the equations turn into

$$\begin{aligned}
& m_{\mathbf{g}}^i n_{\mathbf{g}}^i(\mathbf{r}, t) \frac{\partial}{\partial t} e_{\mathbf{g}}^i(\mathbf{r}, t) + m_{\mathbf{g}}^i n_{\mathbf{g}}^i(\mathbf{r}, t) \mathbf{v}_{\mathbf{g}}^i(\mathbf{r}, t) \cdot \nabla e_{\mathbf{g}}^i(\mathbf{r}, t) \\
&= - p_{\mathbf{g}}^i(\mathbf{r}, t) \nabla \cdot \mathbf{v}_{\mathbf{g}}^i(\mathbf{r}, t) + Q_{\text{drag},\mathbf{g}}^i(\mathbf{r}, t) - Q_{\text{grav},\mathbf{g}}^i(\mathbf{r}, t) \\
&+ Q_{\text{rad},\mathbf{g}}^i(\mathbf{r}, t) - Q_{\text{kin},\mathbf{g}}^i(\mathbf{r}, t) - Q_{\text{int},\mathbf{g}}^i(\mathbf{r}, t) + Q_{\text{rad,int},\mathbf{g}}^i(\mathbf{r}, t)
\end{aligned} \tag{2.55}$$

and

$$\begin{aligned}
& m_{\mathbf{d}}^{\beta,\alpha} n_{\mathbf{d}}^{\beta,\alpha}(\mathbf{r}, t) \frac{\partial}{\partial t} e_{\mathbf{d}}^{\beta,\alpha}(\mathbf{r}, t) + m_{\mathbf{d}}^{\beta,\alpha} n_{\mathbf{d}}^{\beta,\alpha}(\mathbf{r}, t) \mathbf{v}_{\mathbf{d}}^{\beta,\alpha}(\mathbf{r}, t) \cdot \nabla e_{\mathbf{d}}^{\beta,\alpha}(\mathbf{r}, t) = \\
& - Q_{\text{drag},\mathbf{d}}^{\beta,\alpha}(\mathbf{r}, t) + Q_{\text{grav},\mathbf{d}}^{\beta,\alpha}(\mathbf{r}, t) - Q_{\text{rad},\mathbf{d}}^{\beta,\alpha}(\mathbf{r}, t) - Q_{\text{kin},\mathbf{d}}^{\beta,\alpha}(\mathbf{r}, t) - Q_{\text{int},\mathbf{d}}^{\beta,\alpha}(\mathbf{r}, t) + Q_{\text{rad,int},\mathbf{d}}^{\beta,\alpha}(\mathbf{r}, t).
\end{aligned} \tag{2.56}$$

2.1.3.1 Temperature Equations

In order to complete the equations of energy conservation, the temperature equations follow [58]. The inner energy density e is an extensive quantity, resulting from the addition of the different energy reservoirs, i.e.

$$e = e_{\text{th}} + e_{\text{int}} + e_{\text{ch}} + e_{\text{rel}}. \tag{2.57}$$

In order to take into account the different species along the multicomponent description of the fluid, the inner energy density e has to be separated into particular reservoirs coupled by exchange terms among these inner energy reservoirs. The inner energy reservoir e_{th} includes coupling terms due to kinetic collisional heating, and therefore chemical heating by nucleation or growth. Inelastic collisions between the several species and particles also provide the excitation of internal states and deexcitation of excited states of particles of each species e_{int} just like nucleation or growth of dust particles, so that by collision nucleation and growth lead to exchange among the reservoirs by coupling terms. The same consideration applies to the latent chemical inner energy density e_{ch} . The coupling terms describe the net release of latent heat by chemical exothermic or endothermic reaction r producing species i . Latent chemical energy becomes relevant only when a large number of species is involved, and when chemical reactions contribute to the inner energy reservoir, e.g. H_2 -formation or dissociation. Usually latent chemical energy does not play a significant role in cool dust forming circumstellar shells, but rather in the shells of WR- or WC-stars. Assuming the emerging primary clusters

exhibit behaviour like large molecules and do not have noticeable diffusion or drift velocities relative to the bulk of gas, the energy density from relative motion e_{rel} is set equal to zero. With these restrictions, the inner energy density e contains the energy reservoirs e_{th} and e_{int} , so that the equation turns into

$$e = e_{\text{th}} + e_{\text{int}}. \quad (2.58)$$

Even though several energy reservoirs have to be treated almost like open systems, the internal relaxation to partial equilibrium proceeds much faster in each reservoir than between different reservoirs. So, in lowest order approximation, each single reservoir may be considered as being energetically closed, and related to a corresponding *specific heat*. The following equations represent energy-temperature relations, where each particular energy reservoir of a considered species is characterised by a temperature T and a corresponding heat capacity c_v . As with stellar atmospheres and circumstellar shells, the thermal reservoirs of each gas species, highly coupled by collisions, form a local thermal equilibrium for all gas species, so a single thermal temperature may be defined

$$d e_{\text{g,th}} = \frac{1}{m_{\text{g}}} c_{v,\text{th,g}} dT_{\text{th,g}}, \quad (2.59)$$

with m_{g} , the mean mass of a gas particle as defined in equation (2.19). For the dust, only the internal energy reservoir is of interest. The energy-temperature equation of the internal state both of the gas and the dust has to be treated differently for each single considered species in the fluid

$$d e_{\text{int,g}}^i = \frac{1}{m_{\text{g}}^i} c_{v,\text{int,g}}^i dT_{\text{int,g}}^i, \quad (2.60)$$

$$d e_{\text{d,int}}^{\beta,\alpha} = \frac{1}{m_{\text{d}}^{\beta,\alpha}} c_{v,\text{int,d}}^{\beta,\alpha} dT_{\text{d}}^{\beta,\alpha}. \quad (2.61)$$

The heat capacities c_v of the considered multiple components are proportional to the number of degrees of freedom, together with the contribution $\frac{1}{2}k_{\text{B}}$. For the thermal energy reservoir e_{th} , the translational degrees of freedom of a single particle counts with the number of 3. Therefore the thermal heat capacity for constant volume leads to

$$c_{v,\text{th,g}} = c_{v,\text{th,g}}^i = \frac{3}{2} k_{\text{B}} \quad \text{for all } i \text{ with } f_{\text{g,trans}} = 3. \quad (2.62)$$

The identification of the number of degrees of freedom bases on internal energy forms, like the rotational energy ϵ_{rot} of a molecule due to rotation around an axis through the center of mass of the particle or the internal energy ϵ_{vib} by oscillation. A diatomic

molecule with two independent rotational axes possesses two rotational degrees of freedom ($f_{\text{rot}} = 2$). The rotational energy of a spherical dust grain is assumed to be negligible. For linear molecules with f degrees of freedom, $(f - 5)$ degrees of freedom are related to vibrations and $(f - 6)$ for non-linear molecules. The corresponding internal energy is ϵ_{vib} . Since there is only one type of oscillation possible, the degrees of freedom related to vibrations is of the number of $f_{\text{g,vib}} = 1$. The number of the translational degrees of freedom of a single particle is $f_{\text{g,trans}} = 3$. Macroscopic solid grains consisting of N atoms possess $f_{\text{d,int}} = 3N - 6 \simeq 3N$ degrees of freedom as a good approximation. This number provides a continuous phonon spectrum and so ϵ_{vib} is the most important internal energy reservoir. Considering the conditions predominant in dust forming circumstellar shells, with low temperatures, electronic energy does not play a role. The internal energy ϵ_{vib} does not play a role in a cool environment. Electronic degrees of freedom are of interest only in cases, where higher electronic states are excited.

According to the explanations above, the degrees of freedom for diatomic molecules are

$$f_{\text{int,g}}^i = f_{\text{rot,g}}^i + f_{\text{vib,g}}^i = 3. \quad (2.63)$$

This number leads to the internal heat capacities for constant volume

$$c_{\text{v,int,g}} = c_{\text{v,int,g}}^i = \frac{3}{2} k_{\text{B}}. \quad (2.64)$$

With the knowledge that Debye theory for calculating the specific heat of solids applies only to particular solid materials, like e.g. iron, the following consideration should be treated with caution. The heat capacity of probable grain material remains to be defined. Θ_{d}^j describes the Debye temperature of a solid grain, usually $\Theta_{\text{d}}^j < 500$ K, being the internal temperature $T_{\text{d}}^{j,\alpha} > \Theta_{\text{d}}^j$ in a circumstellar dust shell. From the results concerning the number of the degrees of freedom of macroscopic solid grains consisting of N atoms, the internal heat capacities for constant volume may be calculated with the number of degrees of freedom for any macroscopic grain with $N_{\text{d}}^{j,\alpha} > 20$

$$f_{\text{int,d}}^{j,\alpha} = 3N_{\text{d}}^{j,\alpha}, \quad (2.65)$$

as

$$c_{\text{v,int,d}}^{j,\alpha} = \begin{cases} f_{\text{int,d}}^{j,\alpha} \cdot 3k_{\text{B}} \left(\frac{T_{\text{d}}^{j,\alpha}}{\Theta_{\text{d}}^j} \right)^3 \int_0^{T_{\text{d}}^{j,\alpha}/\Theta_{\text{d}}^j} x^4 (e^x - 1)^{-1} dx, & \text{if } T_{\text{d}}^{j,\alpha} < \Theta_{\text{d}}^j, \\ f_{\text{int,d}}^{j,\alpha}, & \text{if } T_{\text{d}}^{j,\alpha} \geq \Theta_{\text{d}}^j. \end{cases} \quad (2.66)$$

According to the expressions for heat capacities, the energy-temperature equation may be rewritten as

$$d e_{\text{g,th}} = \frac{1}{m_{\text{g}}} \frac{3}{2} k_{\text{B}} d T_{\text{th,g}}. \quad (2.67)$$

The energy-temperature equation of the internal state both of the gas and the dust turns into

$$d e_{g,\text{int}}^i = \frac{1}{m_g^i} \frac{3}{2} k_B d T_{\text{int},g}^i. \quad (2.68)$$

By assuming $T_d^{j,\alpha} > \Theta_d^j$ (high temperature approximation of Debye theory for the heat capacity of grains having Debye temperature), for the dust follows

$$d e_{d,\text{int}}^{\beta,\alpha} = \frac{1}{m_d^{\beta,\alpha}} 3N^{j,\alpha} d T_d^{\beta,\alpha} \quad (2.69)$$

For more explanations see [58].

2.1.3.1.1 Temperature Equations by One-Fluid Description

In order to determine gas temperature equations, with replacement of e by equation (2.67) and (2.68), the energy equation (2.43) turns into

$$\begin{aligned} \rho(\mathbf{r}, t) \frac{1}{m_g} \frac{3}{2} k_B \frac{\partial}{\partial t} T_g(\mathbf{r}, t) + \mathbf{v}(\mathbf{r}, t) \rho(\mathbf{r}, t) \frac{1}{m_g} \frac{3}{2} k_B \cdot \nabla T_g(\mathbf{r}, t) + p_g(\mathbf{r}, t) \nabla \cdot \mathbf{v}(\mathbf{r}, t) = \\ \mathbf{v}(\mathbf{r}, t) \cdot \mathbf{f}_{\text{grav}}(\mathbf{r}, t) - \mathbf{v}(\mathbf{r}, t) \cdot \mathbf{f}_{\text{rad}}(\mathbf{r}, t) + Q_{\text{rad},\text{int}}(\mathbf{r}, t) = Q(\mathbf{r}, t) + Q_{\text{rad},\text{int}}(\mathbf{r}, t). \end{aligned} \quad (2.70)$$

In this case, dust temperature is assumed as being in radiative equilibrium and therefore equals radiative temperature T_{rad} .

2.1.3.1.2 Temperature Equations for Gas and Dust

As for the one-fluid description, temperature equations for both gas and dust are specified taking into account the equations (2.67), (2.68), and (2.69).

$$\begin{aligned} m_g^i n_g^i(\mathbf{r}, t) \frac{1}{m_g^i} c_{v,g}^i \frac{\partial}{\partial t} T_g^i(\mathbf{r}, t) + m_g^i n_g^i(\mathbf{r}, t) \frac{1}{m_g^i} c_{v,g}^i \mathbf{v}_g^i(\mathbf{r}, t) \cdot \nabla T_g^i \\ = - p_g^i(\mathbf{r}, t) \nabla \cdot \mathbf{v}_g^i(\mathbf{r}, t) - Q_{\text{drag},g}^i(\mathbf{r}, t) + Q_{\text{grav},g}^i(\mathbf{r}, t) \\ - Q_{\text{rad},g}^i(\mathbf{r}, t) - Q_{\text{kin},g}^i(\mathbf{r}, t) - Q_{\text{int},g}^i(\mathbf{r}, t) + Q_{\text{rad},\text{int},g}^i(\mathbf{r}, t) \end{aligned} \quad (2.71)$$

represents the gas energy equation with

$$Q_{\text{int},g}^i(\mathbf{r}, t) = q_g(\mathbf{r}, t) \frac{1}{m_g^i} c_{v,g}^i T_g^i(\mathbf{r}, t), \quad (2.72)$$

the remanent of the subtraction of the motion equation from energy equation (2.45) with $q_g(\mathbf{r}, t)$, defined in equation (2.12). For the dust energy equation, the replacement of e by the related temperatures leads to

$$\begin{aligned} & m_d^{\beta,\alpha} n_d^{\beta,\alpha}(\mathbf{r}, t) \frac{1}{m_d^{\beta,\alpha}} 3N^{j,\alpha} \frac{\partial}{\partial t} T_d^{\beta,\alpha}(\mathbf{r}, t) \\ & + m_d^{\beta,\alpha} n_d^{\beta,\alpha}(\mathbf{r}, t) \frac{1}{m_d^{\beta,\alpha}} 3N^{j,\alpha} \mathbf{v}_d^{\beta,\alpha}(\mathbf{r}, t) \cdot \nabla T_d^{\beta,\alpha}(\mathbf{r}, t) = \\ & -Q_{\text{drag}}^{\beta,\alpha}(\mathbf{r}, t) + Q_{\text{grav,d}}^{\beta,\alpha}(\mathbf{r}, t) - Q_{\text{rad,d}}^{\beta,\alpha}(\mathbf{r}, t) - Q_{\text{kin,d}}^{\beta,\alpha}(\mathbf{r}, t) - Q_{\text{int,d}}^{\beta,\alpha}(\mathbf{r}, t) + Q_{\text{rad,int,d}}^{\beta,\alpha}(\mathbf{r}, t) \end{aligned} \quad (2.73)$$

with the remanent of the subtraction

$$Q_{\text{int,d}}(\mathbf{r}, t) = q_d(\mathbf{r}, t) \frac{1}{m_d^{\beta,\alpha}} 3N^{j,\alpha} T_d^{\beta,\alpha}(\mathbf{r}, t), \quad (2.74)$$

wherein $q_d(\mathbf{r}, t)$ means the coupling term applied as in (2.17).

2.2 Dust Complex

Describing dust formation, it is fundamental to specify the conditions of generating a surface. The conventional way of describing dust formation is to assume a process which provokes phase transition as an effect of small disturbances. These disturbances with the objective of energy minimisation lead to an stable state. Classical theory is based on three fundamentals, namely: new built grains are spherical, density and surface tension are related to macroscopic values. Cluster size increases by adsorption of monomers and chemical equilibrium is valid just like thermal equilibrium. The assumption of a spherical grain in case of nucleation from the gas phase is justified. In the case of heterogeneous nucleation, the spherical assumption is not founded all the times. The assumed relation to macroscopic quantities is justified by congruence between theory and measurements. Thermodynamical description of nucleation appears first by e.g. Volmer & Weber [108], Becker & Döring [9]. The steps leading to classical nucleation theory are illustrated in the following.

2.2.1 Thermodynamics

Any supersaturated vapor tends to fluctuations from Brownian motion. This leads to variations in density, temperature, and pressure and therefore to aggregations of monomers or molecules. Based on the classical nucleation theory, these aggregations grow by addition of a single monomer, or evaporate by elimination of a single monomer. The life cycle of the new formed conglomerates depends from the stability of the associated thermodynamical state. In case of exceeding the limit of a thermodynamical critical value, the conglomerate, instead of dissociating, grows by adsorption of further

monomers or molecules. This newly formed conglomerate is the so called *critical cluster*.

First, the energetic state of any fluid, which in this case represents our thermodynamical system has to be specified. Each thermodynamical system, e.g. a homogeneous gas phase, is expressed by the state variable of internal energy, which in case of a closed system has to be constant, according to the first law of thermodynamics

$$dU = \delta Q + \delta W. \quad (2.75)$$

The change of the internal energy dU is equal to the heat absorbed or emitted from the environment δQ , and the exchange of work δW done to the system, which includes work from the exchange of matter dN_i through the system boundary. So, the fundamental relation in thermodynamics for gases is given by

$$dU = T dS - p dV + \sum_{i=1}^k \mu_i dN_i. \quad (2.76)$$

Herein

$$T dS = \delta Q \quad (2.77)$$

means the second law of thermodynamics with the differential of the entropy dS and

$$\delta W = -p dV + \sum_{i=1}^k \mu_i dN_i, \quad (2.78)$$

the change of volume V by the pressure p and the exchange of particles N_i with the chemical potential μ_i for an i -type particle. Considering that extensive variables, like e.g. V , S , N , U , are proportional to the absolute size of the system, and, on the other hand, intensive variables, like e.g. p , T , n , are independent from the involved mass of the system, the internal energy changes to

$$U(\xi S, \xi V, \xi N_i) = \xi U(S, V, N_i) \quad (2.79)$$

if the extensive state variables are multiplied by an enlargement factor ξ . All of natural variables of the internal energy U are extensive quantities. So, this causes the fundamental equation of the internal energy to be integrable and it follows from Euler's homogeneous function theorem [6], [11], that

$$U(S, V, N_i) = TS - pV + \sum_i \mu_i N_i. \quad (2.80)$$

The quantity

$$U = U(V, S, N_i) \quad (2.81)$$

is the so called *thermodynamical potential*.

Based on the fact that all thermodynamic potentials include the same complete information about the examined thermodynamic system in equilibrium, thermodynamic

potentials can be determined with respect to specification of the free parameters by Legendre transformation. Assuming reversible processes with constant temperature and pressure in a closed state, a new thermodynamical potential with temperature T , pressure p , and particle species N as natural variables is given by Legendre transformation as the *Gibbs free energy* G [97]:

$$\tilde{U}(V, S, N_i) = U(V, S, N_i) - \frac{\partial f(V, S, N_i)}{\partial V} V - \frac{\partial f(V, S, N_i)}{\partial S} S = U + pV - TS = G \quad (2.82)$$

With equation (2.80) the *Gibbs free energy* G turns to its integral form

$$G = TS - pV + \sum_i \mu_i N_i + pV - TS = \sum_i \mu_i N_i. \quad (2.83)$$

The total derivative of the *Gibbs free energy* G is given by

$$dG = \sum_i d\mu_i N_i + \sum_i \mu_i dN_i \quad (2.84)$$

On the other hand from Legendre transformation results

$$\begin{aligned} dG &= d(U + pV - TS) = dU + p dV + V dp - S dT - T dS = \\ &= T dS - p dV + \sum_{i=1}^k \mu_i dN_i + p dV + V dp - S dT - T dS \end{aligned} \quad (2.85)$$

wherein dU is replaced with the fundamental relation in thermodynamics

$$dG = \sum_{i=1}^k \mu_i dN_i + V dp - S dT. \quad (2.86)$$

Comparison of these two terms leads to

$$0 = S dT - V dp + \sum_{i=1}^k N_i d\mu_i, \quad (2.87)$$

the so called *Gibbs-Duhem-Relation* [89].

The differential of a thermodynamic potential can be assumed equal to a differential of a mechanical potential energy. The equations of state are therefore to be obtained by thermodynamic potentials. To express equilibrium conditions for simple systems as well as for integrated systems under the condition that independent variables are predetermined and constant, the potential has to be completely known. In this case equilibrium behaviour of the system is well-defined.

In the following the equation of *Gibbs free energy* G leads to obtaining a state of equilibrium in a reversible process with constant temperature and pressure in a closed system. Provided the coexistence of two different phases of a fluid, in equilibrium state

with constant pressure, and wherein isobaric and isothermal processes simultaneous proceed, the attention focuses on the change of phase of the two different phases. For every system the conservation of the amount of material has to be applied. First, the pressure p and temperature T are assumed as constant, as is the chemical potential, i.e.

$$\mu_1 = \mu_2 \quad (2.88)$$

$$p = \text{const}, \quad T = \text{const}. \quad (2.89)$$

This leads to the equation for the derivative of the *Gibbs free energy* G , which defines the equilibrium condition

$$dG = 0. \quad (2.90)$$

Due to the dependency on the intensive variables $T, p, \mu_1, \dots, \mu_k$, which are conjugated to form the extensive variables S, V, N_1, \dots, N_k , it is feasible to eliminate an intensive variable. When a system with saturation pressure $p_1(V_1) = p_S$ in the volume V_1 and constant temperature ($T = \text{const.}$) undergoes a fractional change in pressure, the *Gibbs-Duhem-Relation* implies in the following

$$0 = -V dp + \sum_{i=1}^k N_i d\mu_i \quad (2.91)$$

$$\iff V dp = \sum_{i=1}^K N_i d\mu_i \quad (2.92)$$

Then for a chemical potential μ_i the equation turns into

$$V dp_i = N_i d\mu_i, \quad (2.93)$$

wherein $pV = Nk_B T$ is the ideal gas law, and the differential of the chemical potential can be expressed by

$$\frac{1}{p_i} k_B T dp_i = d\mu_i. \quad (2.94)$$

For the chemical potential follows after integration with

$$\int_{p(V_1)}^{p(V_2)} \frac{1}{p_i} k T dp_i = \int_{\mu(V_1)}^{\mu(V_2)} d\mu_i \quad (2.95)$$

a change with pressure:

$$k_B T \ln \left(\frac{p_i(V_2)}{p_{i,S}} \right) = \Delta \mu_i = \mu_i(V_2) - \mu_i(V_1) = k_B T \ln(S), \quad (2.96)$$

with $p_{i,S}$ being the saturation vapour pressure. Knowing this, the chemical potential of the solid phase is associated with $\mu_i(N)$ and the chemical potential of the monomers with $\mu_i(1)$. This leads to

$$\Delta \mu_i = \mu_i(N) - \mu_i(1) = k_B T \ln \left(\frac{p_i}{p_{i,S}} \right) \quad (2.97)$$

and determines the difference between the solid and the fluid phase.

By changing a surface area, work has to be performed to modify the inner energy of the compound. In the case of boundary surfaces, the disposition of forces is highly anisotropic. This anisotropy is specified by surface tension σ . The surface tension tends to minimise the volume of the spherical cluster with radius r_{Cl} . Inside the volume over-pressure holds the mechanical equilibrium. This results in an equilibrium of pressure p_{out} due to surface tension against internal pressure p_{int}

$$p_{int} dV = p_{out} dV + \sigma dA, \quad (2.98)$$

$$p_{int} - p_{out} \Delta p = \frac{8\pi r_{Cl} \sigma}{4\pi r_{Cl}^2} = \frac{2\sigma}{r_{Cl}} \quad (2.99)$$

with $A = 4\pi r_{Cl}^2$, the surface of the cluster, $dA = 8\pi r_{Cl} dr$, the differential of the surface and $V = \frac{4}{3}\pi r_{Cl}^3$, the volume of the cluster. Assuming a spherical cluster, the *Laplace equation* $\Delta p = 0$ is valid, i.e.

$$p_{int} = p_{out} + \frac{2\sigma}{r_{Cl}}. \quad (2.100)$$

The *Laplace equation* represents a special case of the *Kelvin equation*, which sets the internal pressure of a cluster in relation to saturation pressure p_∞ over a flat surface

$$\ln \left(\frac{p_{Cl}}{p_\infty} \right) = \frac{2\sigma V}{r_{Cl} k_B T}. \quad (2.101)$$

In consequence, differences emerge between the *Gibbs-Energies* of the two involved phases, i.e. between the *Gibbs-Energies* of the solid and the monomers. With $G_i(1) = \mu_i(1)$ and $G_i(N) = N \mu_i(N)$, the *Gibbs-Energies* of the monomers and the N -mers, and the work $W_A(N) = 4\pi \cdot r_{N,i}^2 \cdot \sigma$ to form a surface $A(N) = 4\pi \sigma r_i^2$ with the surface tension σ . Assuming $G_i(N) \neq N \cdot \mu_i(1)$, then, in general $G_i(N) > N \cdot \mu_i(1)$ is valid. Furthermore, the difference between the *Gibbs-Energies* of N monomers and an N -mer

leads to:

$$\begin{aligned}
\Delta G_i &= G_i(N) - N\mu_i(1) \\
&= N\mu_i(N) + A(N)\sigma - N\mu_i(1) \\
&= N(\mu_i(N) - \mu_i(1)) + A(N)\sigma \\
&= A(N)\sigma - N(\mu_i(1) - \mu_i(N)) \\
&= A(N)\sigma - N\Delta\mu_i \\
&= A(N)\sigma - Nk_B T \ln \left(\frac{p_i}{p_{i,S}} \right). \tag{2.102}
\end{aligned}$$

With $N = \frac{4}{3} \pi r_i^3(N) \frac{\rho_i}{m_i}$, the size of the N -mer, the difference of the *Gibbs-Energies* can be expressed by

$$\Delta G_i = 4\pi\sigma r_i^2 - \frac{4}{3} \pi r_i^3(N) \frac{\rho_i}{m_i} k_B T \ln \left(\frac{p_i}{p_{i,S}} \right). \tag{2.103}$$

In order to obtain the radius of a nucleus with minimal energy, the *critical radius* r_i^* , i.e. the minimal size of a cluster, the equation has to be differentiated with respect to the radius r_i^* , i.e.

$$0 = \left. \frac{d(\Delta G)^*}{dr_i^*} \right|_{r_i=r_i^*} = 8\pi \sigma r_i^* - \frac{12}{3} \pi r_i^{*2}(N) \frac{\rho_i}{m_i} k_B T \ln \left(\frac{p_i}{p_{i,S}} \right). \tag{2.104}$$

Therefore, the critical radius turns into

$$r_i^* = \frac{2\sigma m_i}{\rho_i k_B T \ln(S)}. \tag{2.105}$$

Then, with the equation of the critical radius r_i^* and with the size of the critical N -mer $N^* = \frac{4}{3} \pi r_i^{*3}(N^*) \frac{\rho_i}{m_i}$, the *Gibbs-Energy* ΔG_i^* can be determined by

$$\Delta G_i^* = 4\pi\sigma r_i^{*2} - \frac{4}{3} \pi r_i^{*3}(N^*) \frac{\rho_i}{m_i} k_B T \ln \left(\frac{p_i}{p_{i,S}} \right) \tag{2.106}$$

$$\iff \Delta G_i^* = \left(4\pi r_i^{*2}(N^*) - \frac{8}{3} \pi r_i^{*2}(N^*) \right) \sigma = \frac{4}{3} \pi r_i^{*2}(N^*) \sigma. \tag{2.107}$$

This leads to a simple expression for the *Gibbs-Energy*

$$\Delta G_i^* = \frac{1}{3} A(N^*) \sigma, \tag{2.108}$$

where $A(N^*)$ is the surface of the critical N -mer.

The next step is to specify the *nucleation rate*. According to Vollmer & Weber [108],

this is the number of clusters, exceeding the energy barrier of the *Gibbs-Energy* ΔG_i^* per volume and time unit. Assuming a thermally activated process of fluctuation of sub-critical nuclei and using the Arrhenius-ansatz, the steady state homogeneous nucleation rate has been given by

$$J_* = \phi \cdot Z \cdot n_{\text{crit}} \cdot \exp\left(\frac{-\Delta G_i^*}{k_B T}\right), \quad (2.109)$$

wherein

$$\mathring{f} = (N_*) n_{\text{crit}} \cdot \exp\left(\frac{-\Delta G_i^*}{k_B T}\right) \quad (2.110)$$

represents the equilibrium concentration of critical size nuclei.

$$\phi = \frac{1}{4} A(N^*) n_i v_{\text{therm}} \quad (2.111)$$

is the frequency of adsorption of a monomer to form a stable nucleus (with n_i , the value of the effective concentration of the condensing species in the gas phase) and $v_{\text{therm}} = \sqrt{8k_B T / (\pi m_i)}$ the thermal velocity. The *Zeldovich-factor*,

$$Z = \left(\frac{1}{2\pi k_B T} \left(-\frac{\partial^2 G^*}{\partial N^2} \right)_{N=N^*} \right)^{1/2}, \quad (2.112)$$

corrects the non-equilibrium concentration of critical nuclei. The *Zeldovich-factor* is the result of an integral realised in the neighborhood of the critical cluster size. It includes that the critical cluster size results both from growth and from evaporation depending on whether the original grain size is smaller or bigger than the critical cluster.

2.2.2 Dust Equations

Based on classical nucleation theory, dust formation, growth, and evaporation is described by the modified theory by H.P. Gail & E. Sedlmayr [47]. Dust formation may be considered as a sequenced process. Small meta-stable clusters are formed from the gas phase up to a significant lower dimension N_* , the so called *critical cluster*. From this dimension, these seeds are able to form macroscopic grains. The formation of a critical cluster can be considered as a stationary problem (H.P. Gail & E. Sedlmayr [53], A. Gauger et al. [55]), provided that hydrodynamical time scales are greater than the growth time scales of the nucleation time scales. The grain growth and formation in the context of the hydrodynamics can be described by the moments K_j of the local size distribution of the dust particles $f(r, N, t)$, i.e.

$$K_j(r, t) = \sum_{N=N_l}^{\infty} N^{j/d} f(r, N, t), \quad (2.113)$$

where the number of monomers contained in a dust particle defines the grain size N . N_l is the minimal limit size of grains in the size contribution, i defines the moment

number, d the spatial dimension of the particles. The following system of equations represents the time evolution of the moments:

$$\frac{\partial}{\partial t} K_0 + \nabla \cdot (\mathbf{v}_g K_0) = J(N_l, t) \quad (2.114)$$

$$\frac{\partial}{\partial t} K_j + \nabla \cdot (\mathbf{v}_g K_j) = N_l^{j/d} J(N_l, t) + \frac{j}{d} \frac{1}{\tau} K_{j-1}, \quad j = 0, 1, 2, 3. \quad (2.115)$$

$J(r, N_l, t)$ is the local formation rate of clusters N_l

$$J(r, N_l, t) = N_l^{\frac{d-1}{d}} \frac{1}{\tau} f(N_l, t). \quad (2.116)$$

The net growth rate $\frac{1}{\tau}$ is the number of monomers per second, per dust particle and monomer surface on the dust particle adsorbed or evaporated from the grain (see also [41]).

$$\begin{aligned} \frac{1}{\tau} = & \sum_{i=1}^I i A_1 v_{\text{th}}(i) \alpha(i) f(i, t) \left\{ 1 - \frac{1}{S^i} \frac{1}{b^i} \alpha_*(i) \right\} \\ & + \sum_{i=1}^I i A_1 \sum_{m=1}^{M_i} v_{\text{th}}(i, m) \alpha^c(i, m) n_{i,m} \left\{ 1 - \frac{1}{S^i} \frac{1}{b_{i,m}^c} \alpha_*^c(i, m) \right\}. \end{aligned} \quad (2.117)$$

Herein,

$$S = n_1 k_B T_g / p_S(1) = \frac{p(1, T_d)}{p_S(1)}, \quad (2.118)$$

means the supersaturation ratio, the ratio of the actual partial pressure of condensible monomers in the gas component $p(1, T_d)$ to the vapor saturation pressure with respect to the dust temperature $p_S(1)$. The quantities b^i and $b_{i,m}^c$ are the generalised departure coefficients of the actual particle densities of the i -mers. Non-TE effects with excitation dust temperatures different from the assumed T_d are represented by α_* . The net growth rate comprises the growth rate $1/\tau_{\text{gr}}$ and the evaporation rate $1/\tau_{\text{ev}}$:

$$\frac{1}{\tau} = \frac{1}{\tau_{\text{gr}}} - \frac{1}{\tau_{\text{ev}}}. \quad (2.119)$$

If $1/\tau_{\text{gr}} < 1/\tau_{\text{ev}}$ the equations (2.114) and (2.115) describe grain destruction caused by sputtering or evaporation. In case of $1/\tau_{\text{gr}} > 1/\tau_{\text{ev}}$ the equations (2.114) and (2.115) describe grain nucleation and growth. For conditions typically prevailing in circumstellar shells of cool stars one can assume that growth from N_* to N_l is a stationary process.

The stationary homogeneous formation rate of critical clusters N_* at time t per hydrogen atom per unit time and unit surface is represented by the nucleation rate

$$J_* = Z \mathring{f}(N) A_{N_*} \sum_{i=1}^I i^2 f(i) v(i) \alpha(i). \quad (2.120)$$

Herein mean the sum over i the sum of all nucleating species, the surface of the critical cluster is represented by

$$A_{N_*} = 4\pi \left(\frac{3Am_p}{4\pi\rho_{\text{solid}}} \right)^{2/3} N_*^{2/3}, \quad (2.121)$$

with the atomic weight A and m_p , the proton mass. $v(i)$ is the thermal velocity (see equation 2.22). The factor α represents the average sticking coefficient for a monomer of the species i according to H.P. Gail & E. Sedlmayr [46]. Herein $\mathring{f}(N)$ denominates the equilibrium distribution of the involved species

$$\mathring{f}(N) = n_1 \exp \left\{ (N-1) \ln S - \frac{\Theta_N}{T_g} (N-1)^{2/3} \right\}. \quad (2.122)$$

Z represents the Zeldovich factor

$$Z = \left(\frac{1}{2\pi} \frac{\partial^2 \ln \mathring{f}(N)}{\partial N^2} \Big|_{N=N_*} \right)^{1/2}. \quad (2.123)$$

In order to focus on stationarity, the explicit time dependency is not discussed. The critical cluster is described as follows

$$N_* = 1 + \frac{N_{*,\infty}}{8} \left\{ 1 + \left[1 + 2 \left(\frac{N_f}{N_{*,\infty}} \right)^{1/3} \right]^{1/2} - 2 \left(\frac{N_f}{N_{*,\infty}} \right)^{1/3} \right\}^3, \quad (2.124)$$

wherein $N_{*,\infty} = (2\Theta_\infty/3 T_g \ln S)^3$ with Θ_∞ , according to the classical nucleation theory, is the surface contribution to the *Gibbs*-Energy (equation (2.107))

$$\Theta_\infty = \sigma 4\pi a_0^2 / k_B. \quad (2.125)$$

$S = n_m k_B T / p_{\text{sat}}$ determines the supersaturation ratio with n_m the number density of the monomers m in the gas phase, and p_{sat} , the saturation vapour pressure over a flat surface. In order to include not only homogeneous growth, but also a corn-mantle heterogeneous growth with several species, the equation turns into

$$J_* = Z \mathring{f}(N) A_{N_*} \left(\sum_{i=1}^I i^2 f(i) v(i) \alpha(i) + \sum_{i=1}^{I'} i^2 \sum_{m=1}^{M_i} v(i, m) \alpha_m^c(i, m) n_{i,m} \right). \quad (2.126)$$

The double sum represents the several species involved in the growth.

The moments are related to the following physical values:

- the number density of monomers condensed in dust particles of size $N \geq N_l$

$$n_C = K_3, \quad (2.127)$$

- the average particle size can be expressed by

$$\langle N \rangle = K_3/K_0, \quad (2.128)$$

- the related average particle radius

$$\langle a \rangle = a_0 K_1/K_0, \quad (2.129)$$

with a_0 , the hypothetical monomer radius,

- the average particle surface is represented by

$$\langle A \rangle = 4 \pi a_0^2 K_2/K_0, \quad (2.130)$$

and

- the particle density of grains of size $N \geq N_l$

$$n_d = \int_{N_l}^{\infty} dN f(r, N, t) = K_0, \quad (2.131)$$

with $N_l \cong 10^2 - 10^3$, the lower limit of the particle size.

2.3 Radiative Transfer

In the following, the radiative transfer is presented in a short version. For more details see e.g. D. Mihalas [88].

Assuming radiative equilibrium for the entire considered atmosphere, the stratification of the temperature of the atmospheric layers can be described by conservation of radiation energy. For that, the radiative transfer problem has to be solved for the outer layers of the star as well as for the circumstellar dust shell. Based on the moment equations of the radiation intensity, one can obtain an approximation for the stratification of the temperature of the atmospheric layers, according to the work of L.B. Lucy [84], [83]. The moments of the specific intensity I_ν in a non-grey description are the following:

$$J_\nu = \frac{1}{2} \int_{-1}^1 I d\mu, \quad H_\nu = 2 \int_{-1}^1 I \mu d\mu, \quad K_\nu = \frac{1}{2} \int_{-1}^1 I \mu^2 d\mu, \quad (2.132)$$

J_ν , H_ν , and K_ν are the 0., 1. and 2. moment of the radiation intensity. At a distance r from the star with a radius R_* , for which $\mu_* \leq \mu \leq 1$, is the cosine of the solid angle, with

$$\mu_* = \sqrt{1 - \left(\frac{R_*}{r}\right)^2}, \quad (2.133)$$

(see Figure 2.2) the moments of intensity can be calculated by using the following angular splitting

$$I_\nu(r, \mu) = I_\nu^+(r) \quad \text{for } \mu \geq \mu_* \quad (2.134)$$

and

$$I_\nu(r, \mu) = I_\nu^-(r) \quad \text{for } \mu < \mu_*, \quad (2.135)$$

i.e. with

$$I_\nu(r, \mu) = \Theta(\mu - \mu_*)I_\nu^+(r) + \Theta(\mu_* - \mu)I_\nu^-(r) \quad (2.136)$$

where Θ is the Heaviside function. The split intensities $I_\nu^+(r)$ and $I_\nu^-(r)$ describe the emission of radiation and respectively the irradiation in a spherical atmosphere surrounding a central, spherical source of radiation [84].

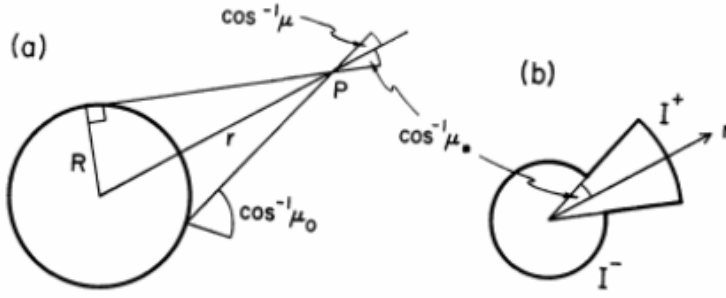


Figure 2.2: Model for the radiation field (adopted from the work of L.B. Lucy [84])

The moments result in

$$J_\nu(r) = \frac{1}{2}(I_\nu^+ + I_\nu^-) - \frac{\mu_*}{2}(I_\nu^+ - I_\nu^-), \quad (2.137)$$

$$H_\nu(r) = (I_\nu^+ - I_\nu^-)(1 - \mu_*^2), \quad (2.138)$$

$$K_\nu(r) = \frac{1}{3} \left[\frac{1}{2}(I_\nu^+ + I_\nu^-) - \frac{\mu_*^2}{2}(I_\nu^+ - I_\nu^-) \right]. \quad (2.139)$$

Elimination of I_ν^+ I_ν^- then gives the 1. intensity moment of radiation

$$J_\nu(r) - 3K_\nu + \frac{1}{2}\mu_*H_\nu. \quad (2.140)$$

The transfer equation (Chandrasekhar, [15]) for a spherical static atmosphere surrounding a spherical source of continuum radiation is represented by

$$\mu \frac{\partial I_\nu}{\partial r} + \frac{1 - \mu^2}{r} \frac{\partial I_\nu}{\partial \mu} = -\kappa_\nu \rho (I_\nu - J_\nu), \quad (2.141)$$

where κ_ν is the mass coefficient of absorption per unit volume. So, the first two moments are

$$\frac{d}{dr} H_\nu + \frac{2H_\nu}{r} = 0 \quad (2.142)$$

and

$$\frac{d}{dr} K_\nu + \frac{3K_\nu - J_\nu}{r} = -\frac{1}{4} \kappa_\nu \rho H_\nu. \quad (2.143)$$

The radiative transfer problem is considered as grey approximation. Assuming local thermodynamical equilibrium (LTE) in addition, radiative equilibrium (RE) can be specified by

$$J = \int J_\nu d\nu = \int \nu B_\nu(T_{\text{RE}}) d\nu, \quad (2.144)$$

where $B_\nu(T_{\text{RE}})$ means the black body radiation field at the radiative equilibrium temperature T_{RE} . Radiative transfer is considered as being time-independent. Assuming radiative equilibrium, radiative emission is balanced by radiative absorption for the entire considered atmosphere. Supposing the isothermal limit case, the gas relaxes without time-delay towards radiative equilibrium. All effects, which may differ from RE, are not considered in the following. The definition of Lucy's optical depth yields

$$\frac{d\tau_L}{dr} = -\kappa \rho \left(\frac{R_*^2}{r^2} \right), \quad (2.145)$$

wherein κ is the mass absorption coefficient and $\tau_L(R_*) = 2/3$ and $\lim_{r \rightarrow \infty} \tau_L(r) = 0$ are the boundary conditions for the optical depth. With the Stefan-Boltzmann law

$$H(R_*) = \frac{\sigma}{4\pi} T_*^4, \quad (2.146)$$

and under condition $\lim_{r \rightarrow \infty} J(r) = 0$, J equals to

$$J = \frac{\sigma}{\pi} T_{\text{RE}}^4 \quad (2.147)$$

with the radiative equilibrium temperature T_{RE} in LTE. So the moment

$$J_\nu(r) = H_\nu(R_*) \left[1/2 \left(1 - \sqrt{1 - \frac{R_*^2}{r^2}} \right) + \frac{3}{4} \int_{R_*}^{\infty} \kappa_\nu \rho \left(\frac{R_*^2}{r^2} \right) dr \right] \quad (2.148)$$

leads to the temperature distribution in radiative equilibrium

$$T_{\text{rad}}^4(r) = \frac{1}{2} T_*^4 \left[1 - \sqrt{1 - \frac{R_*^2}{r^2}} + \frac{3}{2} \tau_L(r) \right]. \quad (2.149)$$

2.4 The Numerical Problem

2.4.1 Differential-algebraic Equations

Ordinary differential equations ([75] [7] [14]) are known in the form of

$$\frac{du}{dx} = f(x, u),$$

wherein $u = u(x)$ represents the unknown function depending on the variable x . The differential quotient $\frac{du}{dx}$ is called a first order scalar ordinary differential equation. An existence and uniqueness theorem exists under weak continuity conditions of the right hand side of the equation, and so, if there are more equations added up, it results in a system of equations

$$\frac{d\mathbf{u}}{dx} = \mathbf{f}(x, \mathbf{u}),$$

with \mathbf{u} , the vector of dependent variables. Each system of this type basically comprises as much equations as unknown functions \mathbf{u} . Every system of higher order may be transformed into an equivalent first order differential equation system by introducing additional variables, representing the derivatives of the originally dependent variables. In case of transformation into a global system of ordinary first order differential equations

$$\mathbf{F}(x, \mathbf{u}, \mathbf{u}') = 0,$$

there is no obligatory assumption of the fact that the number of equations is equal to that of the unknown functions. Both the theoretical as well as the numerical treatment lead to results beyond the common form $\mathbf{u}' = f(x, \mathbf{u})$. The behaviour of the system causes multiple singularities, because of the implicit dependence of \mathbf{u}' . Though, for this system, the question of existence and uniqueness of solutions has to be raised. The implicit first order differential equation system

$$\mathbf{F}(x, \mathbf{u}, \mathbf{u}') = 0, \tag{2.150}$$

with

$$x \in [x_0, x_e], \quad \mathbf{u} : [x_0, x_e] \rightarrow \mathbb{R}^n$$

the initial conditions. Further,

$$\mathbf{F} : [x_0, x_e] \times \mathbb{R}^n \times \mathbb{R}^n \rightarrow \mathbb{R}^n$$

has to be continuous and continuously differentiable by $\mathbf{u}' = \frac{d\mathbf{u}}{dx}$. By introduction of an added variable \mathbf{z} , the system turns into a semi-explicit form with side conditions

$$M(\mathbf{u})\mathbf{u}' = f(x, \mathbf{u}, \mathbf{z}) \tag{2.151}$$

$$0 = g(x, \mathbf{u}, \mathbf{z}), \tag{2.152}$$

wherein is $M(\mathbf{u})$ a regular matrix.

This system of equations comprises differential equations and also algebraic equations, what leads to the notion of DAE, the differential-algebraic-equation system. Each continuously differentiable function

$$\mathbf{u}(x) : [x_0, x_e] \rightarrow \mathbb{R}^n \quad \text{with } \mathbf{F}(x, \mathbf{u}, \mathbf{u}') = 0 \quad \text{and } x \in [x_0, x_e]$$

is called solution of the system of the DAE. The function $\mathbf{u}(x)$ is therefore the solution of the initial value problem, if it solves both the DAE system and the initial conditions. The initial conditions are called consistent if the related initial value problem has at least one solution.

For further treatment, the DAE has to be classified by the index of the differentiation. The index of the differentiation denominates the number of differentiations necessary to transform the system of ordinary first order differential equations

$$\mathbf{F}(x, \mathbf{u}, \mathbf{u}') = 0$$

by differentiating the equations for x and by algebraic transformations into an explicit first order ordinary differential equation system.

$$\mathbf{u}'(x) = \phi(x, \mathbf{u})$$

A first order ordinary differential equation system has the index zero. The index is a measure of the difficulty of the numerical treatment of the DAE by characterising the algebraic part, [101]. In consequence, the system contains potential constraints of the form $r(x, \mathbf{u})$. So, the system has to satisfy the initial conditions, the initial value problem as well as the hidden constraints. It is obvious, that potential differentiations of the algebraic part of the system lead to further independent equations, i.e. conditions of integrability. In general this problem occurs in the case of a system of ordinary differential equation of differing order. An added effect consists of further initial conditions apart from the origin system. So the system has to be treated as “overdetermined”, even if the originally applied equation system consists of the same number of equations as unknown functions. Overdetermined means here the same as for a linear equation system $\mathbf{A} \mathbf{x} = \mathbf{b}$. If a differential equation system is considered as a linear equation system, there exist underdetermined or well determined equation systems. In case of a possible solution, for each matrix $\mathbf{A} = (m \times n)$ it is valid that $\text{rank } \mathbf{A} \leq n$ and the system contains no more than n independent variables. In case of a linear equation system with more equations than unknowns has no solution. So, the system is considered overdetermined and the number of dependent parameters is greater then that of the free chosen parameters.

2.4.2 Shooting Method

In case of ordinary differential equations, which are required to satisfy boundary conditions for more than one value of the independent variable, the resulting problem is

a boundary value problem (see [101], [75]). This includes conditions specified at the endpoints and/or others at interior (usually singular) points. One of the techniques for solving boundary value problems is the so called “(single) shooting” method, which integrates the differential equations as an initial value problem with guesses for the unknown initial values. Since the arbitrarily chosen starting point does not determine a unique solution, the boundary conditions at the other specified points are not necessarily satisfied.

In the present case the multiple shooting method means the full achievement of two boundary conditions. The problem consists in satisfying simultaneously the boundary condition for the singularity of the wind equation and for the boundary values for the optical depths at the radius of the star and at infinity. These conditions have to be solved by varying the velocity to be started with. In addition, the luminosity or the mass loss of the model has to be adjusted for each turn.

The common boundary value problem has to solve a set of N coupled first-order ordinary differential equations, satisfying n_1 boundary conditions at the starting point x_1 , and a remaining set of $n_2 = N - n_1$ boundary conditions at the final point x_2 . The differential equations are

$$\frac{d\mathbf{u}}{dx} = \phi_i(x, \mathbf{u}) \quad i = 1, 2, \dots, N \quad (2.153)$$

wherein \mathbf{u} represents the vector of N dependent variables. At x_1 , the solution is supposed to satisfy

$$B_{1j}(x_1, \mathbf{u}) = 0 \quad j = 1, \dots, n_1 \quad (2.154)$$

though at x_2 , it is supposed to satisfy

$$B_{2k}(x_2, \mathbf{u}) = 0 \quad k = 1, \dots, n_2 \quad (2.155)$$

The values for all of the dependent variables at one boundary must be consistent with any boundary conditions, but otherwise they depend on arbitrary, randomly chosen, free parameters. By integrating the ODE using initial value methods with those initial values, there are discrepancies from the desired boundary values at the other boundary. This leads to a multidimensional rootfinding problem. In order to zero the discrepancies at the other boundary points, the free parameters at the starting point have to be adjusted. The system of differential equations in the form of

$$\frac{d\mathbf{u}}{dx} = \phi_i(x, \mathbf{u}, z) \quad (2.156)$$

is an eigenvalue problem for differential equations. Here the right-hand side depends on a parameter z , The integrated solution has to satisfy $N + 1$ boundary conditions instead of just N . Thus, the problem is overdetermined. In general there is no solution for random values of z . Only a few special values of z , the eigenvalues, lead to a

solution of the equation (2.156). The problem can be reduced to the standard boundary value problem described by equations (2.153) - (2.155) by introducing a new dependent variable

$$u_{N+1} = z. \quad (2.157)$$

The new dependent variable leads to the differential equation

$$\frac{du_{N+1}}{dx} = 0. \quad (2.158)$$

The computational algorithm in its basically form starts with solving the differential equation using a stepping scheme with the initial conditions at x_1 and the equation (2.156).

Step two evaluates the solution $\mathbf{u}(x_2)$ at $x = x_2$ and compares the obtained value with the designated value of $\mathbf{u}(x_2)$.

After adjusting the value at x_1 (either smaller or bigger) with a bisection method for determining values at x_1 , a desired level of tolerance and accuracy is achieved and the numerical solution satisfies the initial conditions.

The shooting method (Fig. 2.3) provides a systematic approach to taking a set of shots allowing to improve the designated result systematically.

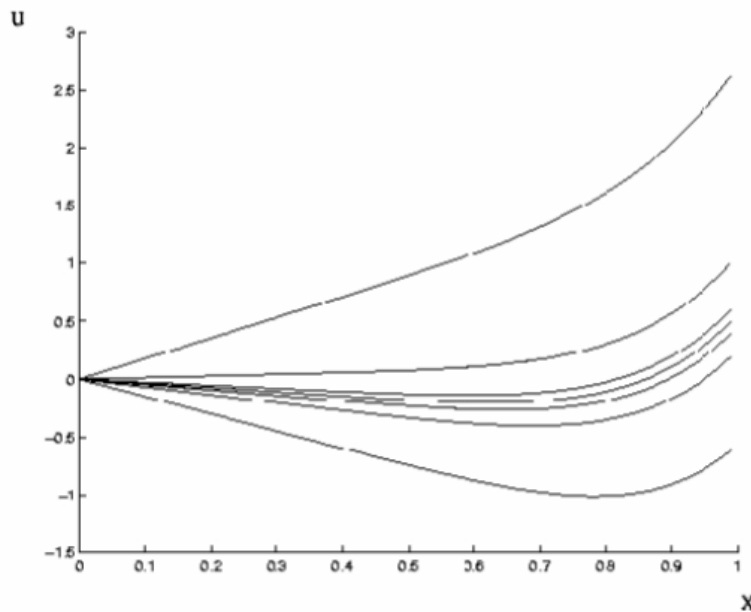


Figure 2.3: Shooting method (schematic). Trial integrations satisfying the boundary condition at one endpoint lead to discrepancies from the designated boundary condition at the other endpoint. These are used to adjust the starting conditions, until boundary conditions at both endpoints are satisfied.

Chapter 3

Models Including Interactions between Gas and Dust

3.1 Stationary Wind Model in Spherical Symmetry

D. Krüger, e. g. [77], investigated the first the influence of the dust component on the momentum coupling between gas and dust based on a stationary dust driven AGB-star wind model in spherical symmetry and in Eulerian description. He presented a system of coupled differential equations including coupling terms. These terms describe the exchange of momentum and energy between gas and dust particles. The presented equations are the following:

The radiative transfer is described as grey (see 2.3), and the temperature distribution follows equation (2.149). First, he uses the mass conservation equation of the gas taking into account a source term from the mass transfer from gas to condensate:

$$\frac{1}{r^2} \frac{\partial}{\partial r} (r^2 v_g \rho_g) = -S. \quad (3.1)$$

Therein, the physical value $-S$ corresponds equation (2.12). Lately, assuming an amount of condensible material about 10^{-3} times the total mass in the wind of an AGB-star, he set the source term S equal zero. In consequence, the continuity equation for the gas phase has to be expressed by the mass loss rate \dot{M}_*

$$r^2 \rho_g v_g = \dot{M}_*/(4 \pi). \quad (3.2)$$

The continuity equation for the dust is given but *not* applied, since the amount of dust issuing from condensible material in the wind is assumed to be negligible (see above). Than one gets

$$\frac{1}{r^2} \frac{\partial}{\partial r} (r^2 v_d \rho_d) = m_d J_*. \quad (3.3)$$

With $m_d J_*$, corresponding equation (2.12). Referring to the text below, where the dust velocity is derived from the drift velocity, the equation of mass conservation for the dust

component is not solved. So the mass conservation is assumed to be only represented by the gas component and by the constant mass loss of the considered stellar object according to the stationary wind model.

Based on the equation of motion for the gas, including a coupling drag force, the equation of motion is represented by

$$\rho_g v_g \frac{\partial v_g}{\partial r} = -\frac{\partial p}{\partial r} + f_{\text{drag}} - \frac{G M_* \rho_g}{r^2}. \quad (3.4)$$

Without remanents resulting from the equation of mass conservation, D. Krüger specified a coupled motion equation by insertion of energy terms from the applied following gas energy conservation equation

$$\frac{1}{r^2} \frac{\partial}{\partial r} (r^2 e_g v_g) + \frac{p}{r^2} \frac{\partial}{\partial r} (r^2 v_g) = q_{\text{rad}} + q_{\text{fric}} + q_{\text{acc}}, \quad (3.5)$$

which leads to the temperature equation for the gas component

$$\frac{\partial T_g}{\partial r} = \frac{T_g}{f v_g} \left(\frac{2 v_g}{r} + \frac{\partial v_g}{\partial r} (v_g^2 - c_S^2) v_g \right) = q_{\text{rad}} + q_{\text{fric}} + q_{\text{acc}} \quad (3.6)$$

with the adiabatic sound velocity c_S . The drag force \mathbf{f}_{drag} is defined after B.T. Draine [32] as

$$f_{\text{drag}} = \rho_g n_d \pi a_d^2 v_{\text{drift}} \left[\left(\frac{4}{3} v_{\text{th}} \right)^2 + v_{\text{drift}}^2 \right]^{1/2}, \quad (3.7)$$

and the average thermal velocity $v_{\text{th}} = \sqrt{\frac{8k_B T_g}{\pi \mu m_H}}$, with μ being the mean molecular weight of the gas phase. The coupling terms are q_{rad} , q_{fric} , q_{acc} , representing

$$q_{\text{fric}} = \left(1 - \frac{\alpha}{2} \right) f_{\text{drag}}, \quad (3.8)$$

$$q_{\text{acc}} = \alpha n_g n_d \pi a_d^2 \frac{f}{2} k_B (T_d - T_g) [v_{\text{th}}^2 + v_{\text{drift}}^2]^{1/2} \quad (3.9)$$

with $\alpha \simeq 0.1$. The energy transfer term q_{acc} from accommodation is adopted from B.T. Draine [31]. The heating-cooling term, describing interactions between dust components and the radiation field (see equation (2.42) et seq.), is derived from

$$q_{\text{rad}}^{\text{vib/rot}} = 4\sigma_r \left(\kappa_J^{\text{vib/rot}} T_{\text{rad}}^4 - \kappa^{T(\text{vib/rot})} T_{\text{vib/rot}}^4 \right), \quad (3.10)$$

using the **Stefan-Boltzmann** law.

So, the stated equation of motion is implemented as follows

$$(v_g^2 - c_S^2) \frac{\partial v_g}{\partial r} = v_g \left[\frac{2c_S^2}{r} - \frac{G M_* \rho_g}{r^2} + \frac{1}{\rho_g} f_{\text{drag}} - \frac{2}{f \rho_g v_g} (q_{\text{rad}} + q_{\text{fric}} + q_{\text{acc}}) \right], \quad (3.11)$$

However, some simplifications made were not so well introduced. The adiabatic sound velocity he defines as

$$\gamma \cdot c_T^2 = c_S^2, \quad (3.12)$$

is not explained. After evaluating the applied equations, the adiabatic coefficient γ has to be equal to $\gamma = 5/2$, as a factor from inserting the temperature equation in (3.4). Though, he applied this factor in the temperature equation from where its originated and gave no details on the validity for this value.

The equation of motion for the dust is introduced as

$$\rho_d v_d \frac{\partial}{\partial r} v_d = -\frac{G M_* \rho_d}{r^2} + f_{\text{rad}} + f_{\text{drag}} + m_d (v_{\text{injection}} - v_d) J_* \quad (3.13)$$

with the remanent $m_d v_d J_*$ resulting from the equation of mass conservation, and the coupling term $m_d v_{\text{injection}} J_*$ that should take into account the velocity of impinging particles. This velocity is assumed to be equal to the newly formed particle velocity, and therefore the coupling term $m_d (v_{\text{injection}} - v_d) J_*$ is set equal zero. D. Krüger specified also an equation for the occurrence of condensible material with the assumption of carbon as the sole component

$$\frac{1}{r^2} \frac{\partial}{\partial r} (r^2 (\epsilon_C n_{(n_H+2n_{H_2})} v_g)) = -N_C \quad (3.14)$$

with N_C , the rate of loss of carbon molecules from the gas phase. The rate N_C is specified by the nucleation rate J_* (see equation (2.120)), m_d , the mass of a condensed cluster and m_C , the mass of a single carbon atom and can be derived from the dust equations (2.12) et seq.

The gas temperature is calculated with respect to heating and cooling terms due to the exchange of energy between gas and dust by friction or accomodating and by exchange with the radiation field. The dust temperature is set equal to the radiation equilibrium temperature $T_d = T_{\text{rad}}$. The momentum coupling is accomplished by coupling terms due to energy exchange between gas and dust. D. Krüger applied non-discrete equations for dust mass conservation and motion.

In consequence of difficulties related to the computing algorithm, he indicated to modify the system of applied equations at the critical point: Under the condition that the relaxation time to reach the equilibrium values is minimal, the differential equations of the dust for the equation of motion as well as the energy equation are both not solved. In this case, they have to be replaced by their equilibrium conditions and correspond to a complete momentum coupling between gas and dust. The drift velocity is therefore solved by an algebraic equation issued from the drag force. But instead of solving the entire system of equations both for gas and for dust motion beyond the critical point, the left over of the applied computed models reveals the equilibrium conditions are held on. More details in the final analysis applied equations follow in Section 4.5.

3.2 Time-Dependent Model

To cite as an example, Y. Simis [102] presented two-fluid time-dependent hydrodynamics in spherical symmetry with included equilibrium gas chemistry as well as grain nucleation and growth. Momentum exchange is introduced by gas-grain collision without

assumptions regarding the completeness of momentum coupling. No stellar pulsation was taken into account. The momentum equation respects the loss of momentum of the gas phase due to the mass transfer from the gas to dust by nucleation. Momentum transfer is described by the drag force. This force is assumed to be proportional to the rate of gas-grain-collisions. Radiation pressure on gas is assumed to be negligible in the circumstellar environment of AGB-stars. They apply a mass conservation equation for the gas as for the dust

$$\frac{\partial}{\partial t} \rho_{g,d} + \frac{1}{r^2} \frac{\partial}{\partial r} (r^2 \rho_{g,d} v_{g,d}) = S_{\text{cond},g,d}(r, t) \quad (3.15)$$

with $S_{\text{cond},g}(r, t) = -S_{\text{cond},d}(r, t)$. The source term S_{cond} representing the condensation of dust from the gas is furthermore not specified and correspond the equation (2.12), respective (2.13). Dust formation is calculated with the equations developed by Gail & Sedlmayr [47] (see 2.2.2). With

$$\rho_d = \frac{4}{3} \pi a_0^3 \rho_{gr} K_3 \quad (3.16)$$

the mass density of the dust is derived from the third moment of the dust formation K_3 , ρ_{gr} , the grain-mass-density and a_0 , the hypothetical monomer radius. Therefore no dust conservation equation is solved. The time dependent momentum equations are indicated in the following form

$$\frac{\partial}{\partial t} (\rho_g v_g) + \frac{1}{r^2} \frac{\partial}{\partial r} (r^2 \rho_g v_g^2) = -\nabla p + f_{\text{rad},g} + f_{\text{kin},g} - f_{\text{grav},g} \quad (3.17)$$

and the same equation for the dust component becomes

$$\frac{\partial}{\partial t} (\rho_d v_d) + v_d \rho_d \frac{\partial}{\partial r} v_d = f_{\text{rad},d} + f_{\text{drag},d} - f_{\text{grav},d} + v_d S_{\text{cond}} \quad (3.18)$$

with $f_{\text{kin},g} = -f_{\text{drag},d}$ with $v_d S_{\text{cond},d}$ from the onset of the dust formation, which means $v_d = v_g = v_{\text{inject}}$, the velocity of an impinging molecule. These terms correspond the equations (2.33) and (2.35). The problem is solved in the isothermal case. The absorption coefficient is assumed as grey and grain temperature is not calculated.

Another example is given by C. Sandin [94]. He presents a time dependent model of a dust driven AGB-star wind with respect to the decoupling of the dust equation of motion from the gas component. Concerning mass conservation, no equation is introduced. The conservation of the equations is performed by introducing coupling terms between the equations of motion of both velocities and for the energy conservation equation. As presented in [94], the resulting equation of motion for the gas is

$$\begin{aligned} \frac{\partial}{\partial t} (\rho v) + \nabla \cdot (\rho v v) = \\ -\nabla p - \frac{GM_r \rho}{r^2} + \frac{4\pi}{c} (\kappa_g) \rho H + f_{\text{drag}} - S_{\text{cond}} v \end{aligned} \quad (3.19)$$

and for the dust

$$\begin{aligned} & \frac{\partial}{\partial t} (\rho_d v_d) + \nabla \cdot (\rho_d v_d v_d) = \\ & -\nabla p - \frac{GM_r \rho_d}{r^2} + \frac{4\pi}{c} (\kappa_d) \rho H - f_{\text{drag}} + S_{\text{cond}} v. \end{aligned} \quad (3.20)$$

The terms S_{cond} correspond the equation (2.12), respective (2.13). The terms S_{cond} correspond the equations (2.33) respective (2.35). The gas opacity follows from Bowen [13], while the dust opacity follows from (cf. Fleischer et al. [43]). The drag force is represented by

$$f_{\text{drag}} = \Sigma \rho n_d \frac{v_d^2 C_D}{2}, \quad (3.21)$$

wherein

$$\Sigma = \pi r_0^2 K_1^2 / K_0^2 \quad (3.22)$$

is the cross section of the dust particle with the dust moments K_1 and K_0 and the *drag coefficient* C_D introduced by (Bird [10]). The dust equation of internal energy is not included, the grain temperature is assumed to be determined by radiative equilibrium. The energy equation is not introduced in particular. For reasons of stability, v_d is set equal v in dust forming regions where the dust/gas ratio is small. The effects of stellar pulsations on the atmosphere are simulated by a sinusoidal radially varying inner boundary, located at $0.91 R_*$. The emulation of the κ -mechanism by piston approximation provides similiar effects on the dynamics of the wind as levitated atmosphere and strong shocks. For more details see also Bowen [13].

Chapter 4

Multi-Component Description of a Stellar Wind

4.1 Aim

Compared to other models describing flows including multicomponent effects (Chapter 3), in this work, the completely elaborated conservation equations of mass, motion, and energy lead to a set of remanents. These remanents have to be included in the study of multicomponent description of winds of AGB-stars on purpose of consistency. In the case of the equation of mass conservation, this term describes the mass transfer from gas phase to the condensed components. The equation of motion gets an additional velocity-dependent term, which may be categorised as a repulsion force from the phase change, leading to a gain of momentum for the gas phase. The added terms to the energy conservation equation may be interpreted in the same manner. The newly formed grains transport kinetic energy. In order to examine the multicomponent description, the applied equations are considered in the stationary case, assuming spherical symmetry and grey radiation transfer. The investigation bases on two models: First, the model is implemented as a single-fluid model, completely coupled by friction to reproduce stationary works (e.g.(Section 3.1)). Second, the finite differences Euler method model is extended by introducing the separate equations for gas and dust.

In both cases, the model is described by the parameters of the investigated stellar object as follows. The mass loss \dot{M}_* and the temperature T_* are predetermined. The luminosity L_* results as eigenvalue from the applied shooting method. The radius R_* is derived from the Stefan-Boltzmann law from the temperature T_* and the luminosity L_* . The initial values for the gas density $\rho(R_*)$ are derived from the free initial parameter of the velocity $v(R_*)$ of the gas phase from mass conservation and the mass loss rate \dot{M}_* , assumed to be constant in time. Treating the radiative transfer as introduced in Section 2.3, there is an additional differential equation to consider as well as two resulting constraints. First, the value of τ_L at the position $r = R_*$, is set equal 2/3, and

for $r = \infty$, the value of τ_L has to vanish. The pressure of the gas phase is represented by the ideal gas law

$$p = \rho_g k_B T_g / (\mu m_H), \quad (4.1)$$

with ρ_g , the gas density, k_B , the Boltzmann constant T_g , the temperature of the gas phase and μm_H , the product of the mean molecular weight of the gas phase and the atomic weight of the hydrogen atom. The mean molecular weight is determined as

$$\mu \approx \frac{n_H + 2n_{H_2} + 4n_{He}}{n_H + n_{H_2} + n_{He}} \quad (4.2)$$

and furthermore approximated with the constant value of $\mu = 1.26$. That equals to a ratio of H : He = 10:1. n_H, n_{H_2}, n_{He} are the particle number densities of the considered species.

4.2 The Restriction To C-Rich Cases

The mechanisms leading to the formation of carbonaceous dust in the stellar outflows are similar to those important for soot formation in flames, nevertheless the physical data related with the nucleation of dust grains in circumstellar environments are not sufficient to describe the processes in an adequate way. Even in C-rich environments, many questions remain unsolved. The formation of amorphous carbon is deduced from the conditions of grain formation under laboratory conditions. Thus, nucleation is treated as combustion or pyrolysis of hydrocarbons. Dust formation begins with nucleation of acetylene molecules. The further accumulation tends to PAH (Polycyclic Aromatic Hydrocarbon) molecules and through dehydration carbon grains are formed. In case of metalcarbides, there are laboratory studies investigating various metal-carbon clusters by laser induced plasma reactor experiments [57]. Results tend to consider a “cage” structure of the cluster, whatever the hydrocarbon reactant used. The mechanism leading to such a form are not yet well understood.

In the work of H.P. Gail & E. Sedlmayr [58], it is shown that in an oxygen-rich circumstellar outflow with dust forming elements like Si, Fe, and Mg, the nucleation of seed from the gas phase for subsequent growth is rather unlikely.

A.B.C. Patzer et al. [90] pointed out, that despite an enhancement of the nucleation theory with the inclusion of the effects of chemical non-equilibrium in the gas phase, different types of laboratory experiments or experimental studies concerning physical parameters underlying the nucleation process have to be required to benefit from the developed theoretical treatment.

K.S. Jeong [71] investigated in an oxygen-rich circumstellar environment the formation

of seed nuclei for subsequent growth of dust grains. The work led to the conclusion, that the formation of seed nuclei is not possible by nucleation of abundant gas phase species bearing the abundant dust forming element like Si, Fe, and Mg. The most abundant candidate for nucleation in oxygen-rich circumstellar shells, the SiO molecule nucleates at temperatures close to 600 K. Though, the alternative solid-forming element Al_2O_3 persisting at very high temperatures seemed to be virtually not present as monomer in the gas phase.

A. Ferrarotti [39], studied the behaviour of stars with an oxygen rich element mixture, applying a stationary wind model in spherical symmetry with focus on dust formation. Instead of solving the entire system of coupled equations at the radius of the star, the equation of motion is integrated after the sonic point when dust condensation sets in. Before the sonic point, the velocity is predetermined on the value of the sound velocity.

Heterogeneous nucleation seems not to apply to silicate grains, since Al_2O_3 is found as corundum and amorphous grain in presolar grains [36].

Only carbon grains seem to be suited for heterogeneous nucleation [22]. Other primary condensates suffer from the problem how to nucleate under the conditions prevailing in the outflow. Therefore, J.A. Nuth & F.T. Ferguson [70] investigated a new vapor pressure equation for SiO. The reported increases of the level of supersaturation in outflows are insufficient to induce SiO nucleation in most circumstellar outflows. They pointed out that a better understanding of the radiative transfer in a dust-forming stellar outflow would be helpful, as the calculated nucleation rate is very sensitive to the temperature. Furthermore, they complained problems with both the physical parameters used, with the application of classical nucleation theory to silicate condensation, as well as with the potential violation of the assumptions essential to the derivation of the model when it is applied to circumstellar outflows. They ask for some version of classical nucleation theory to provide a working model for silicate condensation.

Woitke et al. [113] pointed out, that the observed magnitude of mass loss-rates from oxygen-rich AGB-stars can not be reproduced even by detailed dynamical models with frequency-dependent formation of dirty dust grains. He noted that in case of previous grey models, e.g. K.S. Jeong [71] or A. Ferrarotti and H.P. Gail [40], the radiation pressure is overestimated by applying Rosseland mean opacities in O-rich cases. Even a combination of stellar pulsations and radiation pressure are therefore insufficient to drive a wind with a mass loss of observed strength.

S. Höfner [64] suggested with both estimated and results of dynamical radiation-hydrodynamical models, that micron-sized Fe-free grains are the solution to drive the wind. Though, the nucleation is not calculated. The seed nuclei are assumed as already formed.

In consequence, nucleation in oxygen-rich outflows is not yet fully understood. There is still a lack on required data. Hence, for the purpose of this work, the carbon rich case is exemplarily chosen, where only a single condensing species has to be considered and the classical theory of homogeneous nucleation can be used. In a first step, the equations are reduced to a simple two fluid case with gas and dust as components of the fluid.

4.3 Single Fluid Model

In order to implement the single fluid case, a program code was developed which utilises the explicit Euler method. The applied equations are presented in the following. The Euler method based on a finite difference approximation (e.g. [37]). The model was calculated in several step sizes to verify. Furthermore, the model was implemented in LIMEX. LIMEX is an extrapolation integrator for the solution of linearly-implicit differential-algebraic systems, developed by P. Deuffhard and U. Nowak, [34]. The equations representing the hydrodynamics are treated in stationary case with respect to spherical symmetry. The density of the gas phase ρ_g is derived from the time-constant mass loss \dot{M}_* of the considered stellar object

$$4 \pi r^2 \rho_g(r) v_g(r) = \dot{M}_*. \quad (4.3)$$

Since the amount of condensible material in the gas phase is assumed to be 10^{-3} times the non-condensable, the dust component is not taken into account.

The equation of motion of the gas component is treated as follows with respect to the singularity of the equation

$$\frac{\partial}{\partial r} v_g(r) = \frac{1}{v_g(r)} \left\{ \frac{2c_T^2(r)}{r} - \frac{k_B}{\mu m_H} \frac{\partial T(r)}{\partial r} + \frac{f_{\text{rad}}(r)}{\rho_g(r)} - \frac{f_{\text{grav}}(r)}{\rho_g(r)} \right\} / \{v_g^2(r) - c_T^2(r)\}. \quad (4.4)$$

The term c_T denotes the isothermal sound velocity.

$$c_T(r) = \sqrt{\frac{k_B T(r)}{\mu m_H}} \quad (4.5)$$

and μ , the mean molecular weight.

The grain growth and formation are covered by the equations of the moment method of dust formation as stated in Section 2.2.2 with all terms defined there, represented by the equations (2.114), respective (2.115).

The gravitational acceleration force f_{grav} is represented by the equation (2.39), so is the radiative acceleration f_{rad} represented by the equation (2.40), the external force due to the radiative acceleration in case of radiative equilibrium, with $4 \pi H = L_*/(4 \pi r^2)$,

and χ_{H} are the flux weighted opacities of the gas or dust species. The treatment of the gas phase follows the work of Fleischer [41]. Considering C-stars, a reduced set of hydrocarbons, H, H₂, C, C₂, C₂H₂, is used to calculate the particle densities of the condensing species. The included hydrocarbons are treated in chemical equilibrium and are therefore time-independent. They depend on the temperature and the density of hydrogen $\langle n_{\text{H}} \rangle$, and the chemical abundances ϵ_i of each element, relative to hydrogen. The partial pressure of p_i is derived from the law of mass action, assuming the validity of ideal gas law and chemical equilibrium. It yields a system of two quadratic equations, being aware that the constraint of the set of hydrocarbons leads to an underestimation of the nucleation rate J_* . The chemistry assumes solar abundances [3].

L_*/L_{\odot}	T_* (K)	C/O ratio
$4.35 \cdot 10^3$	$2.0 \cdot 10^3$	2.0
$7.64 \cdot 10^3$	$2.0 \cdot 10^3$	2.0
$1.28 \cdot 10^4$	$2.0 \cdot 10^3$	2.0

Table 4.1: The implemented models

The radiative transfer as introduced in Section 2.3 (equation (2.145)), leads to an additional differential equation for the value τ_L . This value τ_L defines the optical depth applied in the radiative transfer after L.B. Lucy [84], [83].

$$\frac{d\tau_L}{dr} = -\kappa\rho_g \left(\frac{R_*^2}{r^2} \right). \quad (4.6)$$

wherein $\lim_{r \rightarrow \infty} \tau_L(r) = 0$ is the boundary condition for the optical depth and κ the mass absorption coefficient. The value of κ is derived from the third moment of the dust equations K_3 [43], [48]

$$\kappa = \frac{3V_0}{4} \frac{K_3 Q'(T)}{\rho_g} = \frac{\pi a_0^3 K_3 5.9T}{\rho_g} \quad (4.7)$$

with a_0 , the hypothetical monomer radius and $Q'(T)$ [12], the extinction efficiency of the grain divided by the grain radius.

The Figures 4.1, 4.2, 4.3, 4.6, 4.5, 4.4 show the results for three different stellar luminosities.

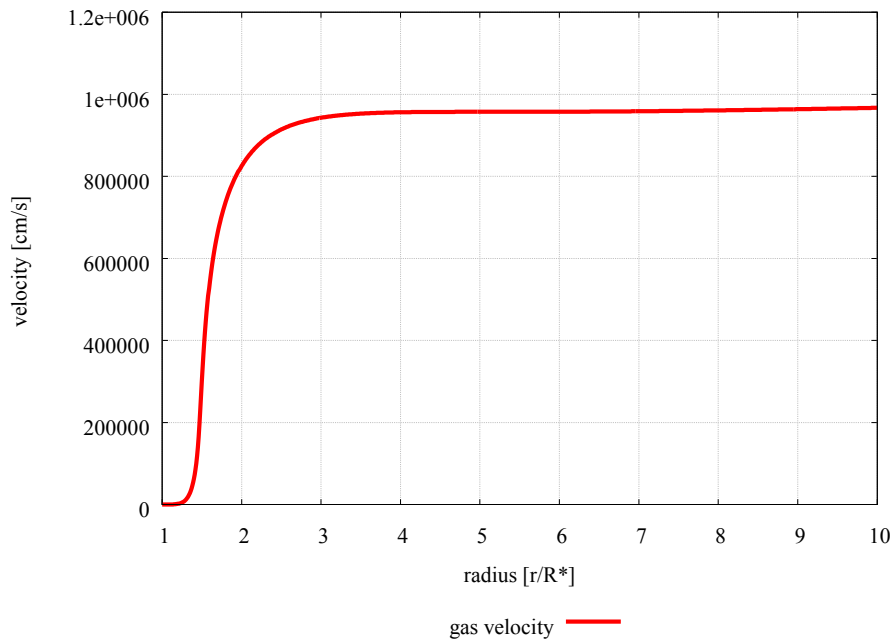


Figure 4.1: Velocity structure of a stellar wind with a luminosity of $4.35 \cdot 10^3 \cdot L_{\odot}$ (Euler-method)

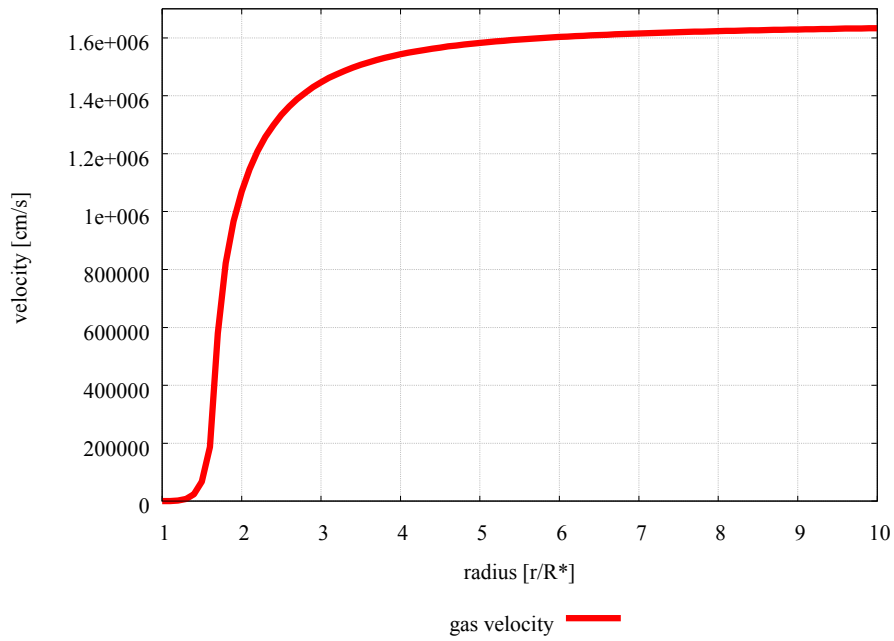


Figure 4.2: Velocity structure of a stellar wind with a luminosity of $7.64 \cdot 10^3 \cdot L_{\odot}$ (Euler-method)

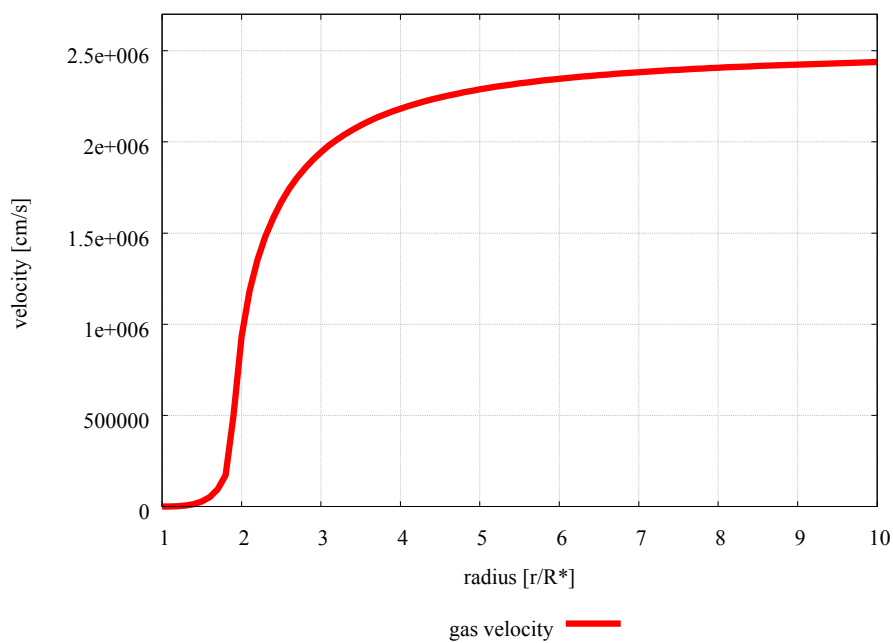


Figure 4.3: Velocity structure of a stellar wind with a luminosity of $1.28 \cdot 10^4 \cdot L_{\odot}$ (Euler-method)

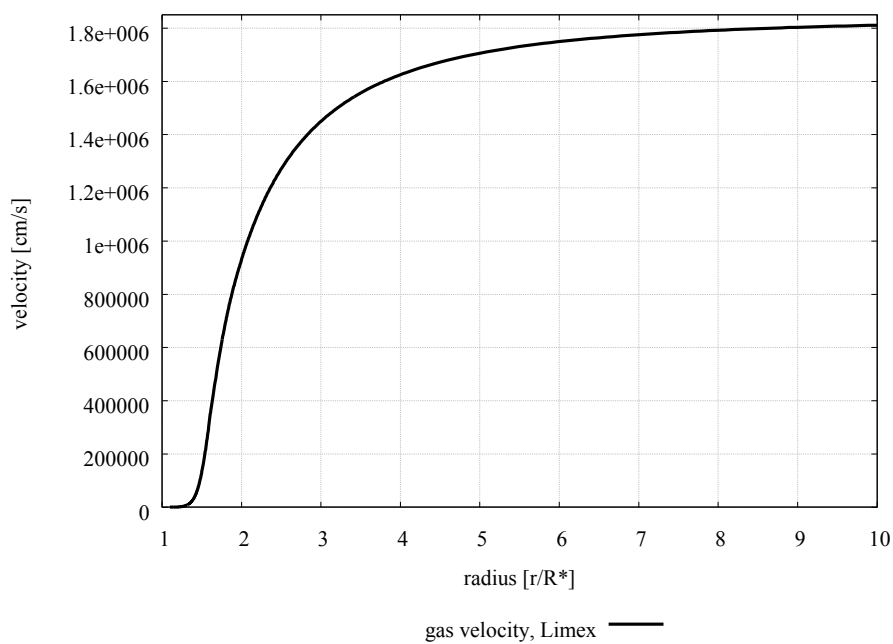


Figure 4.4: Velocity structure of a stellar wind with a luminosity of $4.35 \cdot 10^3 \cdot L_{\odot}$ (Limex)

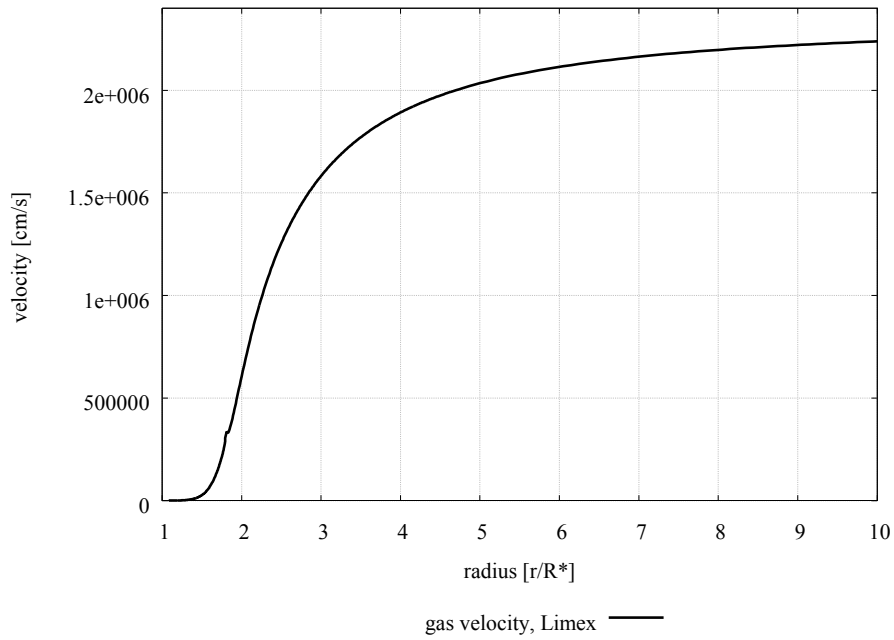


Figure 4.5: Velocity structure of a stellar wind with a luminosity of $7.64 \cdot 10^3 \cdot L_{\odot}$ (Limex)

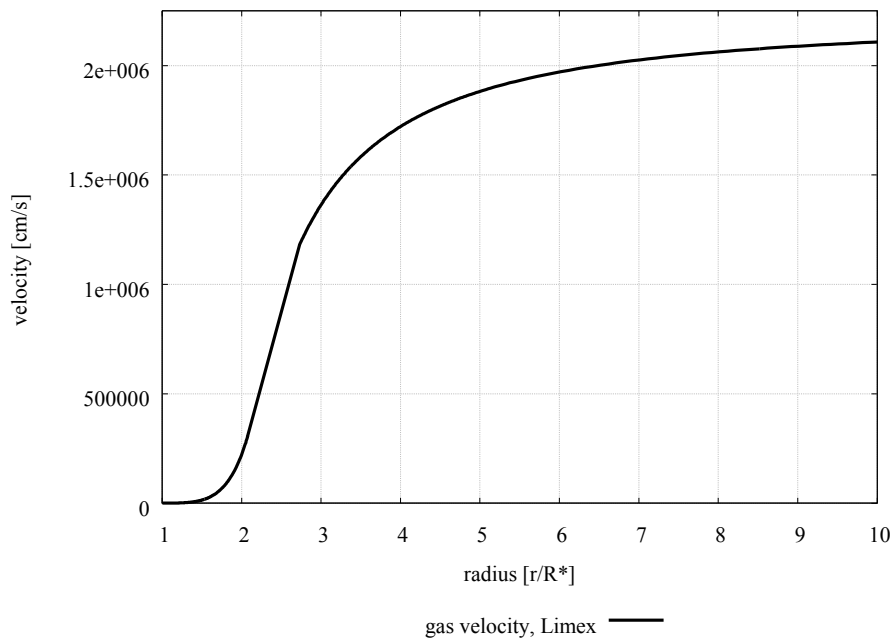


Figure 4.6: Velocity structure of a stellar wind with a luminosity of $1.28 \cdot 10^4 \cdot L_{\odot}$ (Limex)

The LIMEX implementation versus the implementation in the Euler method showed smaller values for the mass loss due to smaller initial values for the gas velocity. The comparison of the results is shown in Figure (4.7). The resulting final velocities are comparable. Then, in addition, these two models are compared with the implementation as presented by Gail & Sedlmayr (Dust formation in stellar winds III [51]), cf. Table 4.2. In this case, in comparison with the two other model calculations, the final velocities are smaller, though the mass loss was comparable, exceptional for the luminosity of $L_*/L_\odot = 7.64 \cdot 10^3$. Nevertheless, the similarity of the variations of the obtained values by the Euler method compared to Limex as to the results presented by Gail & Sedlmayr and as well as Limex compared to the method as presented by Gail & Sedlmayr show the same qualitative behaviour. The result of the developed program code utilising the explicit Euler method is considered being sufficient close and therefore validated. So, the simple Euler method therefore served as a basic tool for the next studies.

model	L_*/L_\odot	$v_\infty/(\text{cm/s})$	\dot{M}/M_*
Euler	$4.35 \cdot 10^3$	$1.15 \cdot 10^6$	$5.33 \cdot 10^{-6}$
	$7.64 \cdot 10^3$	$1.6 \cdot 10^6$	$1.64 \cdot 10^{-5}$
	$1.28 \cdot 10^4$	$2.55 \cdot 10^6$	$3.3 \cdot 10^{-5}$
Limex	$4.35 \cdot 10^3$	$1.84 \cdot 10^6$	$1.83 \cdot 10^{-6}$
	$7.64 \cdot 10^3$	$2.38 \cdot 10^6$	$7.89 \cdot 10^{-6}$
	$1.28 \cdot 10^4$	$2.22 \cdot 10^6$	$2.98 \cdot 10^{-5}$
Dust formation in stellar winds III [51]	$4.35 \cdot 10^3$	$1.28 \cdot 10^6$	$3 \cdot 10^{-6}$
	$7.64 \cdot 10^3$	$1.62 \cdot 10^6$	$1 \cdot 10^{-5}$
	$1.28 \cdot 10^4$	$1.83 \cdot 10^6$	$3 \cdot 10^{-5}$

Table 4.2: Comparison of the implemented models

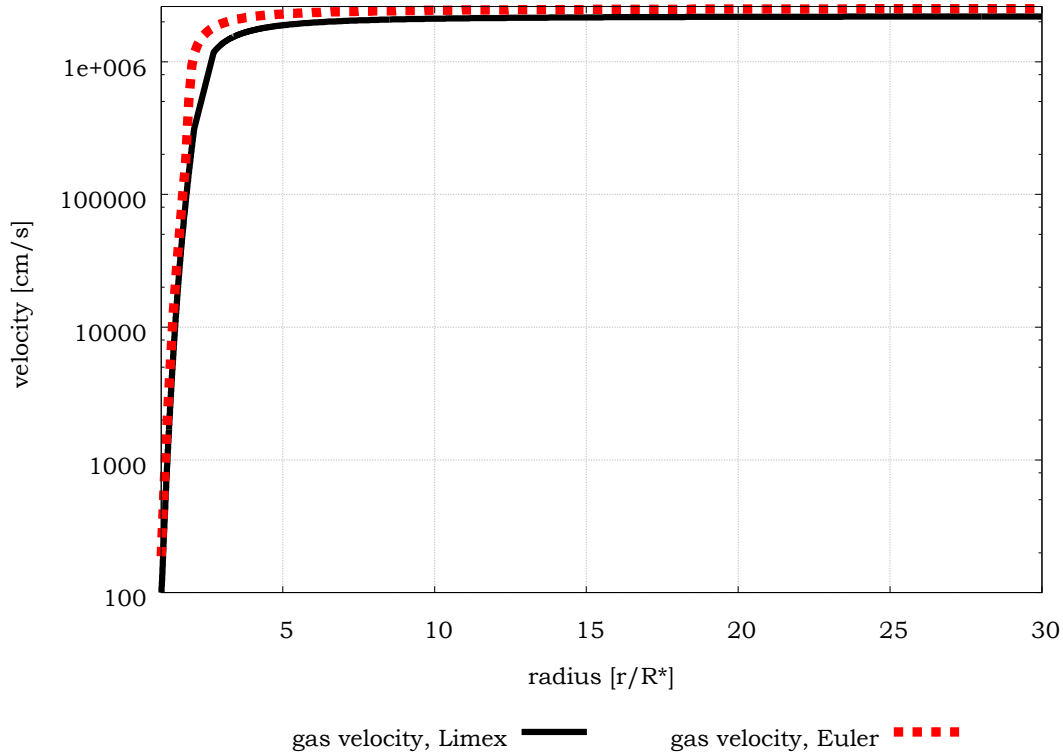


Figure 4.7: Comparison of the implemented numerical models: E.g. velocity structure of a stellar wind with a luminosity of $1.28 \cdot 10^4 \cdot L_{\odot}$

4.4 Two-Fluid-Model

In order to implement the multicomponent description in the Euler method, the equations of the single fluid model are extended in a first step to a simple two fluid case. This is applicable in circumstellar shells with a high C/O ratio, and therefore only one single condensing species has to be considered. The multicomponent model is simplified to prove the existence of a solution of the coupled system of ordinary differential equations in conjunction with the equations of the dust-complex with chemistry.

In order to determine the differential-algebraic-equation system in a consistent way, all terms are derived from setting up the equations. In comparison to e.g. D. Krüger (see Section 3.1), who used a simplified two fluid description implemented in a stationary model, in the present work, all terms are included. The aim is to get a consistent description in this way. The time-dependent models (e.g. Simis [102]) include exchange terms for the equation of motion derived from the continuity equation . Otherwise, the source term, representing the condensation of dust from the gas is furthermore not specified in these models.

4.4.1 Applied Equations

The model is treated in radiative equilibrium (RE). The following equations represent the hydrodynamics with the continuity equation, the equations of motion, both for the gas phase as well as the dust component in stationary case with respect to spherical symmetry

$$\frac{1}{r^2} \frac{\partial}{\partial r} (r^2 \rho_g(r) v_g(r)) = q_g(r) \quad (4.8)$$

and

$$\frac{1}{r^2} \frac{\partial}{\partial r} (r^2 \rho_d(r) v_d(r)) = q_d(r). \quad (4.9)$$

Instead of not solving dust conservation equation and deriving the mass density of the dust from the third moment of the dust formation K_3 , the applied terms $q_g(r)$ and ($q_d(r)$) are referred to the equations (2.12) and (2.13) in Section 2.1.1. These terms are not considered in previous works in this form.

All terms involved in the following equations of motion are introduced in Section 2.1.2.2. The resulting equations for the gas and the dust in stationary case with respect to spherical symmetry are for the gas component

$$\rho_g(r) v_g(r) \frac{\partial}{\partial r} v_g(r) = -\frac{\partial}{\partial r} p_g(r) + f_{g,\text{rad}}(r) - f_{g,\text{grav}}(r) + f_{g,\text{drag}}(r) - q_{g,\text{acc}}(r) \quad (4.10)$$

and the dust motion equation equals to

$$\rho_d(r) v_d(r) \frac{\partial}{\partial r} v_d(r) = f_{d,\text{rad}}(r) - f_{d,\text{grav}}(r) - f_{d,\text{drag}}(r) - q_{d,\text{acc}}(r) \quad (4.11)$$

with the gravitational force $f_{\text{grav}}(r)$ (equation (2.39)), and

$$q_{d,\text{acc}}(r) = v_d(r) q_d(r) = J_*(r) m_d v_d(r). \quad (4.12)$$

The drag force $f_{g,d,\text{drag}}(r)$ follows the work of D. Krüger [76]. For reference, see equation (3.7). The terms $q_{g,\text{acc}}(r)$ and $q_{d,\text{acc}}(r)$ are introduced in consequence of the exchange terms resulting from the continuity equations both for gas and for dust. They are definite by deduction. After total derivation of the ideal gas law (4.1), the two components are included in the momentum equation. The equation of motion of the gas component is treated as follows with respect to the singularity of the equation

$$v_g(r) \frac{\frac{\partial}{\partial r} v_g(r) = \frac{\frac{2c_T^2(r)}{r} - \frac{k_B}{\mu m_H} \frac{\partial T(r)}{\partial r} + \frac{f_{g,\text{rad}}(r)}{\rho_g(r)} - \frac{f_{g,\text{grav}}(r)}{\rho_g(r)} + \frac{f_{g,\text{drag}}(r)}{\rho_g(r)} - \frac{q_{g,\text{acc}}(r)}{\rho_g(r)}}{v_g^2(r) - c_T^2(r)}}{v_g^2(r) - c_T^2(r)}}{v_g^2(r) - c_T^2(r)}. \quad (4.13)$$

The term c_T denotes the isothermal sound velocity. Since the velocity distribution is assumed to be proportional to the size of the grains, the size of the drift velocity and

therefore the drag force is assumed average-sized.

The radiative transfer is introduced in Section 2.3, so is the grain growth and formation are covered in Section 4.3 with further definitions given there. The set of stellar parameters follows the single fluid model, and may be seen there (Table (4.1)).

4.4.2 Results of the Two-Component Description

Based on the equations of the last Section (4.4.1), the effect of two components was studied. The underlying model is realised in a simple Euler method as developed in the single fluid case, with the model data of $\dot{M} = 2.4 \cdot 10^{-5} \cdot M_*/\text{year}$, the mass loss per year and $L_* = 1 \cdot 10^4 L_\odot$, the stellar luminosity. With these parameters, the single fluid model provides a physically solution for the coupled case. For the two-fluid-model, each component was described by its own equation both for mass and moment conservation as pointed up. They were coupled as by coupling terms issued from elaboration of the extended equations for two components as by the drag force. The results are presented in the form of a reduced figure in order to point out the critical values at the onset of dust formation.

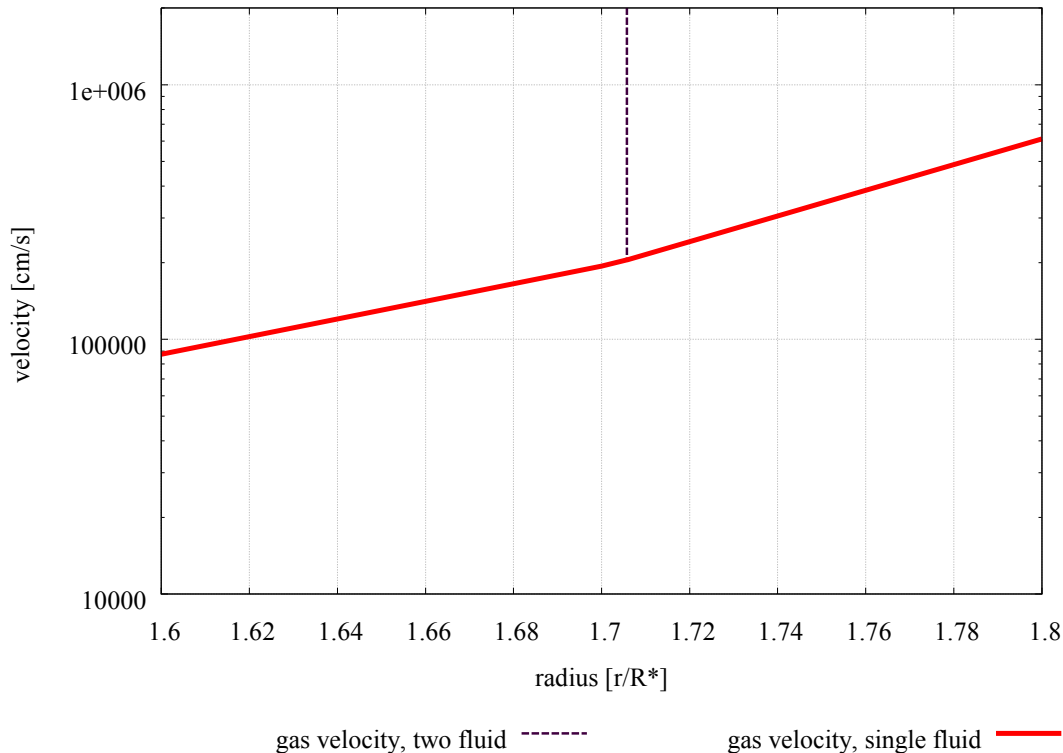


Figure 4.8: Velocity structure: Comparison of the single fluid description and the two fluid description of a stellar wind with a luminosity of $1 \cdot 10^4 \cdot L_\odot$

The Figure 4.8 shows, that the results of the implementation suffered from the small amount of the dust density by dust formation onset. This led to a high influence of the drag force by decelerating the dust component. The resulting gradient of the dust velocity was highly negative and led to a dust velocity lower than the gas velocity. In consequence, the drift velocity turned negative and the system of equations collapsed. Even by substituting the gas density differential equation for the constant mass loss equation, neglecting the mass exchange between the two components, the results with regard to the role of the drag force show the same behaviour.

4.5 Decoupled Description of the Dust Component

The disappointing results of the two component description of the fluid led to further considerations relating to the behaviour of the several parameters at the onset of dust formation. So, at the beginning, the model is reduced to the decoupled case leading to different studies analysing the onset values. These studies refer to the work of D. Krüger (Section 3.1). The equations applied on his work are extended by dust formation and growth and used for studies about the behaviour of the dust component and the influence of, and respective for, the dust velocity in Section 4.4. Though the equations D. Krüger implemented suggest a two component treatment of the fluid, most likely he lately applied the equations representing the single fluid case with an extension for the dust component based on an average grain size. These extensions of the equations he finally applied are extracted by the left over of his computed models. The Figure (4.9) shows a reproduction D. Krüger similarly had applied of a decoupled fluid with derived drift velocity. In this reproduction however, the dust moments are calculated.

The principal equations are these from the Section 4.3 with assumptions and restrictions indicated there. In addition to these basic equations, the following equations are implemented without coupling with the gas component. The extension component consists therefore of a mass flux differential equation for the dust component, represented by the dust velocity v_d multiplied by the density of the dust component ρ_d . They describe the dust component for the density as well as for its velocity. To begin with the mass flux j , it is assumed that the product of velocity and density is treated as an entity. The resulting equations in their time independent, spherical symmetric description are stated as follows:

$$\frac{1}{r^2} \frac{\partial}{\partial r} (r^2 \rho_d(r) v_d(r)) = \frac{1}{r^2} \frac{\partial}{\partial r} (r^2 j_d(r)) = 4 \pi \cdot J_*(r) \cdot m_d. \quad (4.14)$$

The equation of motion of the dust component provides the equilibrium equation between deceleration by moment transfer, the gravitation and the radiative acceleration

$$f_{\text{drag}}(r) = -\frac{G M_* \rho_d(r)}{r^2} + f_{\text{rad}}(r). \quad (4.15)$$

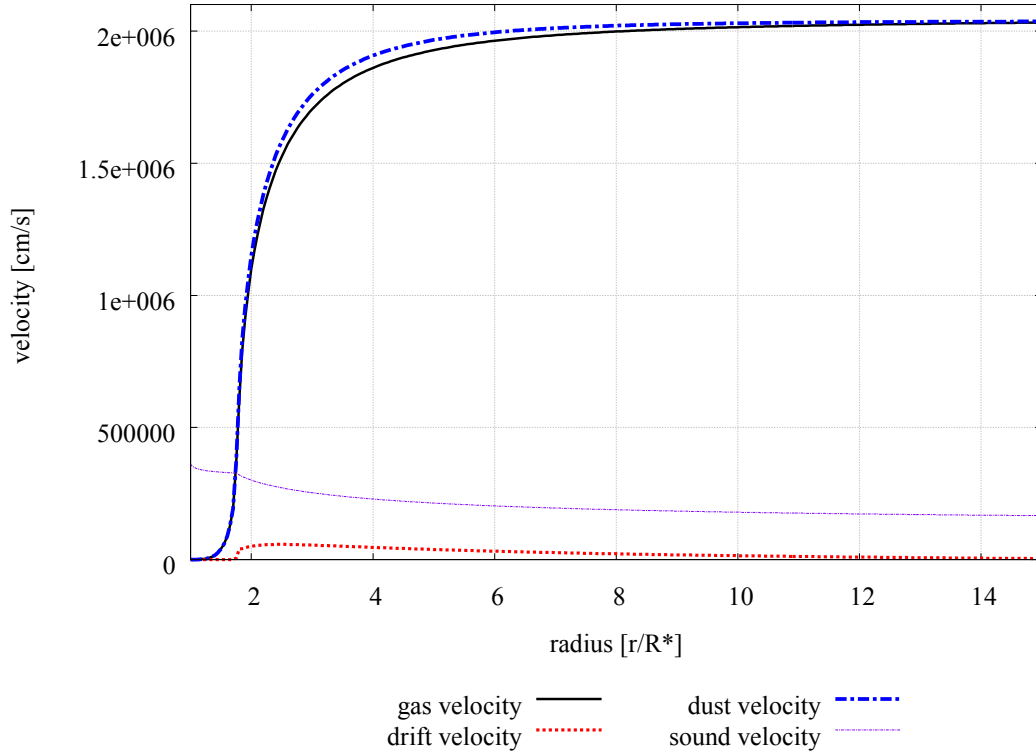


Figure 4.9: The decoupled model with derived drift velocity with a stellar luminosity of $1 \cdot 10^4 \cdot L_{\odot}$

So, the equilibrium between deceleration by moment transfer, the gravitation on the one hand and the radiative acceleration on the other hand is used to calculate the drift velocity v_{drift} using the drag force f_{drag} [32], (Section 3.1)

$$f_{\text{drag}}(r) = \rho_{\text{g}}(r)n_{\text{d}}(r)\pi a_{\text{d}}^2(r)v_{\text{drift}}(r) \left[\left(\frac{4}{3}v_{\text{th}}(r) \right)^2 + v_{\text{drift}}^2(r) \right]^{1/2}. \quad (4.16)$$

The drift velocity v_{drift} is the result of an algebraic equation. The dust velocity is derived by the drift velocity with $v_{\text{drift}}(r) = v_{\text{d}}(r) - v_{\text{g}}(r)$. Since the product of velocity and density is treated as an entity the calculated mass flux density j divided by the dust velocity v_{d} provides the dust density

$$\rho_{\text{d}}(r) = \frac{j_{\text{d}}(r)}{v_{\text{d}}(r)}. \quad (4.17)$$

The mass of a dust grain is represented by $m_{\text{d}} = m_{\text{C}} \cdot a_0^3 \cdot \frac{K3^3}{K0^3}$, wherein m_{C} determines the mass of a carbon monomer and a_0 the hypothetical monomer radius. In the model Krüger applied, the size of the grain is predetermined and therefore does not refer to

the moment equations. The model parameters are applied as follows: The mass M_* is set equal M_\odot , the stellar temperature amounts to 2000 K and $\dot{M} = 2.4 \cdot M_*/\text{year}$, the mass loss per year. The C/O ratio is set equal 2.0. At the radius of the star, the velocity starts with the value of $v_0 = 1.236 \cdot 10^2 \text{cm/s}$ and reaches the value of $v_\infty = 2.069 \cdot 10^6 \text{cm/s}$ at the radius of $100 R_*$. The critical point is located at 1.73 times the radius of the star. Without exception, these values (Figure 4.10) are valid for the following studies.

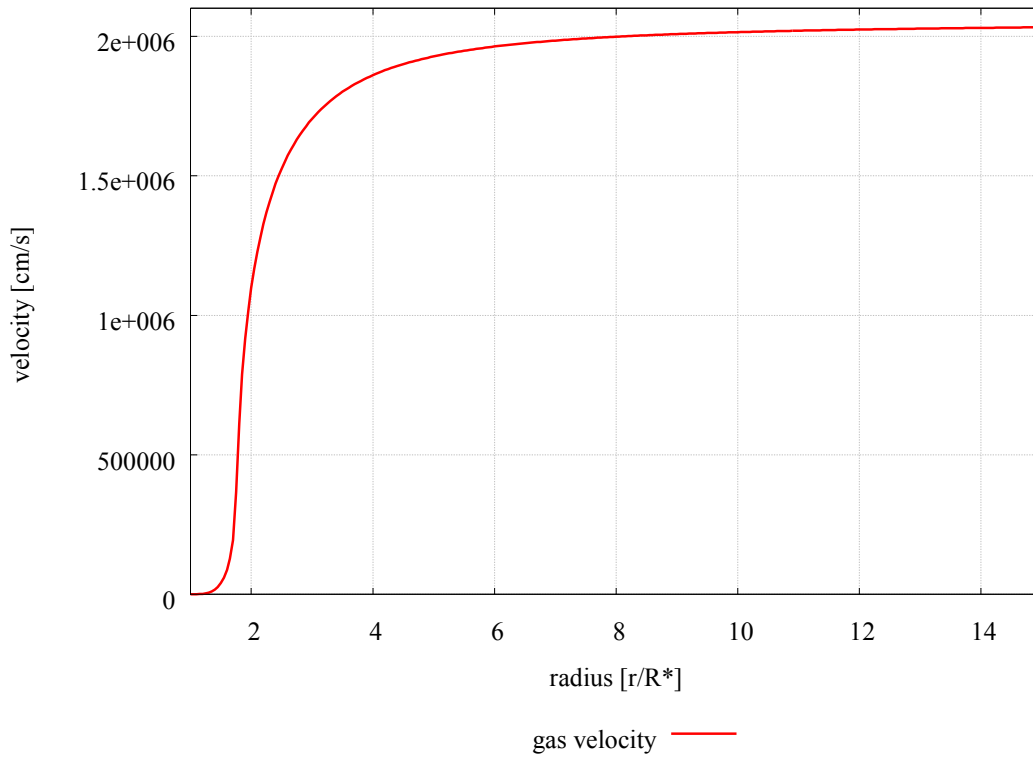


Figure 4.10: Velocity structure of a stellar wind with a luminosity of $1 \cdot 10^4 \cdot L_\odot$ (Euler-method)

This ansatz is used as a basis to modify the results from the single-fluid-model. The aim is to elaborate some onset conditions for starting the two-fluid-model, and clarify the resulting difficulties calculating the drag force. The aim is to avoid the difficulties based on the high influence of decreasing back coupling by the drag force in the two-fluid-model.

4.5.1 Results of the Decoupled Description and Consequences for the Two Fluid Description

The following study of the mass flux description is focused on the behaviour around the onset point of dust formation. Due to the modality of treatment of the dust equation of motion, further exceeding results are not expected, though the equilibrium equation does not apply for outer regions where the gradient of the dust velocity is not expected to vanish.

r/R_*	$\rho_g/(g/cm^3)$	$\rho_d/(g/cm^3)$	$v_{\text{drift}}/(cm/s)$
1.707000e+000	5.997842e-014	0.000000e+000	0.000000e+000
1.707350e+000	5.974379e-014	1.563831e-028	0.000000e+000
1.707360e+000	5.973709e-014	3.127704e-028	0.000000e+000
....			
1.745000e+000	3.564853e-014	6.484791e-022	0.000000e+000
1.746000e+000	3.481854e-014	6.729802e-022	0.000000e+000
1.747000e+000	3.422216e-014	7.002767e-022	3.734633e-003
1.748000e+000	3.366699e-014	7.270024e-022	1.009205e-002
1.749000e+000	3.313413e-014	7.527687e-022	1.699015e-002

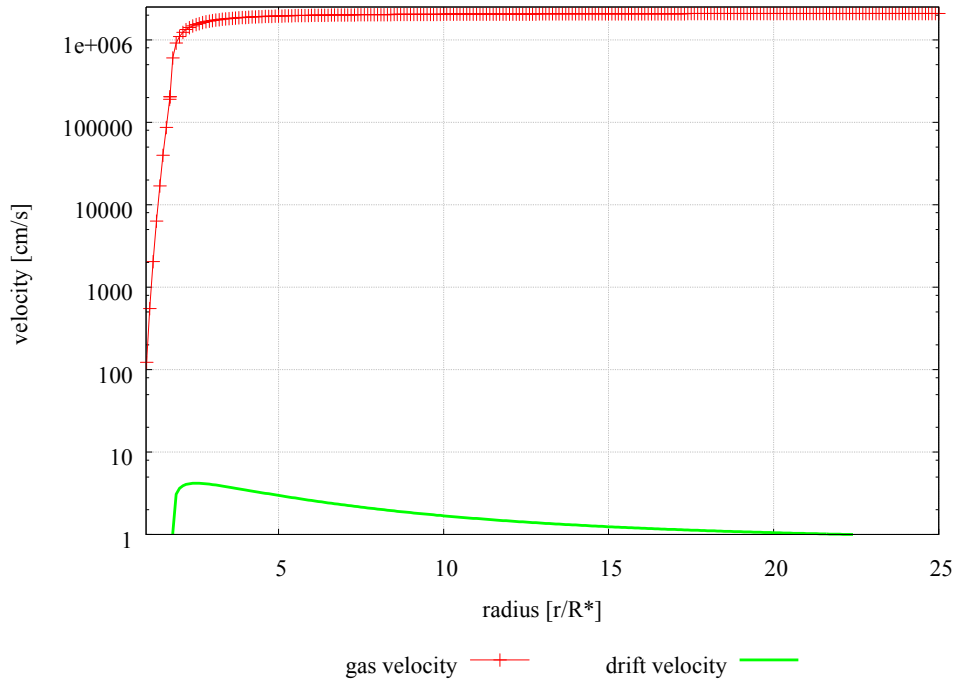


Figure 4.11: Gas and drift velocity structure

The Table 4.5.1 shows the resulting dust density around the onset point in the range of 10^{-28}g/cm^3 . The nature of the equilibrium equation allows a solution for the drift velocity just for radiative acceleration terms $L_* \cdot \kappa_d / (4 \pi c)$ greater than the gravitational term $G \cdot M_*$. The Figure 4.11 shows the gas and drift velocity structure calculated by the equilibrium equation. This model forms the basis of the modified two-fluid-system. In comparison to the results of the original two-fluid-model, the starting values of the dust density with 10^{-28}g/cm^3 and 10^{-29}g/cm^3 are almost about the same range. So, if in case of decoupled description the size of the dust density onset does not increase in a considerable dimension, the two fluid model was not expected to provide other results as shown before. In order to examine the behaviour of the equations, the model was now varied just around the onset of dust formation. There, the two fluid model is calculated as coupled single fluid. The equations are these of Section 4.4.1. As the drag force tended to get collapsed the system of equations, the equilibrium equation as had applied by D. Krüger is used to obtain a value for the drift velocity, (equation 4.16). The grain formation and growth is described as indicated in Section 2.2.2.

If ever the acceleration term due to the two fluid description exceeds this one of the single fluid description, the model is expected to run on the two fluid description applying the full set of equations of the two fluid model (Section 4.4.2). The Figures 4.12, 4.13, 4.14 show the behaviour of single aspects of the fluid and the related values.

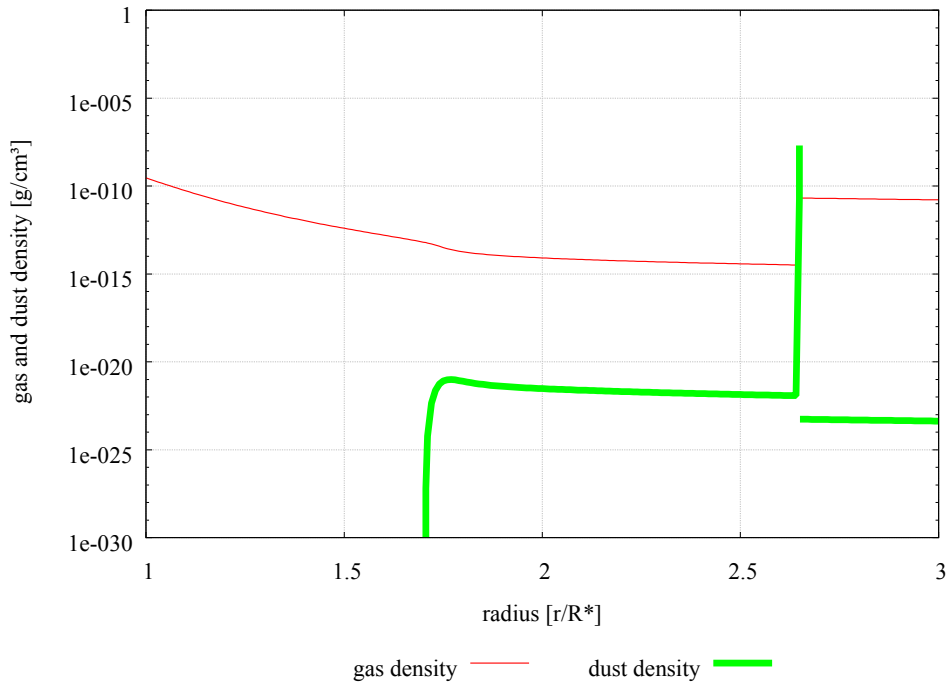


Figure 4.12: Dust and gas densities, calculated as coupled single fluid around the onset of dust formationl

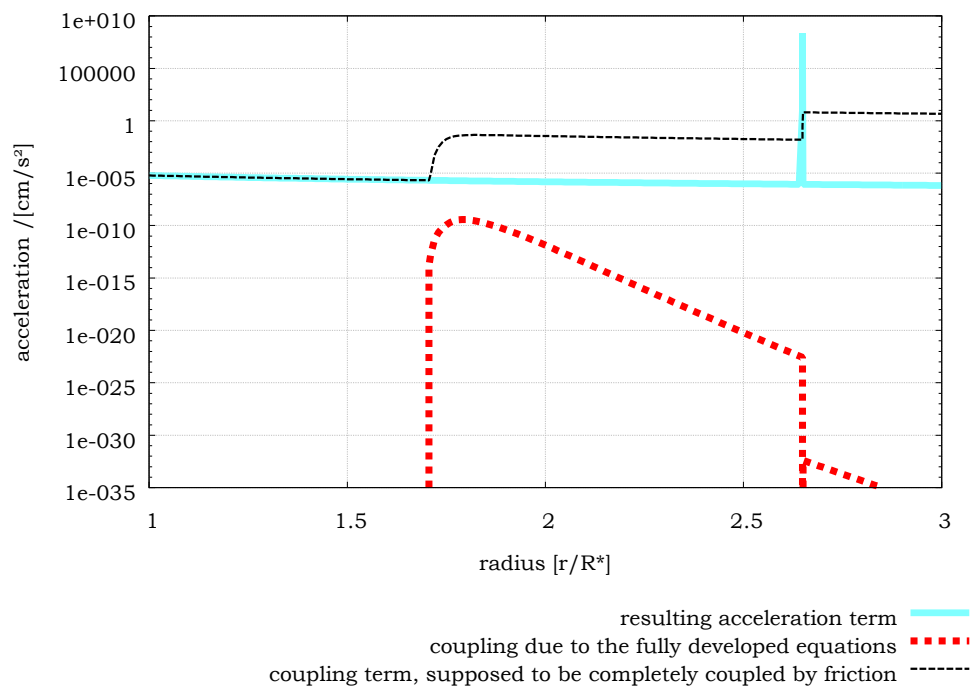


Figure 4.13: Acceleration terms, calculated as coupled single fluid around the onset of dust formation

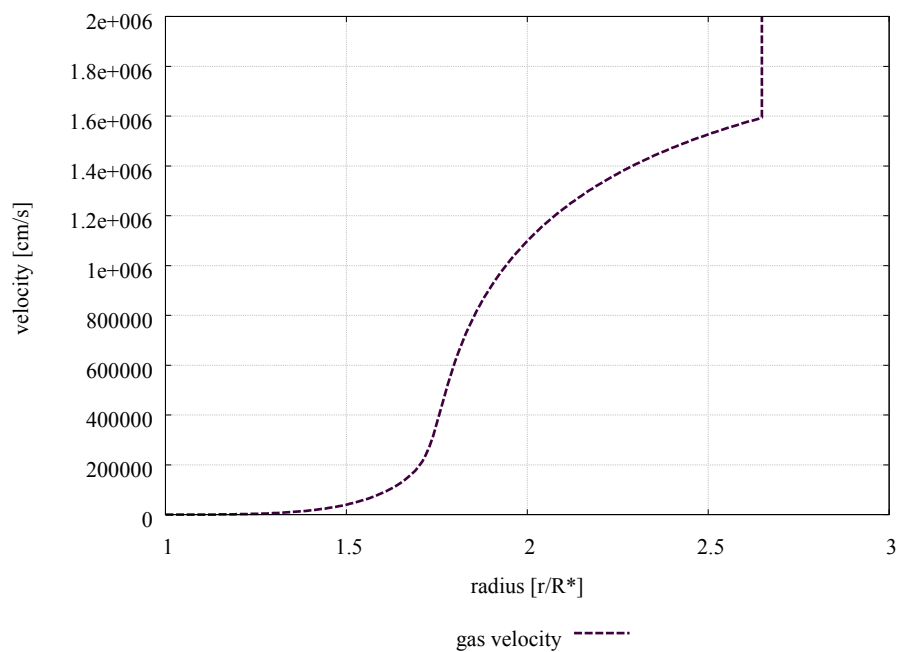


Figure 4.14: Velocity structure, calculated as coupled single fluid around the onset of dust formation

The listed figures show the non-consistency of the change between the two methods. The desired smooth changeover lacks by the jump around the onset of the two fluid description located around $2.649 R_*$. The Figure 4.12 shows a single peak of increasing dust density. Then, after leaping, the dust density increases below the value before. In addition, the gas density increases in a non-realistic way. The resulting calculated mass loss \dot{M} therefore is incorrect. Given that $f_{\text{rad}}(r)$ represents the acceleration term, coupled by friction, and $f_{\text{g,rad}}(r) + f_{\text{g,drag}}(r) - q_{\text{g,acc}}(r)$ represents the acceleration due to the two-fluid description, the Figure 4.13 does not show any congruence of the values of acceleration for both cases. The coupling term $-q_{\text{g,acc}}(r)$ does not provide a significant change in the amount of acceleration. Therefore, the drag force f_{drag} increases immediately when the acceleration term due to the two fluid description exceeds this one of the single fluid description. The gas velocity increases due to the acceleration term (Figure 4.14).

The abandonment of the differential equation for the gas phase does not improve the result either. The following Figure 4.15 shows a fortified increase of the dust density after leaping, exceeding the value of the gas density. The velocity structure resembles the structure with differential equation for the gas phase. As for the fully described system, the equations turned to collapse.

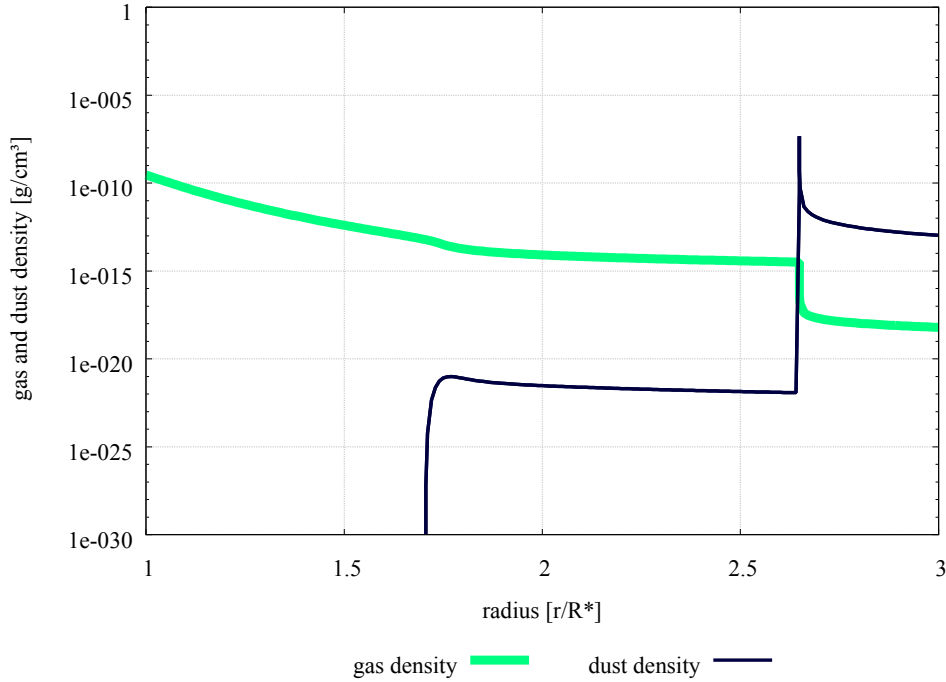


Figure 4.15: Density structure of the model without a differential equation for the gas component calculated as coupled single fluid around the onset of dust formation

The results of the study indicate a need to clarify the behaviour of the equations at the onset point of the dust formation. At the point where the coupled case has to be substituted by the two component equations, the drag force and the coupling term increase in consequence of the non-realistic increasing dust density.

4.6 Closer Inspection of the Equations of the Model

Given that the results of the two-component description suffer from the lack of consistency, the equations underlying the model are analysed in detail. Operating on the premise that the product of the dust velocity and the dust density was represented by the mass flux density $j(r) = \rho_d(r) \cdot v_d(r) = n_d(r) \cdot m_C \cdot v_d(r)$, as well as the dust density may be neglected against the gas density, two different approaches to obtain data both for dust density and velocity are applied in one model. The model bases on the single fluid data velocity structure with added equations from Section 4.5 with the luminosity of $L_* = 10^4 \cdot L_\odot$ and the mass loss $\dot{M} = 2.04 \cdot 10^{-5} M_*/\text{year}$ (Figure 4.10). The comparison consists in two cases where the mass flux density provides along with the moment equations for the dust formation the dust density as well as the dust velocity and besides the drag force.

On the one hand, the dust density is derived by the third moment of the dust formation and growth equations $\rho_d(r) = K_3(r) \cdot \rho_{\text{solid}} \cdot a_0^3 \cdot \pi \cdot \frac{4}{3}$, with a_0 , being the hypothetical monomer radius and ρ_{solid} , the density of the grain material. This equation refers to the work of Simis, Section 3.2. The mass of a dust grain is calculated by $m_d = \frac{K_3}{K_0} \cdot m_C$. Herein means m_C the mass of a monomer (see equation 2.128). The velocity of the dust $v_d(r)$ is the result of the division of the mass flux density $j(r)$ by the density of the dust $\rho_d(r)$. So, the resulting drift velocity leads to the drag force f_{drag} (equation 4.16).

On the other hand, the mass flux density applied to the velocity structure of the coupled single fluid model yields the values for the drift velocity v_{drift} by an algebraic equation (and therefore the dust velocity) based on the equilibrium equation for the gradient of the dust velocity (see Section 4.5). The dust formation is calculated as stated in Section 4.3. The result of the mass flux density divided by the dust velocity provides the dust density $\rho_d(r) = \frac{j(r)}{v_d(r)}$. The aim of the study is to examine the obtained results around the dust formation onset in order to compare the equality of the approaches.

The resulting Table 4.3 and Figures 4.16, 4.17, and 4.18, show the differences between the two methods describing the drift velocities as well as the dust densities around the onset of dust formation. Both methods bases on the moments of the dust formation

equations and are coupled by the nucleation rate J_* .

The effect on the acceleration term reveals the excessive driving force on the gas phase in the beginning dust formation zone. The drift velocity based on the equilibrium equation for the dust differential equation starts at $1.747 R_*$.

n term. The drift velocities derived from the moment equations of dust formation and growth are in the order of $v_{\text{drift}} \approx 10^{11}$. These values do not seem realistic. The comparison between the values of the dust density for both cases are in the order 10^6 . So, these results lead to the suggestion that different types of description not only result in non-realistic values, but also may not allow a bidirectional conversion between.

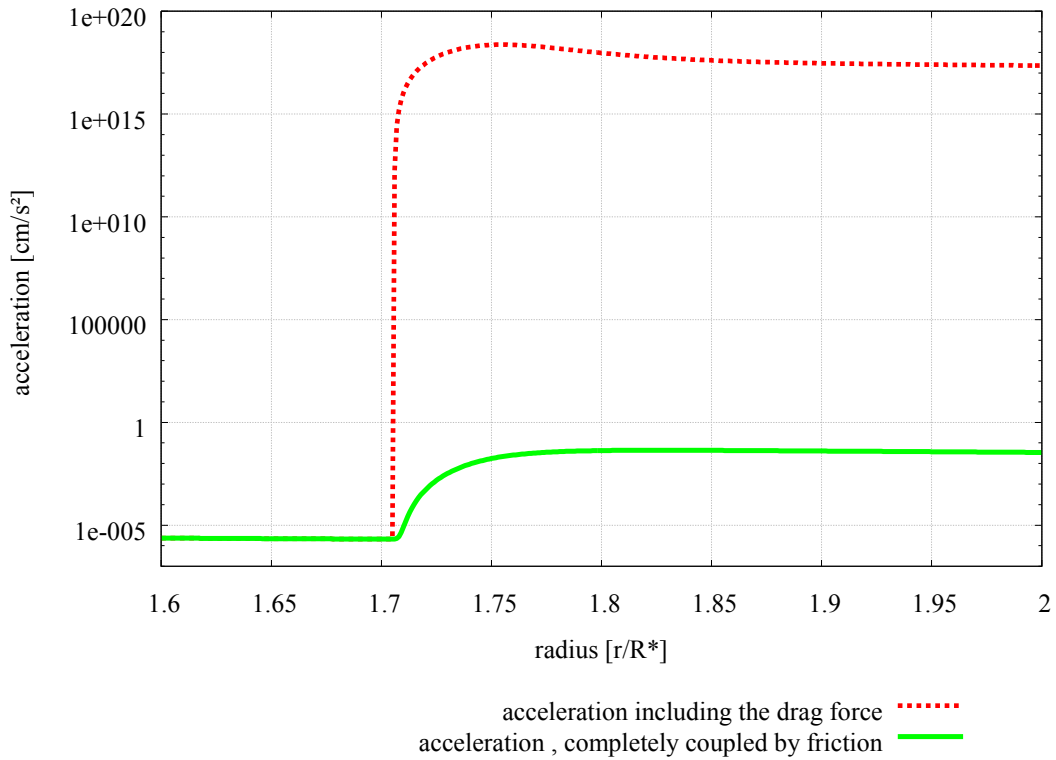


Figure 4.16: Comparison of the acceleration terms

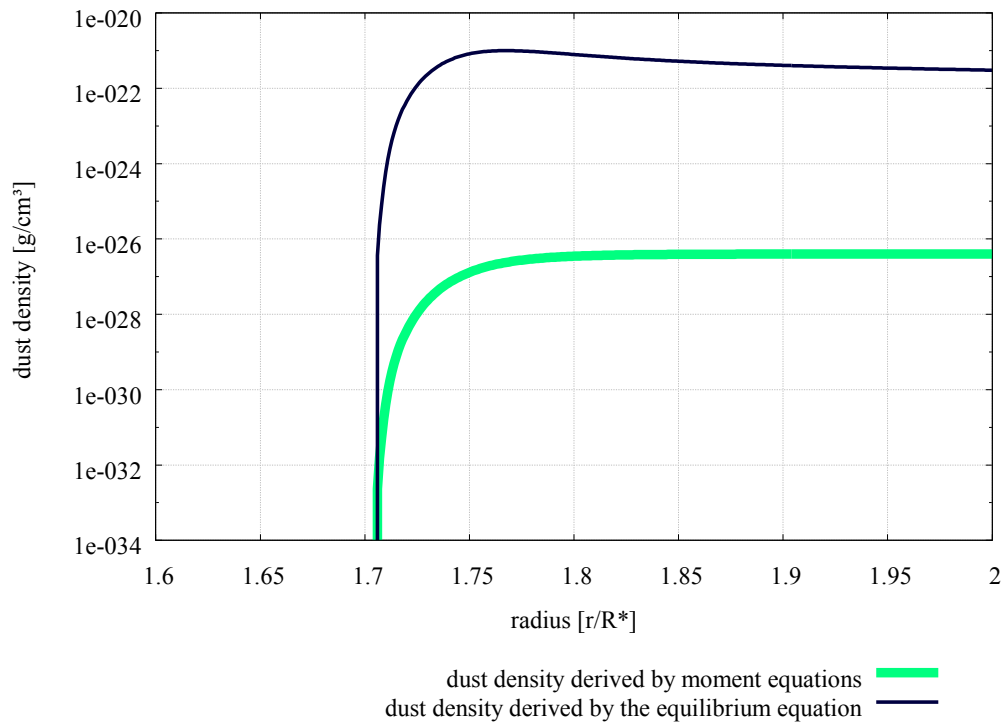


Figure 4.17: Comparison of the dust densities

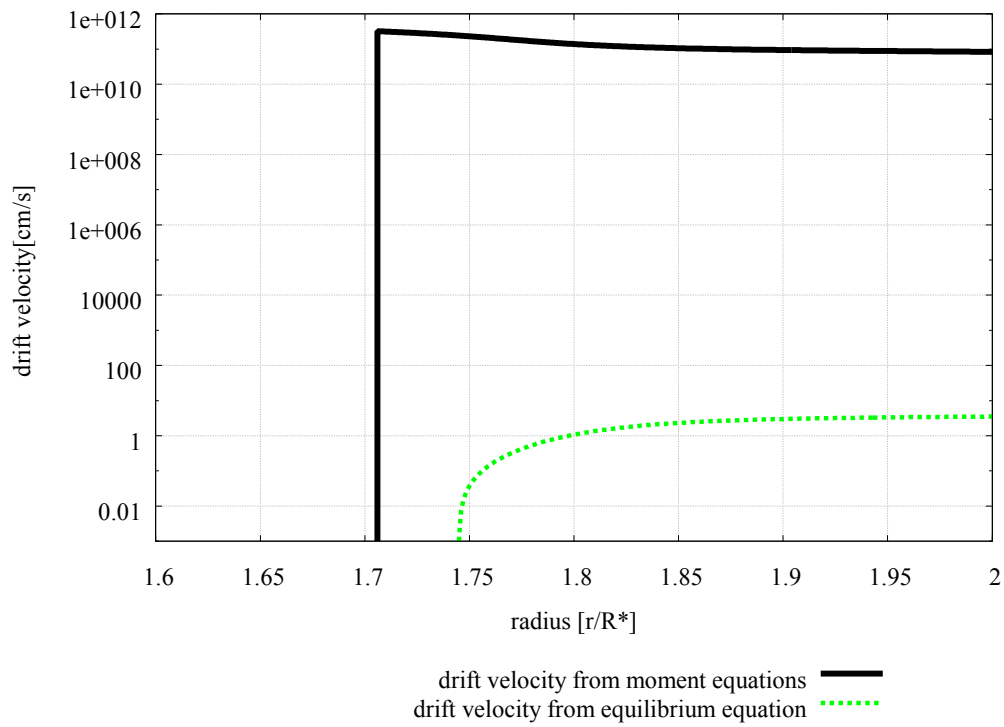


Figure 4.18: Comparison of the drift velocities

r/R_*	values derived by moment equations with f_{drag}				values based on the equilibrium equation with the coupled acceleration term			
	$\rho_d / (\text{g/cm}^3)$	$v_{\text{drift}} / (\text{cm/s})$	acceleration term / (cm/s^2)		$\rho_d / (\text{g/cm}^3)$	$v_{\text{drift}} / (\text{cm/s})$	acceleration term / (cm/s^2)	
1.707000e+000	1.524650e-032	3.217870e+011	2.763622e+014		2.363590e-026	0.000000e+000	2.293679e-006	
1.708000e+000	5.242123e-032	3.197749e+011	1.609322e+015		7.993215e-026	0.000000e+000	2.818846e-006	
1.709000e+000	1.611073e-031	3.177623e+011	4.757514e+015		2.415823e-025	0.000000e+000	4.356887e-006	
1.710000e+000	4.119169e-031	3.157486e+011	1.038038e+016		6.073155e-025	0.000000e+000	7.904231e-006	
1.711000e+000	8.956996e-031	3.137335e+011	1.904549e+016		1.298186e-024	0.000000e+000	1.473867e-005	
1.712000e+000	1.720603e-030	3.117167e+011	3.123376e+016		2.450959e-024	0.000000e+000	2.637607e-005	

Table 4.3: Table demonstrating differences of dust density based on moment equations and mass flux

4.7 Results of the Studies

By extending the single fluid model system of equations, this new system of equations leads to further restricting conditions apart the origin single fluid system in the coupled case. These initial respective boundary conditions apply twice: for the first time at the so called critical point where the velocity gradient results in a singularity and for the second time at the onset of dust formation.

The attempt to yield a physical solution like in the coupled case, the assumption is made that the driving force on the gas at the critical point is the same as in the coupled single fluid description. So, the coupling terms in the two fluid case, including drag force, radiation pressure on the gas component and coupling term due to the fully elaboration of the conservation equations, have to be substituted by the driving force as in the coupled case.

$$\begin{aligned} \rho_g(r)v_g(r)\frac{\partial}{\partial r}v_g &= -\frac{\partial}{\partial r}p_g(r) + f_{g,\text{rad}}(r) - f_{g,\text{grav}}(r) + f_{g,\text{drag}}(r) - q_{g,\text{acc}}(r) \\ &= -\frac{\partial}{\partial r}p_g(r) - f_{g,\text{grav}}(r) + f_{\text{rad,coupled}}(r). \end{aligned} \quad (4.18)$$

This leads to an algebraic expression for the drag force at the critical point:

$$f_{g,\text{drag}}(r) = \frac{L_\star}{4\pi c r^2} \chi_{d,\text{H}} - J_\star(r)m_d v_g(r). \quad (4.19)$$

In the case of the dust density, there is no algebraic condition serving as boundary condition at this point.

At the onset of dust formation, the dust velocity is assumed to be the same size as the gas velocity

$$v_d = v_g. \quad (4.20)$$

The dust density on the other hand, is not well-defined, the assumption of no dust at this point does surely not correspond the real situation.

The informations of dust densities from observation are neither available at dust formation onset nor at the critical point, and the calculated value on the dust formation onset depends strongly on the applied description. So, these conditions are not sufficient to provide unique conditions for the shooting method.

The realisation of a two fluid description in the actual implementation does not seem feasible. The calculated drag force term does not allow a coupling between the two components that correspond the radiative coupling in the single fluid case. Furthermore, the back-coupling on the dust component leads to a decrease of the dust velocity gradient in consequence of a small amount of dust at the dust formation onset.

The coupling term due to the full elaboration of the conservation equations of mass

and motion adds only an amount of 10^{-8} times the value of the acceleration term (see Figure 4.13). So this term may not play a significant role.

It still needs to be clarified whether the full set of equations is not in the ability to start the driving force. The coupled case of the single-fluid-model only works with positive values, whereas the two component model yields negative results for the equation of dust motion. The huge momentum transfer decelerates the wind and lead to the collapsing system of equations due to the drag force to the gas component as a consequence of a small amount of dust.

In order to avoid the negative values for the dust velocity gradient, the change between different types of description as performed in the studies above suffers from the lack of consistency. This behaviour of the equations does not allow a physical solution in a stationary description.

Chapter 5

Conclusions and Outlook

All modeling descriptions of dust formation in circumstellar shells are in need of well-defined data. Discrepancies between observed and calculated physical parameters of outflows from AGB-stars such as mass loss or the nature of the dust grains question the possible accuracy of the description of these outflows based on the physical data so far. Many studies investigated the lack of both data and theoretical enhancement (e.g. J.A. Donn & B. Nuth [28], A.B.C. Patzer [91]) in order to allow future researches the complete description of dust formation in stellar outflows. Even in C-rich cases, derived from examination of presolar grains in meteorites, many of the formation processes in heterogeneous dust formation are not yet well repeatable.

Applying nonequilibrium condensation theory involving chemical reactions to the gas outflows from carbon-rich AGB-stars, the formation of TiC and graphite grains was investigated in order to reproduce the solar TiC core-graphite-mantle spherules extracted from the Murchison meteorite by T. Chigai & T. Yamamoto [21]. They identified a discrepancy of a third of the size between the observed core/mantle ratio and the predicted values. In addition, the amount of the total gas pressure at the formation site is considered to be slightly higher than those applied by A.J. Fleischer [43] or I. Cherchneff [19].

Despite these general deficiencies of knowledge, the enhancement of theoretical equipment to describe the dust formation region would be preferred and essential. The partial extension of the generally applied single fluid model has been performed in the hydrodynamic case by C. Sandin [94], [95], [96], or Y. Simis, [102], e.g.

The stationary case of the two fluid case, though it is stated by D. Krüger [77], is not achieved. He only applied a single fluid model with derived back-calculated values for the drift velocity without applying the moment equations for the dust formation. His thesis suffered from the lack of problem definition and suggested a successful completion

of the two fluid implementation in restricted form.

So, the present thesis attempts the first implementation of a two fluid description of a circumstellar stationary outflow. The implementation consists of fully elaborated equations with coupling terms and dust formation based on the moment equations. In order to obtain a consistent outflow, the results from different studies indicate difficulties both from the configuration of the system of equations and from the incoming coupling terms like the drag force.

The configuration of the equations leads to negative gradients of the dust velocity due to the back coupling of the drag force. The momentum transfer to the gas component leads to these inadvertent gradients. Even a restriction to positive values by substituting the dust moment equation for the equilibrium equation for the dust moment around the crucial interval, does not provide any amelioration.

The lack of consistency of the results of the two-component description led to further detailed analyses of the equations underlying the model.

Therefore, two different approaches to obtain data both for dust density and velocity are applied in one model. On the one hand, the dust density was derived by the third moment of the dust formation and growth equations. The mass flux density and the density of the dust provided the velocity of the dust and the drag force.

The other path utilised the mass flux density applied to the velocity structure of the coupled single fluid model from where the values for the drift velocity are therefore derived by an algebraic equation. So, the derived values both result from the moment equations and from the simplified hydrodynamical equations. The divergent values for the dust density, and apparently unrealistic results for the drift velocity, suggested therefore a fundamental lack of equal value of the two ways of description. The coupling term due to the full elaboration of the conservation equations of mass and motion was too small to support the lack of acceleration from the drag force. The two fluid model system of equations led to further restricting conditions apart the origin single fluid system in the coupled case. The obtained values from Section 4.6 for the dust density as initial values for the shooting method were not well-defined and therefore unsuitable to start the integration.

In consequence, the attempt to implement the two fluid case in stationary and spherical symmetry description with the available system of equations even in the carbon-restricted case, does not succeed.

However, the results of this work cleared the way for revision and adaptation of the present system of equations in order to allow a consistent description of multicomponent fluids. Here, new approaches concerning the coupling terms are needed, providing a compatible value to the single fluid description. The problem of the influence of the dust density on the drag force has to be clarified. In case of perpetuated investigation of a multicomponent fluid system, it has to be sustained by further studies on the coupling

terms, the missing initial conditions, a reconsideration of the nucleation theory, and, in addition, more data are required.

Appendix A

In order to exemplify the elaboration of the conservation equations, the following equations are treated in detail for the gas phase.

To begin with:

$$\frac{\partial}{\partial t} \rho_g(\mathbf{r}, t) + \nabla \cdot (\mathbf{v}_g(\mathbf{r}, t) \rho_g(\mathbf{r}, t)) = q_g(\mathbf{r}, t) \quad (\text{A.1})$$

Multiplication with $\mathbf{v}_g(\mathbf{r}, t)$ yields

$$\begin{aligned} \mathbf{v}_g(\mathbf{r}, t) \frac{\partial}{\partial t} \rho_g(\mathbf{r}, t) + \mathbf{v}_g(\mathbf{r}, t) \rho_g(\mathbf{r}, t) \nabla \cdot \mathbf{v}_g(\mathbf{r}, t) + (\mathbf{v}_g(\mathbf{r}, t) \cdot \nabla \rho_g(\mathbf{r}, t)) \mathbf{v}_g(\mathbf{r}, t) \\ = q_g(\mathbf{r}, t) \mathbf{v}_g(\mathbf{r}, t) \end{aligned} \quad (\text{A.2})$$

Elaboration of

$$\begin{aligned} \frac{\partial}{\partial t} (\rho_g(\mathbf{r}, t) \mathbf{v}_g(\mathbf{r}, t)) + \nabla \cdot (\rho_g(\mathbf{r}, t) \mathbf{v}_g(\mathbf{r}, t) \otimes \mathbf{v}_g(\mathbf{r}, t)) = \\ - \nabla \cdot p_g(\mathbf{r}, t) + \mathbf{f}_{g,rad}(\mathbf{r}, t) - \mathbf{f}_{g,grav}(\mathbf{r}, t) + \mathbf{f}_{drag}(\mathbf{r}, t) \end{aligned} \quad (\text{A.3})$$

leads to

$$\begin{aligned} \rho_g(\mathbf{r}, t) \frac{\partial}{\partial t} \mathbf{v}_g(\mathbf{r}, t) + \mathbf{v}_g(\mathbf{r}, t) \frac{\partial}{\partial t} \rho_g(\mathbf{r}, t) + 2 \mathbf{v}_g(\mathbf{r}, t) \rho_g(\mathbf{r}, t) \nabla \cdot \mathbf{v}_g(\mathbf{r}, t) + (\mathbf{v}_g(\mathbf{r}, t) \cdot \nabla \rho_g(\mathbf{r}, t)) \mathbf{v}_g(\mathbf{r}, t) \\ = - \nabla \cdot p_g(\mathbf{r}, t) + \mathbf{f}_{g,rad}(\mathbf{r}, t) - \mathbf{f}_{g,grav}(\mathbf{r}, t) + \mathbf{f}_{drag}(\mathbf{r}, t) \end{aligned} \quad (\text{A.4})$$

and after subtraction of the mass conservation equation, the equation turns into

$$\begin{aligned} \rho_g(\mathbf{r}, t) \frac{\partial}{\partial t} \mathbf{v}_g(\mathbf{r}, t) + \mathbf{v}_g(\mathbf{r}, t) \rho_g(\mathbf{r}, t) \nabla \cdot \mathbf{v}_g(\mathbf{r}, t) \\ = - \nabla \cdot p_g(\mathbf{r}, t) + \mathbf{f}_{g,rad}(\mathbf{r}, t) - \mathbf{f}_{g,grav}(\mathbf{r}, t) + \mathbf{f}_{drag}(\mathbf{r}, t) - q_g(\mathbf{r}, t) \mathbf{v}_g(\mathbf{r}, t). \end{aligned} \quad (\text{A.5})$$

The simplified final equation follows as

$$\begin{aligned} \rho_g(\mathbf{r}, t) \left(\frac{\partial}{\partial t} \mathbf{v}_g(\mathbf{r}, t) + \mathbf{v}_g(\mathbf{r}, t) \nabla \cdot \mathbf{v}_g(\mathbf{r}, t) \right) \\ = - \nabla \cdot p_g(\mathbf{r}, t) + \mathbf{f}_{g,rad}(\mathbf{r}, t) - \mathbf{f}_{g,grav}(\mathbf{r}, t) + \mathbf{f}_{drag}(\mathbf{r}, t) - q_g(\mathbf{r}, t) \cdot \mathbf{v}_g(\mathbf{r}, t). \end{aligned} \quad (\text{A.6})$$

with $q_g(\mathbf{r}, t) = -J_* m_d$, and therefore $-q_g(\mathbf{r}, t) = J_* m_d$ leads to a gain of momentum for the gas phase.

The same procedure has to be applied to the energy equation.

$$\begin{aligned} & \frac{\partial}{\partial t} \left[\rho_g(\mathbf{r}, t) \left(e_g(\mathbf{r}, t) + \frac{1}{2} v_g^2(\mathbf{r}, t) \right) \right] + \\ & \nabla \cdot \left[\rho_g(\mathbf{r}, t) \left((e_g(\mathbf{r}, t) + \frac{1}{2} v_g^2(\mathbf{r}, t)) \mathbf{v}_g(\mathbf{r}, t) \right) + p_g(\mathbf{r}, t) \mathbf{v}_g(\mathbf{r}, t) \right] = Q_{\text{rad, int, g}}(\mathbf{r}, t) \end{aligned} \quad (\text{A.7})$$

leads to

$$\begin{aligned} & \rho_g(\mathbf{r}, t) \frac{\partial}{\partial t} e_g(\mathbf{r}, t) + e_g(\mathbf{r}, t) \frac{\partial}{\partial t} \rho_g(\mathbf{r}, t) + \rho_g(\mathbf{r}, t) \frac{\partial}{\partial t} \left(\frac{1}{2} v_g^2(\mathbf{r}, t) \right) + \\ & \frac{1}{2} v_g^2(\mathbf{r}, t) \frac{\partial}{\partial t} \rho_g(\mathbf{r}, t) + \rho_g(\mathbf{r}, t) e_g(\mathbf{r}, t) \nabla \cdot \mathbf{v}_g(\mathbf{r}, t) + \\ & \rho_g(\mathbf{r}, t) \mathbf{v}_g(\mathbf{r}, t) \cdot \nabla e_g(\mathbf{r}, t) + e_g(\mathbf{r}, t) \mathbf{v}_g(\mathbf{r}, t) \cdot \nabla \rho_g(\mathbf{r}, t) + \\ & \frac{1}{2} v_g^2(\mathbf{r}, t) \rho_g(\mathbf{r}, t) \nabla \cdot \mathbf{v}_g(\mathbf{r}, t) + \frac{1}{2} v_g^2(\mathbf{r}, t) \mathbf{v}_g(\mathbf{r}, t) \cdot \nabla \rho_g(\mathbf{r}, t) + v_g(\mathbf{r}, t) \rho_g(\mathbf{r}, t) v_g(\mathbf{r}, t) \nabla \cdot \mathbf{v}_g(\mathbf{r}, t) + \\ & p_g(\mathbf{r}, t) \nabla \cdot \mathbf{v}_g(\mathbf{r}, t) + \mathbf{v}_g(\mathbf{r}, t) \cdot \nabla p_g(\mathbf{r}, t) = Q_{\text{rad, int, g}}(\mathbf{r}, t). \end{aligned} \quad (\text{A.8})$$

After rearranging it yields

$$\begin{aligned} & \rho_g(\mathbf{r}, t) \left(\frac{\partial}{\partial t} e_g(\mathbf{r}, t) + \mathbf{v}_g(\mathbf{r}, t) \cdot \nabla e_g(\mathbf{r}, t) \right) + \frac{1}{2} v_g^2(\mathbf{r}, t) \left(\frac{\partial}{\partial t} \rho_g(\mathbf{r}, t) + \nabla \cdot (\mathbf{v}_g(\mathbf{r}, t) \rho_g(\mathbf{r}, t)) \right) \\ & + e_g(\mathbf{r}, t) \left(\frac{\partial}{\partial t} \rho_g(\mathbf{r}, t) + \nabla \cdot (\mathbf{v}_g(\mathbf{r}, t) \rho_g(\mathbf{r}, t)) \right) + \\ & \mathbf{v}_g(\mathbf{r}, t) \left(\rho_g(\mathbf{r}, t) \left(\frac{\partial}{\partial t} \mathbf{v}_g(\mathbf{r}, t) + \mathbf{v}_g(\mathbf{r}, t) \nabla \cdot \mathbf{v}_g(\mathbf{r}, t) \right) + \nabla p_g(\mathbf{r}, t) \right) \\ & + p_g(\mathbf{r}, t) \nabla \cdot \mathbf{v}_g(\mathbf{r}, t) = Q_{\text{rad, int, g}}(\mathbf{r}, t). \end{aligned} \quad (\text{A.9})$$

The final version consists in

$$\begin{aligned} & \rho_g(\mathbf{r}, t) \left(\frac{\partial}{\partial t} e_g(\mathbf{r}, t) + \mathbf{v}_g(\mathbf{r}, t) \cdot \nabla e_g(\mathbf{r}, t) \right) = -\frac{1}{2} v_g^2(\mathbf{r}, t) q_g - e_g(\mathbf{r}, t) q_g \\ & - \mathbf{v}_g(\mathbf{r}, t) \cdot (\mathbf{f}_{g, \text{rad}}(\mathbf{r}, t) - \mathbf{f}_{g, \text{grav}}(\mathbf{r}, t) + \mathbf{f}_{\text{drag}}(\mathbf{r}, t) - q_g(\mathbf{r}, t) \mathbf{v}_g(\mathbf{r}, t)) \\ & - p_g(\mathbf{r}, t) \nabla \cdot \mathbf{v}_g(\mathbf{r}, t) + Q_{\text{rad, int, g}}(\mathbf{r}, t) \\ & = -\frac{1}{2} v_g^2(\mathbf{r}, t) q_g(\mathbf{r}, t) - e_g(\mathbf{r}, t) q_g(\mathbf{r}, t) - \mathbf{v}_g(\mathbf{r}, t) \cdot \mathbf{f}_{\text{rad, g}}(\mathbf{r}, t) + \mathbf{v}_g(\mathbf{r}, t) \cdot \mathbf{f}_{g, \text{grav}}(\mathbf{r}, t) - \mathbf{v}_g(\mathbf{r}, t) \cdot \mathbf{f}_{\text{drag}}(\mathbf{r}, t) \\ & - q_g(\mathbf{r}, t) \mathbf{v}_g(\mathbf{r}, t) \cdot \mathbf{v}_g(\mathbf{r}, t) - p_g(\mathbf{r}, t) \nabla \cdot \mathbf{v}_g(\mathbf{r}, t) + Q_{\text{rad, int, g}}(\mathbf{r}, t) \\ & = -Q_{\text{kin, g}}(\mathbf{r}, t) - Q_{\text{int, g}} - Q_{\text{rad, g}}(\mathbf{r}, t) + Q_{\text{grav, g}}(\mathbf{r}, t) - Q_{\text{drag, g}}(\mathbf{r}, t) - Q_{\text{acc, g}}(\mathbf{r}, t) \\ & - p_g(\mathbf{r}, t) \nabla \cdot \mathbf{v}_g(\mathbf{r}, t) + Q_{\text{rad, int, g}}(\mathbf{r}, t) \end{aligned} \quad (\text{A.10})$$

with the replacements both for the mass conservation equation and for the motion equation and the definition of the newly inserted terms.

Bibliography

- [1] Chorin A.J. and J.E. Marsden. A MATHEMATICAL INTRODUCTION TO FLUID MECHANICS. Springer Verlag.
- [2] C.M.O.D. Alexander. LABORATORY STUDIES OF CIRCUMSTELLAR AND INTERSTELLAR MATERIALS. EAS Publications Series, 35:75–102, 2009.
- [3] C.W. Allen. ASTROPHYSICAL QUANTITIES. The Athlone Press, London.
- [4] A. C. Andersen, S. Höfner, and R. Gautschy-Loidl. DUST GRAIN PROPERTIES IN ATMOSPHERES OF AGB STARS. arXiv: astro-ph/0209247, 2002.
- [5] A. C. et al. Anderson. DUST FORMATION IN WINDS OF LONG PERIOD VARIABLES, V. THE INFLUENCE OF MICRO-PHYSICAL DUST PROPERTIES IN CARBON STARS. Astronomy & Astrophysics, 400:981–992, 2003.
- [6] T. M. Apostol. CALCULUS, 2D. ED. Waltham, Massachusetts: Blaisdell., 1, 1967.
- [7] U.M. Ascher and L.R. Petzold. COMPUTER METHODS FOR ORDINARY DIFFERENTIAL EQUATIONS AND DIFFERENTIAL-ALGEBRAIC EQUATIONS . SIAM.
- [8] Williams I.P. Baines, M.J. and A.S. Asebiomo. RESISTANCE TO THE MOTION OF A SMALL SPHERE MOVING THROUGH A GAS. Monthly Notices of the Royal Astronomical Society, 130:63, 1965.
- [9] R. Becker and W. Döring. KINETISCHE BEHANDLUNG DER KEIMBILDUNG IN ÜBERSÄTTIGTEN DÄMPFEN. Annalen der Physik, Issue 8, 416:719–752, 1935.
- [10] G. A. Bird. MOLECULAR GAS DYNAMICS AND THE DIRECT SIMULATION OF GAS FLOWS, 2ND EDN. (OXFORD UNIVERSITY PRESS) . 1994.
- [11] C. Blatter. 20. MEHRDIMENSIONALE DIFFERENTIALRECHNUNG, AUFGABEN, 1. ANALYSIS II (2ND ED.). Springer Verlag ISBN 3-540-09484-9.
- [12] G.H. Bowen. DYNAMICAL MODELING OF LONG-PERIOD VARIABLE STAR ATMOSPHERES. Astrophysical Journal, 329:299, 1988.

- [13] G.H. Bowen. DYNAMICAL MODELING OF LONG-PERIOD VARIABLE STAR ATMOSPHERES. The Astrophysical Journal, 329:299–317, 1988.
- [14] K. Brenan, S. Campbell, and L. Petzold. NUMERICAL SOLUTION OF INITIAL VALUE PROBLEMS IN DIFFERENTIAL ALGEBRAIC EQUATIONS, NORTH HOLLAND, 1989. republished by SIAM.
- [15] S. Chandrasekhar. RADIATIVE TRANSFER. Clarendon Press, Oxford, Dover 1960, 1950.
- [16] I. Cherchneff. FORMING DUST PRECURSORS IN THE INNER ENVELOPES OF CARBON-RICH AGB STARS. Astrophysics and Space Science, 224:379, 1995.
- [17] I. Cherchneff. ABUNDANCES IN CIRCUMSTELLAR DUST. ASP Conference Series, 147:179, 1998.
- [18] I. Cherchneff. NUCLEATING DUST IN CARBON-RICH AGB STARS. IAUS, 177:331, 2000.
- [19] I. Cherchneff, J. R. Barker, and A. G. G. M. Tielens. POLYCYCLIC AROMATIC HYDROCARBON FORMATION IN CARBON-RICH STELLAR ENVELOPES. Astrophysical Journal, 401:269–287, 1992.
- [20] I. Cherchneff and P. Cau. THE CHEMISTRY OF CARBON DUST FORMATION. IAUS, 191:251, 1999.
- [21] T. Chigai, T. Yamamoto, and T. Kozasa. FORMATION CONDITIONS OF PRESOLAR TIC CORE-GRAPHITE MANTLE SPHERULES IN THE MURCHISON METEORITE. The Astrophysical Journal, 510, Issue 2:999–1010, 1999.
- [22] Thomas K. Croat, Frank J. Stadermann, and Thomas J. Bernatowicz. PRESOLAR GRAPHITE FROM AGB STARS: MICROSTRUCTURE AND s-PROCESS ENRICHMENT. The Astrophysical Journal, 631, Issue 2:976–987, 2005.
- [23] L. Decin, I. Cherchneff, S. Hony, S. Dehaes, C. De Breuck, and K. M. Menten. DETECTION OF “PARENT” MOLECULES FROM THE INNER WIND OF AGB STARS AS TRACERS OF NON-EQUILIBRIUM CHEMISTRY . Astronomy & Astrophysics, 480, Issue 2:431–438, 2008.
- [24] C.F. Delale and G.E.A. Meier. A SEMI-PHENOMENOLOGICAL DROPLET MODEL OF HOMOGENEOUS NUCLEATION FROM THE VAPOR PHASE. Journal of Chemical Physics, 98, Nr. 12:9850 – 9858, 1993.
- [25] R. Dettmer. THERMODYNAMISCHE BETRACHTUNGEN ZUR KONDENSATION, PHD THESIS PHILIPPS-UNIVERSITÄT MARBURG. 1997.

- [26] C. Dominik, H.-P. Gail, and E. Sedlmayr. SELFCONSISTENT MODELS OF DUST DRIVEN WINDS AROUND C-STARS . Mitteilungen der Astronomischen Gesellschaft, 70:364D, 1987.
- [27] C. Dominik, H.-P. Gail, and E. Sedlmayr. THE SIZE DISTRIBUTION OF DUST PARTICLES IN A DUST-DRIVEN WIND. Astronomy & Astrophysics, 223:227D, 1989.
- [28] B. Donn and J. A. Nuth. DOES NUCLEATION THEORY APPLY TO THE FORMATION OF REFRACTORY CIRCUMSTELLAR GRAINS? Astrophysical Journal, 288:187–190, 1985.
- [29] B. T. Draine. TIME-DEPENDENT NUCLEATION THEORY AND THE FORMATION OF INTERSTELLAR GRAINS. Astrophysics and Space Science, 65:313–335, 1979.
- [30] B.T. Draine. TIME DEPENDENT NUCLEATION THEORY AND THE FORMATION OF INTERSTELLAR GRAINS. Astrophysics and Space Science, 65:313–335, 1979.
- [31] B.T. Draine. INTERSTELLAR SHOCK WAVES WITH MAGNETIC PRECURSORS. The Astrophysical Journal, 241:1021–1038, 1980.
- [32] B.T. Draine. MULTICOMPONENT, REACTING MHD FLOWS. Royal Astronomical Society, Monthly Notices, 220:133–148, 1986.
- [33] B.T. Draine and E.E. Salpeter. TIME DEPENDENT NUCLEATION THEORY . The Journal of Chemical Physics, 67, No. 5:2230, 1977.
- [34] R. Ehrig, U. Nowak, and P. Deuffhard. HIGHLY SCALABLE PARALLEL LINEARLY-IMPLICIT EXTRAPOLATION ALGORITHMS, TECHNICAL REPORT . Konrad-Zuse-Zentrum für Informationstechnik (Berlin).
- [35] H.-P.Gail et al. CHEMISTRY IN CIRCUMSTELLAR SHELLS . Mit Ag, 70:365G, 1987.
- [36] Stroud et al. CHONDRITES AND THE PROTOPLANETARY DISK. Science, 305.
- [37] J.D. Faires and R.L. Burden. NUMERISCHE METHODEN: NHERUNGSVERFAHREN UND IHRE PRAKTISCHE ANWENDUNG. Spektrum Akademischer Verlag; Auflage: Studienausgabe.
- [38] J. Feder, K. C. Russell, J. Lothe, and G. M. Pound. HOMOGENEOUS NUCLEATION AND GROWTH OF DROPLETS IN VAPOURS. Advances in Physics, 15, Issue 57:111–178, 1966.
- [39] A. S. Ferrarotti and H.-P. Gail. MINERAL FORMATION IN STELLAR WINDS V. FORMATION OF CALCIUM CARBONATE. Astronomy & Astrophysics, 430:995, 2005.

- [40] A. S. Ferrarotti and H.-P. Gail. COMPOSITION AND QUANTITIES OF DUST PRODUCED BY AGB-STARS AND RETURNED TO THE INTERSTELLAR MEDIUM . Astronomy & Astrophysics, 447, Issue 2:553–576, 2006.
- [41] A. J. Fleischer. HYDRODYNAMICS AND DUST FORMATION IN THE CIRCUMSTELLAR SHELLS OF MIRAS AND LONG-PERIOD VARIABLES, PhD THESIS, TECHNISCHE UNIVERSITÄT BERLIN. 1994.
- [42] A. J. Fleischer, A. Gauger, and E. Sedlmayr. GENERATION OF SHOCKS BY RADIATION PRESSURE ON NEWLY FORMED CIRCUMSTELLAR DUST. Astronomy & Astrophysics, 242L:1, 1991.
- [43] A. J. Fleischer, A. Gauger, and E. Sedlmayr. CIRCUMSTELLAR DUST SHELLS AROUND LONG-PERIOD VARIABLES. I - DYNAMICAL MODELS OF C-STARS INCLUDING DUST FORMATION, GROWTH AND EVAPORATION. Astronomy & Astrophysics, 266:321, 1992.
- [44] A. J. Fleischer, A. Gauger, and E. Sedlmayr. CIRCUMSTELLAR DUST SHELLS AROUND LONG-PERIOD VARIABLES. III. INSTABILITY DUE TO AN EXTERIOR κ -MECHANISM CAUSED BY DUST FORMATION. Astronomy & Astrophysics, 297:543, 1995.
- [45] A. J. Fleischer, A. Gauger, E. Sedlmayr, and H.-P. Gail. DYNAMICAL MODELS OF DUST SHELLS AROUND MIRA VARIABLES. ASPC, 11:431, 1990.
- [46] H.-P. Gail and E. Sedlmayr. DUST FORMATION IN STELLAR WINDS. I - A RAPID COMPUTATIONAL METHOD AND APPLICATION TO GRAPHITE CONDENSATION. Astronomy & Astrophysics, 133:320, 1984.
- [47] H.-P. Gail and E. Sedlmayr. FORMATION OF CRYSTALLINE AND AMORPHOUS CARBON GRAINS . Astronomy & Astrophysics, 132:163–167, 1984.
- [48] H.-P. Gail and E. Sedlmayr. DUST FORMATION IN STELLAR WINDS II. Astronomy & Astrophysics, 148:183–190, 1985.
- [49] H.-P. Gail and E. Sedlmayr. THE MAXIMUM POSSIBLE MASS LOSS RATE FOR DUST DRIVEN WINDS. Astronomy & Astrophysics, 161:201–202, 1986.
- [50] H.-P. Gail and E. Sedlmayr. THE PRIMARY CONDENSATION PROCESS FOR DUST AROUND LATE M-TYPE STARS . Astronomy & Astrophysics, 166:225–236, 1986.
- [51] H.-P. Gail and E. Sedlmayr. DUST FORMATION IN STELLAR WINDS III. Astronomy & Astrophysics, 171:197–204, 1987.
- [52] H.-P. Gail and E. Sedlmayr. DUST FORMATION IN STELLAR WINDS. V - THE MINIMUM MASS LOSS RATE FOR DUST-DRIVEN WINDS. Astronomy & Astrophysics, 177:186, 1987.

- [53] H.-P. Gail and E. Sedlmayr. DUST FORMATION IN STELLAR WINDS IV. Astronomy & Astrophysics, 206:153–168, 1988.
- [54] H.-P. Gail and E. Sedlmayr. MINERAL FORMATION IN STELLAR WINDS I. Astronomy & Astrophysics, 347:594–616, 1999.
- [55] A. Gauger, E. Sedlmayr, and H.-P. Gail. DUST FORMATION, GROWTH AND EVAPORATION IN A COOL PULSATING CIRCUMSTELLAR SHELL. ASPC, 235:345, 1990.
- [56] R. Gautschy-Loidl, S. Höfner, U. G. Jorgensen, and B. Aringer. DYNAMIC MODEL ATMOSPHERES OF AGB STARS. IV. A COMPARISON OF SYNTHETIC CARBON STAR SPECTRA WITH OBSERVATIONS. Astronomy & Astrophysics, 422:289–306, 2004.
- [57] B. C. Guo, K. P. Kerns, and Jr. A. W. Castleman. Ti8C12^+ -METALLO-CARBOHEDRENES: A NEW CLASS OF MOLECULAR CLUSTERS? . Science, 255:1411, 1992.
- [58] E. Sedlmayr H.-P. Gail. PHYSICS AND CHEMISTRY OF CIRCUMSTELLAR DUST SHELLS. in press.
- [59] T. W. Hartquist, S. van Loo, S.A.E.G. Falle, P. Caselli, and I. Ashmore. DUST IN INTERSTELLAR CLOUDS, EVOLVED STARS AND SUPERNOVAE. AIP Conference Proceedings, 397, no. 2:101–104.
- [60] Ch. Helling, J. M. Winters, and E. Sedlmayr. CIRCUMSTELLAR DUST SHELLS AROUND LONG-PERIOD VARIABLES. VII. THE ROLE OF MOLECULAR OPACITIES. Astronomy & Astrophysics, 358:651, 2000.
- [61] R. Henkel, E. Sedlmayr, and H.-P. Gail. NONEQUILIBRIUM CHEMISTRY IN CIRCUMSTELLAR SHELLS. Reviews in Modern Astronomy, 1:231, 1988.
- [62] S. Höfner. WINDS OF COOL GIANT , proc. 13th cool stars workshop, hamburg, 5-9 july 2004. F. Favata et. eds.
- [63] S. Höfner. DYNAMICAL MODELLING OF AGB STAR ATMOSPHERES. Asymptotic Giant Branch Stars, IAU Symposium, Edited by T. Le Bertre, A. Lebre, and C. Waelkens, 191:159, 1999.
- [64] S. Höfner. WINDS OF M-TYPE AGB STARS DRIVEN BY MICRON-SIZED GRAINS. Astronomy & Astrophysics, 491, Issue 2:L1–L4, 2008.
- [65] S. Höfner. DUST FORMATION AND WINDS AROUND EVOLVED STARS: THE GOOD, THE BAD AND THE UGLY CASES. Cosmic Dust - Near and Far ASP Conference Series, 414:3, 2009.

- [66] S. Höfner and E.A. Dorfi. DUST FORMATION IN WINDS OF LONG-PERIOD VARIABLES. IV. ATMOSPHERIC DYNAMICS AND MASS LOSS. Astronomy & Astrophysics, 319:648, 1997.
- [67] S. Höfner, U. G. Jorgensen, R. Loidl, and B. Aringer. DYNAMIC MODEL ATMOSPHERES OF AGB STARS. I. ATMOSPHERIC STRUCTURE AND DYNAMICS. Astronomy & Astrophysics, 340:497, 1998.
- [68] S. Höfner, U. G. Jorgensen, R. Loidl, and B. Aringer. DYNAMIC MODEL ATMOSPHERES OF AGB STARS I. ATMOSPHERIC STRUCTURE AND DYNAMICS. Astronomy & Astrophysics, 340:497–507, 1998.
- [69] S. Höfner, R. Loidl, B. Aringer, and U. G. Jorgensen. DYNAMICAL ATMOSPHERES AND MASS LOSS OF PULSATING AGB STARS. ASPC, 259:534, 2002.
- [70] J.A. Nuth III and F.T.Ferguson. SILICATES DO NUCLEATE IN OXYGEN-RICH CIRCUMSTELLAR OUTFLOWS: NEW VAPOR PRESSURE DATA FOR SiO. Astrophysical Journal, 649:1178, 2006.
- [71] K.S. Jeong. DUST SHELLS AROUND OXYGEN-RICH MIRAS AND LONG-PERIOD VARIABLES, PHD THESIS. 2000.
- [72] A. P. Jones. INTERSTELLAR AND CIRCUMSTELLAR GRAIN FORMATION AND SURVIVAL. Origin and early evolution of solid matter in the Solar System. Roy Soc of London Phil Tr A, 359, Issue 1787:1961, 2001.
- [73] J. L. Katz. HOMOGENEOUS NUCLEATION THEORY AND EXPERIMENT: A SURVEY. Pure Appl. Chem., Vol. 64, No. 11:1661–1666, 1992.
- [74] A. King, T. Henkel, S. Chapman, H. Busemann, D. Rost, C. Guillermier, M. R. Lee, I. A. Franchi, and I. C. Lyon. AMORPHOUS CARBON GRAINS IN THE MURCHISON METEORITE. 42nd Lunar and Planetary Science Conference, held March 711, 2011 at The Woodlands, Texas. LPI, Contribution No. 1608:2604, 2011.
- [75] W.M.Seiler und J.Tuomela K.Krupchyk. OVERDETERMINED ELLIPTIC SYSTEMS. Foundations of Computational Mathematics, 6, Number 3:309–351, 2006.
- [76] D. Krüger. A COMPUTATIONAL MULTI-COMPONENT METHOD FOR MODELING THE EVOLUTION OF SIZE DISTRIBUTION FUNCTIONS AND ITS APPLICATION TO COSMIC DUST GRAINS, PHD THESIS. 1999.
- [77] D. Krüger, A. Gauger, and E. Sedlmayr. TWO-FLUID MODELS FOR STATIONARY DUST-DRIVEN WINDS. I. MOMENTUM AND ENERGY BALANCE. Astronomy & Astrophysics, 290:573–589, 1994.

- [78] J. Kuipers. THEORY AND SIMULATION OF NUCLEATION, PHD THESIS. ISBN: 978-90-9024619-2, 2009.
- [79] S.Höfner L. Mattsson, R. Wahlin. DUST DRIVEN MASS LOSS FROM CARBON STARS AS A FUNCTION OF STELLAR PARAMETERS I. Astronomy & Astrophysics, 509:A14, 2010.
- [80] T. Lebzelter, W. Nowotny, S. Höfner, M. T. Lederer, K. H. Hinkle, and B. Aringer. ABUNDANCE ANALYSIS FOR LONG PERIOD VARIABLES. VELOCITY EFFECTS STUDIED WITH O-RICH DYNAMIC MODEL ATMOSPHERES. Astronomy & Astrophysics, 517A:6L, 2010.
- [81] K. Lodders and Jr. Fegley. THE ORIGIN OF CIRCUMSTELLAR SILICON CARBIDE GRAINS FOUND IN METEORITES. Meteoritics, 30, Issue 6:661, 1995.
- [82] R. Loidl, S. Höfner, U. G. Jorgensen, and B. Aringer. DYNAMIC MODEL ATMOSPHERES OF AGB STARS. II. SYNTHETIC NEAR INFRARED SPECTRA OF CARBON STARS. Astronomy & Astrophysics, 342:531–541, 1999.
- [83] L. B. Lucy. MASS LOSS BY COOL CARBON STARS. Astrophysical Journal, 205:482, 1976.
- [84] L.B. Lucy. THE FORMATION OF RESONANCE LINES IN EXTENDED AND EXPANDING ATMOSPHERES. The Astrophysical Journal, 163:95–110, 1971.
- [85] K. B. MacGregor and R. E. Stencel. ON THE INTERACTION BETWEEN DUST AND GAS IN LATE-TYPE STELLAR ATMOSPHERES AND WINDS. Astrophysical Journal, 397, no. 2:644–651, 1992.
- [86] L. Mattsson and S. Höfner. DUST-DRIVEN MASS LOSS FROM CARBON STARS AS A FUNCTION OF STELLAR PARAMETERS II. EFFECTS OF GRAIN SIZE ON WIND PROPERTIES. Astronomy & Astrophysics, 533:A42, 2011.
- [87] R. B. McClurg. HOMOGENEOUS NUCLEATION THEORY, PHD THESIS, CALIFORNIA INSTITUTE OF TECHNOLOGY. 1997.
- [88] D. Mihalas. STELLAR ATMOSPHERES. W.H. Freeman & Co,eds., 1978.
- [89] W. Nolting. GRUNDKURS THEORETISCHE PHYSIK,4., SPEZIELLE RELATIVITTS-THEORIE, THERMODYNAMIK . Springer, Berlin,Heidelberg.
- [90] A.B.C. Patzer, A. Gauger, and E. Sedlmayr. DUST FORMATION IN STELLAR WINDS. VII. KINETIC NUCLEATION THEORY FOR CHEMICAL NON-EQUILIBRIUM IN THE GAS PHASE. Astronomy & Astrophysics, 337:847–858, 1998.

- [91] A.B.C. Patzer, M. Wendt, C. Chang, and D. Sülzle. NUCLEATION STUDIES UNDER THE CONDITIONS OF CARBON-RICH AGB STAR ENVELOPES: TiC. ASPC, Why Galaxies care about AGB-stars II, 445:361, 2011.
- [92] W.H. Press, S.A. Teukolski, W.T. Vetterling, and B.P. Flannery. NUMERICAL RECIPES IN FORTRAN 77. Cambridge University Press, ISBN 0-521-43064-X, 1986-1992.
- [93] E.E. Salpeter. NUCLEATION AND GROWTH OF DUST GRAINS. The Astrophysical Journal, 193:579–584, 1974.
- [94] C. Sandin and S. Höfner. THREE COMPONENT MODELING OF C-RICH AGB STAR WINDS, I. METHOD AND FIRST RESULTS. Astronomy & Astrophysics, 398:253–266, 2003.
- [95] C. Sandin and S. Höfner. THREE COMPONENT MODELING OF C-RICH AGB STAR WINDS, II. THE EFFECTS OF DRIFT IN LONG-PERIOD VARIABLES. Astronomy & Astrophysics, 404:798–807, 2003.
- [96] C. Sandin and S. Höfner. THREE COMPONENT MODELING OF C-RICH AGB STAR WINDS, III. MICRO-PHYSICS OF DRIFT-DEPENDENT DUST FORMATION. Astronomy & Astrophysics, 413:789–798, 2004.
- [97] F. Schwabl. STATISTISCHE MECHANIK . Springer, Berlin,Heidelberg.
- [98] E. Sedlmayr. DIE ENTSTEHUNG DES INTERSTELLAREN STAUBS. Mitteilungen der Astronomischen Gesellschaft, 63:75, 1986.
- [99] E. Sedlmayr. DUST FORMATION IN C-STAR SHELLS. Symposium of the International Astronomical Union, 122:543, 1987.
- [100] E. Sedlmayr. DUST CONDENSATION IN STELLAR OUTFLOWS. IAUS, 135:467, 1989.
- [101] W.M. Seiler. UNTER- UND BERBESTIMMTE SYSTEME VON DIFFERENTIALGLEICHUNGEN. Mathematische Semesterberichte, 57:231–268, 2010.
- [102] Y. Simis. MASS LOSS MODULATION IN DUST FORMING STELLAR WINDS, PHD THESIS, LEIDEN UNIVERSITY. 2001.
- [103] J. R. Stephens and B. K. Kothari. LABORATORY ANALOGUES TO COSMIC DUST. Conference on Protostars and Planets, Tucson, Ariz., Moon and the Planets, 19:139–152, 1978.
- [104] S.Höfner M.T.Lederer K.H.Hinkle B.Aringer T.Lebzelter, W.Nowotny. ABUNDANCE ANALYSIS FOR LONG PERIOD VARIABLES VELOCITY EFFECTS STUDIED

- WITH O-RICH DYNAMIC MODEL ATMOSPHERES. *Astronomy & Astrophysics*, 517,:A6, 2010.
- [105] T.M.Koehler, H.-P.Gail, and E. Sedlmayr. MGO DUST NUCLEATION IN M-STARS: CALCULATION OF CLUSTER PROPERTIES AND NUCLEATION RATES. *Astronomy & Astrophysics*, 320:553–567, 1997.
- [106] P. Ulmschneider, W. Rammacher, and H.-P. Gail. ATMOSPHERIC PULSATIONS AND MASS LOSS DRIVEN BY OVERTAKING ACOUSTIC SHOCKS. *ASPC*, 147:471, 1992.
- [107] Dr. Hanna Vehkamäki, Ari Asmi, and MSc (ed). CLASSICAL HOMOGENOUS NUCLEATION THEORY IN MULTICOMPONENT SYSTEMS. *Springer*, 1 edition , no. 2, 2006.
- [108] M. Volmer and A. Weber. KEIMBILDUNG IN ÜBERSÄTTIGTEN GEBILDEN. *Z. phys. Chem.*, 119:277301, 1926.
- [109] J. M. Winters, C. Dominik, and E. Sedlmayr. THEORETICAL SPECTRA OF CIRCUMSTELLAR DUST SHELLS AROUND CARBON-RICH ASYMPTOTIC GIANT BRANCH STARS. *Astronomy & Astrophysics*, 288:255, 1994.
- [110] J. M. Winters, A. J. Fleischer, and A. Gauger. OPTICAL APPEARANCE OF DYNAMICAL MODELS OF CIRCUMSTELLAR DUST SHELLS AROUND LONG-PERIOD VARIABLES. *Astron. Ges., Abstr. Ser.*, 7:107, 1992.
- [111] J. M. Winters, A. J. Fleischer, A. Gauger, and E. Sedlmayr. CIRCUMSTELLAR DUST SHELLS AROUND LONG-PERIOD VARIABLES. IV. BRIGHTNESS PROFILES AND SPATIAL SPECTRA OF C-STARS. *Astronomy & Astrophysics*, 302:483, 1986.
- [112] J. M. Winters, A. J. Fleischer, A. Gauger, and E. Sedlmayr. CIRCUMSTELLAR DUST SHELLS AROUND LONG-PERIOD VARIABLES. II. THEORETICAL LIGHTCURVES OF C-STARS. *Astronomy & Astrophysics*, 290:623, 1995.
- [113] P. Woitke. TOO LITTLE RADIATION PRESSURE ON DUST IN THE WINDS OF OXYGEN-RICH AGB STARS. *Astronomy & Astrophysics*, 460:L9–L12, 2006.